Conducting Polymer and Zeolite Modified Carbon Electrodes for the Determination of Drugs and Biological Fluids

Solomon Mehretie

A Thesis Submitted to

The Department of Chemistry

Presented in Partial Fulfillment of the Requirements for Degree of

Doctor of Philosophy (Analytical Chemistry)

Addis Ababa, Ethiopia
May 2013

Addis Ababa University

School of Graduate Studies

This is to certify that the thesis prepared by Solomon Mehretie Yeniesew entitled: Conducting Polymer And Zeolite Modified Carbon Electrodes For The Determination of Drugs And Biological Fluids and submitted in partial fulfillment of the requirement of the Doctor of Philosophy (Analytical Chemistry) complies with the regulation of the University and meets the accepted standards with respect to originality and quality.

Signed by examining committee

Name	Signature	Date
1. Dr. Merid Tessema (Advisor)		30 | 05 | 13
2. Prof. Theodros Solomon (Advisor)		30 | 05 | 13
3. Dr. Shimelis Admassie (Advisor)		30 | 05 | 13
4. Prof. Antonio Lopez de Lacey (External Examiner)		30 | 05 | 13
5. Prof. B.S. Chandravanshi (Internal Examiner)		30 | 05 | 13
6. Dr. Negussie Megersa (Internal Examiner)		__ | __ | __
7. Dr. Mesfin Redi (Chairman)		30 | 05 | 13
_____ Chairman, College Academic Commission	_____	__ | __ | __

ABSTRACT

Conducting Polymer and Zeolite Modified Carbon Electrodes for the Determination of Drugs and Biological Fluids

Solomon Mehretie
Addis Ababa University, 2013

Electrochemical signals can be enhanced by specifically modifying electrode surfaces with the aim of providing suitable environment to the analyte of interest. Poly(3,4-ethylenedioxythiophene) and activated iron(III) doped zeolite were used to modify carbon electrodes for the determination of drugs and biological fluids. 3,4-Ethylenedioxythiophene was electropolymerized on glassy carbon electrode by running multi-sweep cyclic voltammetry whereas iron(III) doped zeolite was coated on the electrode surface. Both modified carbon electrodes were characterized by using cyclic voltammetry. The poly(3,4-ethylenedioxythiophene) modified electrodes were employed for the determination of niclosamide and N-acetyl-p-aminophenol while the iron(III) doped zeolite modified electrodes were used to determine pyridine-2-aldoxime methochloride and uric acid. Cyclic voltammetry and differential pulse voltammetry were used to investigate the electrochemical behavior of N-acetyl-p-aminophenol and its degradation product, p-aminophenol at poly(3,4-ethylenedioxythiophene) modified electrode in pH 7.0 buffer solution. Both N-acetyl-p-aminophenol and p-aminophenol showed quasi-reversible redox reactions with formal potentials of 367 mV and 101 mV (versus Ag/AgCl), respectively. The significant peak potential difference (266 mV) between N-acetyl-p-aminophenol and p-aminophenol enabled the simultaneous

determination of these species using differential pulse voltammetry. The voltammetric responses gave linear ranges of 1.0–100 μM and 4.0–320 μM, with detection limits of 0.40 μM and 1.2 μM for N-acetyl-p-aminophenol and p-aminophenol, respectively. Furthermore, the poly(3,4-ethylenedioxythiophene) modified electrode showed a very good electrochemical behavior for niclosamide with a significant enhancement of the peak current compared to the bare electrode. A linear voltammetric response for niclosamide was obtained in the concentration range 0.075–7.50 μM, with a detection limit of 0.01 μM. When the iron(III) doped zeolite modified glassy carbon electrode was treated with sulfuric acid (2.5 mM), it showed a better electrochemical response compared to the untreated zeolite modified electrode. Cyclic voltammetry and square wave voltammetry were employed to investigate the electrochemical behavior of pyridine-2-aldoxime methochloride and uric acid at the modified electrode. The analytical performance of the modified electrode was evaluated using anodic stripping voltammetry in a buffer solution (pH 7.0), and a linear response for pyridine-2-aldoxime methochloride was obtained in the concentration range 0.5–100.0 μM with a detection limit of 0.16 μM. The iron(III) doped zeolite was also responsible for the electrocatalytic oxidation of uric acid in a buffer solution (pH 4.6). The analytical performance of the iron(III) doped zeolite modified electrode was evaluated using square wave voltammetry. A linear anodic response for uric acid in the concentration range 0.6–60.0 μM, a detection limit of 0.09 μM and sensitivity of 0.64 μA μM^{-1} were obtained. Finally, the proposed methods were successfully applied for the determination of the analytes in pharmaceutical formulations and/or biological samples.

List of publications

1. Solomon Mehretie, José Losada, Merid Tessema, Shimelis Admassie, Theodros Solomon, Isabel Díaz, Joaquin Perez-Pariente, Voltammetric determination of Uric acid at activated iron (III) doped zeolite modified glassy carbon electrode (manuscript).
2. Solomon Mehretie, José Losada, Merid Tessema, Shimelis Admassie, Theodros Solomon, Isabel Díaz, Joaquin Perez-Pariente, Stripping voltammetric determination of pyridine-2-aldoxime methochloride at iron (III) doped zeolite modified glassy carbon electrode, *Analyst* **2012**, 137, 5625.
3. Solomon Mehretie, Shimelis Admassie, Merid Tessema and Theodros Solomon, Electrochemical Study of Niclosamide at Poly(3,4-ethylenedioxythiophene) Modified Glassy Carbon Electrode, *Sensors and Actuators B: Chemical* **2012**,168, 97.
4. Solomon Mehretie, Shimelis Admassie, Tadele Hundie, Merid Tessema and Theodros Solomon, Simultaneous determination of N-acetyl-p-aminophenol and p-aminophenol with poly(3,4-ethylenedioxythiophene) modified glassy carbon electrode, *Talanta*, **2011**, 85, 1376.
5. Solomon Mehretie, Shimelis Admassie, Merid Tessema and Theodros Solomon, Voltammetric Determination of Paracetamol with Poly(3,4-Ethylenedioxy-thiophene) Modified Glassy Carbon Electrode, *Anal. Bioanal. Electrochem.* **2011**, 3, 38.

ACKNOWLEDGEMENTS

I would like to express my sincere gratitude to my advisors Dr. Merid Tessema, Dr. Shimelis Admassie and Prof. Theodros Solomon. I am fortunate to have three different but complementary supervisors: Dr. Merid, I appreciate your encouragement and continuous guidance and meticulous editing of the manuscripts and thesis; Dr. Shimelis, I owe you a lot for introducing me to electroanalytical experiments and for pushing me to write manuscripts side-by-side with my experiments; and Prof. Theodros, I thank you for your critical comments on manuscripts and constructive criticism in my first topic course, that was a turning point for my PhD study.

I would like to thank Prof. Lo Gorton for hosting and supervising me as a guest student in his lab, Lund, Sweden. I am grateful to Prof. Lo for introducing to flow injection analysis and biosensors. I never forget your encouragement and patience during my hard time in the lab.

I would like to extend my sincere gratitude to Prof. Isabel Diaz for her help in obtaining the scholarship in Spain. It would have been difficult to get the fund without your help. I am grateful to Prof. José Losada and Prof. Joaquin Perez-Pariente for their advice during my stay in Spain. Prof. José, thanks a lot for your guidance in your lab and continuous encouragement. Prof. Joaquin, I owe you for introducing me to zeolite chemistry and your valuable comments.

My sincere thanks go to Prof. Negussie Reta, for triggering me to join the PhD program, Prof. Teketel Yohannes, for the electrochemistry course with him and providing books, Prof. Wendimagegn Mamo, for his help during my niclosamide experiment, Prof. Chandravanshi and Dr. Negussie Megerssa, for their comments on the thesis and support, and Dr. Ahmed Mustefa for providing me with necessary facilities from the Department. I have also been privileged to get different kinds of assistance from the staff members of the Department of Chemistry, AAU.

I am highly indebted to Addis Ababa University for allowing me to join the PhD program and covering my travel and living expenses during my six months stay in Sweden; to the Swedish Research Council (project 621-2007-4124 "Bioelectrochemical studies of direct and mediated electron transfer between redox enzymes, biological membranes, living cells and electrodes) for the financial support; and to the Spanish Ministry of Foreign Affairs-Spanish Agency for Cooperation and Development through the "Becas Institucionales" Program for the financial support during my 11 months stay in Spain.

I would like to express my gratitude to Dr. Siraye Esubalew for sharing idea, friendship and unreserved support to me and my family. My lab-mates: you have always been a source of idea and encouragement; Maereg, for your idea of activation of zeolite with acid; Alemnew, for sharing idea and support, and Birhanu, for your fun in the lab room.

I would like to extend my gratitude to Andualem and Wendimagegn, for our common denominator, and Negesh (Amigo), for sharing many things together during our stay in Spain (never forget "en casa"). I am also grateful to Dr. Mesay Mulugeta; he was

encouraging me to do more research and was involved in valuable discussion with me on analytical chemistry. I owe a lot to Samson Tamene for providing me the niclosamide standard.

I am greatly indebted to Dr. Gashaw Mamo and his wife Rekike for their support, encouragement and Ethiopian dishes during my stay in Lund.

I am grateful to *Gashe* Sahilemichael Deme for his support and patience in completing my clearance while I was in Spain. I would also like to thank W/os Lemlem, Aster and Megabit for their support.

I would like to thank all my lab-mates in Lund, especially Roberto, Nadeem, Christopher, Gabor, Hiro, Mitra and Alireza for friendship, joyful time we had together in the labs and parties.

My thanks also go to Nacho, Teresa, Manuel and Irene, for the tour we had around in Madrid, Segovia or Burgos for introducing me to the culture and history of the Spanish people. I am immensely grateful to Victory Gascon for her support and always being with us. Many thanks also go to all GTM members for their profound support and Birth day parties.

My warmest gratitude goes to all my friends who helped me a lot, especially, Legesse, Mulugeta, Sisay, Zewdu, Tibebu, Hymero, Meskerem and Alazar for their moral and material support.

Let me also take this opportunity to thank my family for their unconditional love and co-operation, *abey* Merra, *etita* Siraye, Mulu, Welle, Anie and Mark have always been with me with their whole hearted support, encouragement and prayers.

I would also like to extend my sincere thanks to Hana's family, especially Hareg and Abebaw for their encouragement and support.

The immense moral support I received from my wife Hana helped me to materialize this PhD work. I am indebted to her for taking the full responsibility of managing the home and caring for our daughter, understanding and love. My joy with our daughter Bethewoin has given me the energy in fact I forget my exhausting lab work when I look at your daily development (God bless you! Bethe). I would like to thank Anguach for being always there at home and take caring of my daughter.

Contents

List of abbreviations

CME	– Chemical modified electrode
PEDOT	– Poly(3,4-ethylenedioxythiophene)
EDOT	– 3,4-Ethylenedioxythiophene
$Fe^{3+}Y$	– Iron(III) doped zeolite
pbs	– Phosphate buffer solution
APAP	– N-acetyl-p-aminophenol
PAP	– P-aminophenol
PAM-2	– Pyridine-2-aldoxime methochloride
UA	– Uric acid
DMF	– Dimethylformamide
GCE	– Glassy carbon electrode
CPGCE	– Zeolite-free carbon paste glassy carbon electrode
CV	– Cyclic voltammetry
DPV	– Differential pulse voltammetry
SWV	– Square wave voltammetry
DPASV	– Differential pulse anodic stripping voltammetry
SWASV	– Square wave anodic stripping voltammetry
VB	– Valence band
CB	– Conduction band
η	– Overpotential
SCE	– Saturated calomel electrode
SOD	– Sodalite
WE	– Working electrode
CE	– Counter electrode
n	– Number of electron(s)
T	– Temperature
α	– Electron transfer coefficient
Γ	– Surface coverage
ν	– Potential scan rate

List of figures

List of tables

1. Introduction to conducting polymer and zeolite

1.1. Background

Electrochemistry was earlier begun by emphasizing the equilibrium aspect of a redox reaction, particularly focusing on subjects such as galvanic cell, potentiometry and conductometry [1]. Attention was not given to the dynamic aspect of electrochemistry until the beginning of the 1920s. The change in the course of electrochemistry was started in 1922 when Heyrovskey published the first paper dealing with polarography [2] for which he was awarded the Noble Prize in Chemistry in 1959. Polarography deals with current-potential relationships of a redox reaction exhibited by the dropping mercury electrode, proved to be the first electroanalytical technique in electrochemistry.

The discovery of polarography opened a new area of study in electrochemistry such as the kinetics of redox reactions and reversible or irreversible electron transfer processes [3]. Mercury was the metal that pushed electroanalytical chemistry to the highest level in the field of electrochemistry in the 1940s. Apart from the huge experimental work made with this unique metal, polarography also constituted the experimental benchmark for the enormous theoretical work dealing with different types of electrode mechanisms [4-7]. Although mercury was still taken in great consideration in the 1970s, 1980s and even nowadays, its toxicity to the environment reduces its use.

The era of solid electrodes instead of the dropping mercury electrode began in the 1960s [8]. This change of the working electrode gave rise to a technique called voltammetry which is more sensitive and faster than polarography [9]. The presence of higher charging

current in polarography made it less sensitive than voltammetry. In 1969, Ralph Adams published a volume that constitutes a reference point for different solid electrode materials other than mercury [10]. These substrates include platinum, gold and various forms of carbon. The 1960s and the 1970s were also the decades when theoretical studies made for different complex electrode mechanisms, based on linear sweep and cyclic voltammetry [11].

Although solid electrodes such as gold, platinum and carbon are currently in widespread use in electroanalytical chemistry, because of their broad potential range, low background current and suitability for various sensing and detection applications, they are prone to poisoning by contaminants (fouling), sluggish electron transfer and difficulty in obtaining the desired selectivity and sensitivity. In order to address these drawbacks, modification of solid electrodes was begun in the 1970s [12, 13]. Royce Murray's exhaustive treatment of chemically modified electrodes (CMEs) appeared in a chapter in the Electroanalytical Chemistry series by Bard in 1984 [14]. In his review, Murray gave a definition for modified electrode: "...one deliberately seeks in some hopefully rationale fashion to immobilize a chemical on the electrode surface so that the electrode thereafter displays the chemical, electrochemical, optical, and other properties of the immobilized molecules ...." Hence, CMEs are deliberate placement of chemical species onto an electrode surface to meet a desired goal in order to accelerate the electron transfer reactions, preferentially (pre)concentrate and/or enhance selectivity. Since Murray's review, there have been huge amounts of work on CMEs for the last 28 years [15-17].

Electrocatalytic property is one of the important features of CME to be utilized in electroanalytical chemistry. Figure 1.1 illustrates an example of electrocatalytic process at a CME with decrease in overpotential (η). The reversible redox mediator M_{ox}/M_{red} with a standard potential of $E^o_{M_{ox/red}}$ was immobilized on an electrode to promote the irreversible oxidation reaction of $A_{red} \rightarrow A_{ox} + e^-$. A relatively high overpotential was observed at a bare electrode (Figure 1.1A) while in the presence of the mediator the reaction was promoted by redox mediation with a low overpotential at $E^o_{M_{ox/red}}$ (Figure 1.1B). This type of heterogeneous CMEs is not only selective and sensitive but also fast and reusable in electroanalytical measurements.

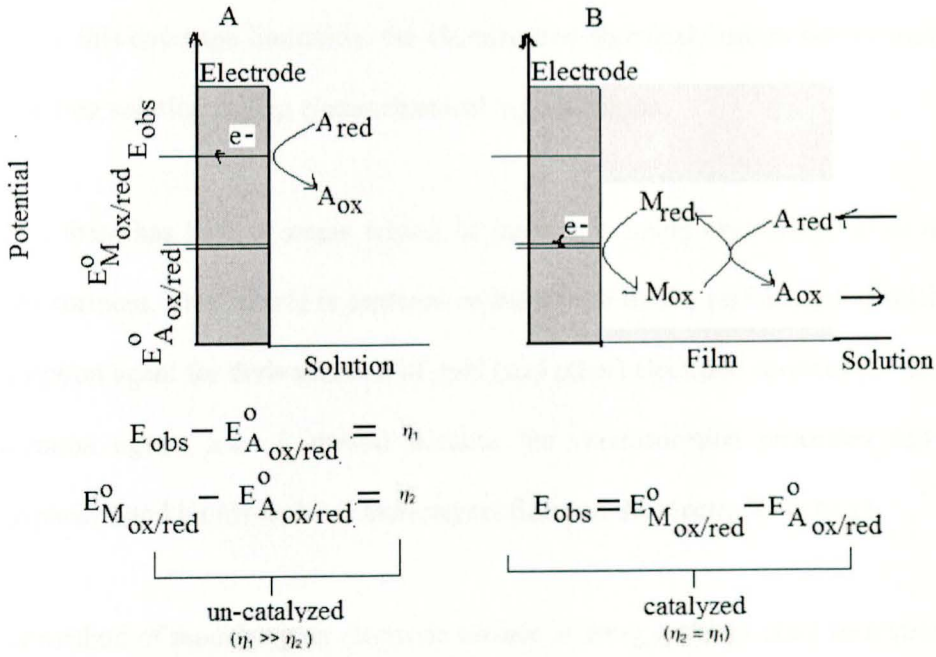

Figure 1.1. Schematic representation for the oxidation reaction of analyte ($A_{red} \rightarrow A_{ox}$) on: (A) bare electrode and (B) modified electrode with mediators (M_{red}/M_{ox}). The E_{obs}, $E^o_{M_{red/ox}}$ $E^o_{A_{red/ox}}$ and η correspond to un-catalyzed, $M_{red/ox}$ mediated standard potentials and over potential, respectively

There are four methods of preparing CMEs, based on the nature of the modifying process [16, 18]. Sorption is considered the first method to place a chemical species at a conductive surface. It is an adsorptive interaction between a chemical species and the surface of an electrode. The chemical species consists of π systems containing functional groups suitable to interact selectively with species in solution. For the case of sorption-based CMEs, physical and chemical interaction properties are utilized as modifying procedures to form monolayer structures [19, 20].

Chemisorption requires direct contact between the chemisorbed molecule and the electrode surface; as a result, the highest coverage achievable is a monomolecular layer. Apart from this coverage limitation, the chemisorbed chemical species slowly leach into the contacting solution during electrochemical investigations.

However, there has been a recent rebirth of interest in using chemisorption to modify electrode surfaces. This rebirth is centered on the use of thiols, sulfides and disulfides as chemisorption agent for derivatization of gold (and other) electrode surfaces [21-23]. The derivatization agents are of interest because the chemisorption processes can yield densely-packed and highly-ordered monolayers films on the electrode surfaces.

Another method of modifying an electrode surface is using covalent bond formation. The formation of covalent bond between specific functional groups on the electrode surface and the chemical species to be attached to the surface involves reaction of a surface hydroxyl with hydrolytically-unstable siline [24]. The silane will be hydrolyzed in the presence of trace water to form a siloxane that will ultimately become covalently attached

to the electrode surface. In addition, carbon surface is found to be efficient for the covalent modification due to its alterable functionalities and hence numerous investigations are made on variety of carbon surfaces [25].

Polymer-based multilayer CMEs provide another way of modification of an electrode surface. A number of polymers have been used to prepare CMEs, they can be classified into: redox polymers, ion exchange polymers and electronically conducting polymers. Redox polymers are polymers that contain electroactive functionalities either within the main polymer chain or side-chain pendant on the polymer. A typical example is poly(vinylferrocene) in which the ferrocene groups attached to the polymer chain are the electroactive functionality [15].

Ion exchange polymers are not themselves electroactive but can incorporate electroactive guest molecules. They incorporate electroactive counterions via an ion exchange reaction. For example, Nafion (perfluorosulfonate ionomer) is a strong acid ion exchange polymer in which the proton can be replaced with an electroactive cation ion [15, 26].

The third class of polymer used to prepare CMEs is electronically conducting polymer which attracts a lot of attention as voltammetric transducers [27]. Conducting polymer modified electrodes were used to detect a number of electroactive compounds such as dopamine [28-31], ascorbic acid [32-34], uric acid [35], morphine [36], and serotonin [37]. The advantage of conducting polymer modified electrodes over conventional metal or carbon electrodes is their electrocatalytic ability. This often leads to better separation of oxidation (or reduction) peaks of the different analytes in electrochemical responses.

Clay, zeolite and other inorganic, microcrystalline structured materials have also been used to modify electrode surfaces [38-40]. These inorganic materials are of interest because they are ion exchangers, like ion exchange polymers; clays and zeolites can withstand high temperatures and highly oxidizing solution media. In addition, these inorganic materials have well-defined microstructures. For example, clays have a sheet-like structure and zeolite contain pores and channels of well-defined diameter. The four possible routes for the preparation of CMEs are schematically summarized as shown in Figure 1.2.

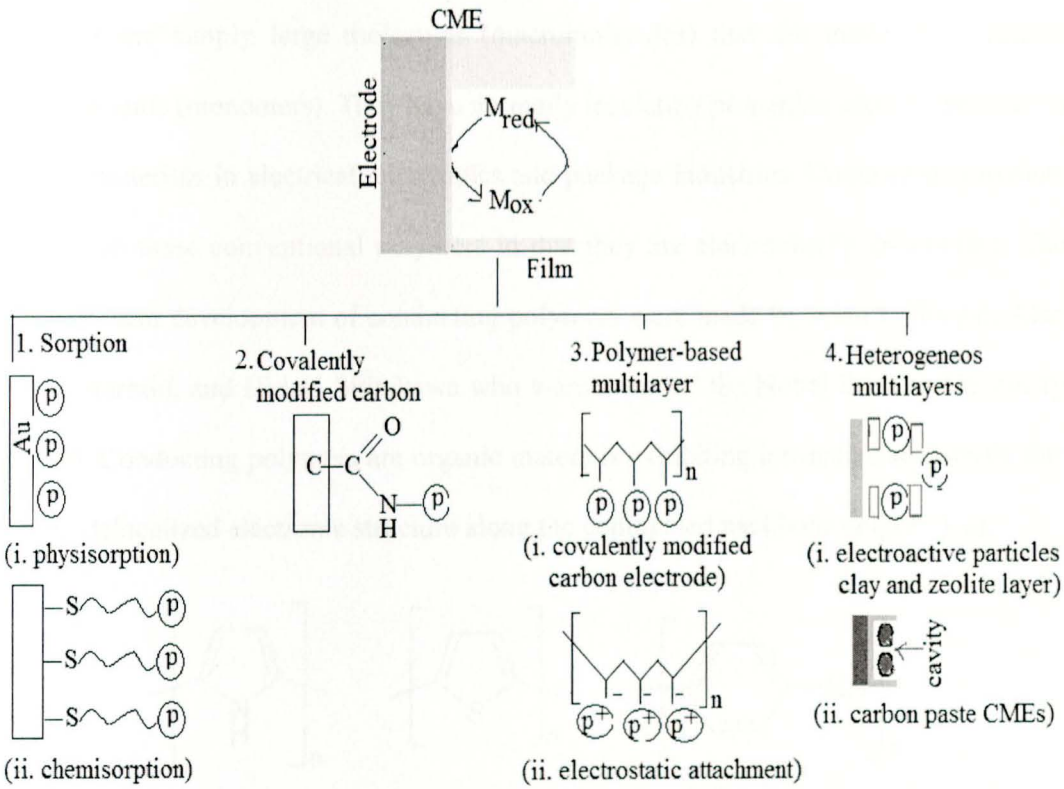

Figure 1.2. Schematic representation for various types of CME preparation routes

In general, CMEs have been shortened into three main categories [41]: (1) monolayer modified electrodes, (2) homogeneous multimolecularly layered electrodes (mainly based on polymer films), and (3) composite electrodes based on multicomponent heterogeneous matrixes that are constituted by either (bio)organic or inorganic modifiers. This thesis mainly focuses on the latter two categories in which modification of electrodes by conducting polymers and zeolite will be discussed.

1.2. Conducting polymer

Polymers are simply large molecules (macromolecules) that are made from smaller repeating units (monomers). They have normally insulating properties used extensively to insulate materials in electrical, electronics and package industries. Conducting polymers differ from these conventional polymers in that they are electronically conducting. The discovery and development of conducting polymers were made by Alan J. Heegar, Alan J. MacDiarmid, and Hideki Shirakawa who were awarded the Nobel Prize in Chemistry in 2000. Conducting polymers are organic materials exhibiting intrinsic conductivity due to their delocalized electronic structure along the conjugated backbone (Figure 1.3).

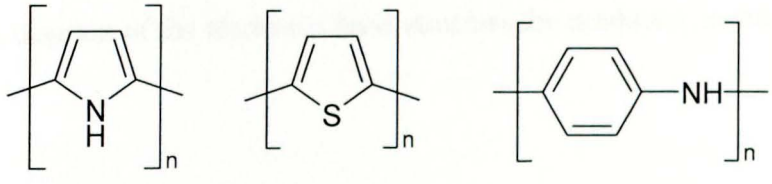

1 2 3

Figure 1.3. Structure of polypyrrole (**1**), polythiophene (**2**) and polyaniline (**3**)

The conductivity exhibited by conducting polymers was in earlier days explained by using the Band theory [42]. Materials depending on their electrical conductivity can generally be classified into insulators, semiconductors and conductors. This classification depends on the energy gap (band gap) between the valence band and the conduction band as depicted in Figure 1.4. The band gap of insulator materials is more than 10 eV and hence, it is difficult to promote an electron from the valence band to the conduction band. The band gap for semiconductors is smaller (about 1 eV) so it is possible to excite electrons from the valence band to the conduction band at room temperature. In conductors, the valence band and conduction band overlap; in fact some portion of the conduction band is filled by electrons.

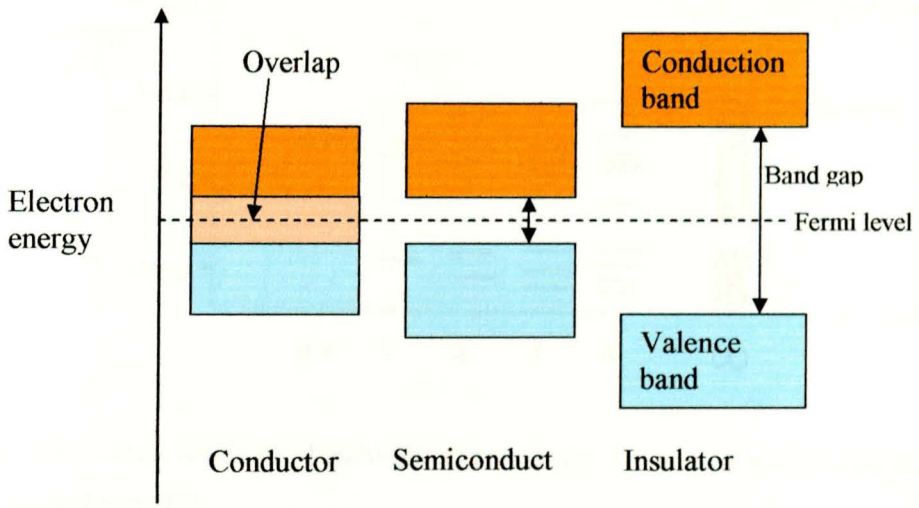

Figure 1.4. A diagram of the electronic band structure for conductor, semiconductor and insulator

The band structure of a conducting polymer comes from the interaction of the π-orbitals of the repeating units. The calculated energies of oligothiophenes with n = 1-4 and of polythiophene as a function of oligomer length are shown in Figure 1.5 [43]. The addition

of every new thiophene unit causes hybridization of the energy levels yielding more and more levels until a point is reached at which there are bands rather than discrete levels. Interaction between the π-electrons of the neighboring molecules leads to a three-dimensional band structure.

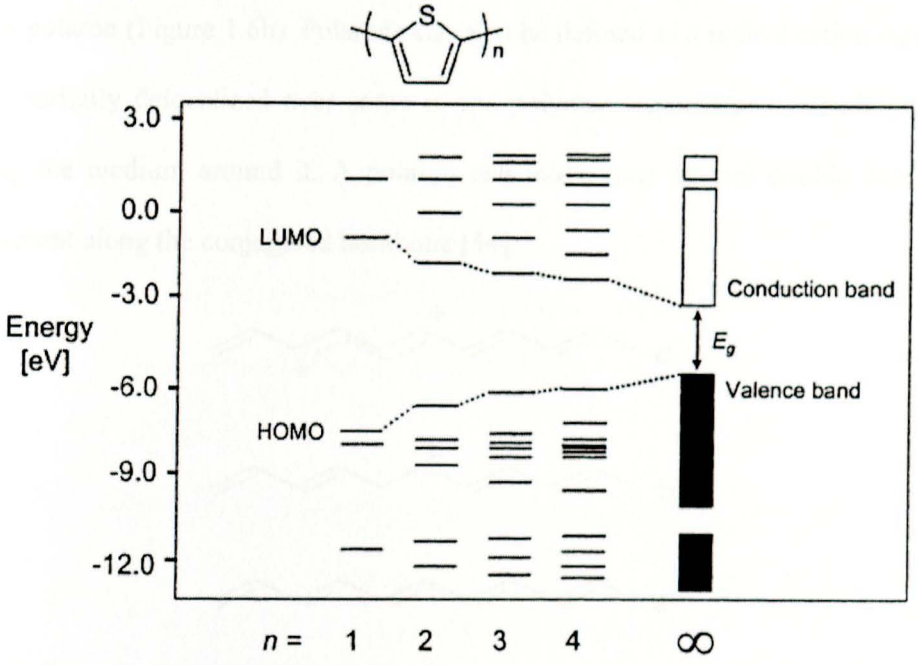

Figure 1.5. Energy levels of oligothiophenes with n = 1-4 and of polythiophene, where E_g is the band gap [43]

The band gap of conducting polymers is around 1 eV, indicating that conducting polymers are semiconductor materials. In a semiconductor, doping produces an acceptor energy level close to the valence band or a donor energy level close to the conduction band. But the conduction of conducting polymers is a little different.

The conduction mechanism of conducting polymers is due to the interaction of a number of atomic orbitals leading to the formation of electron band structure. When oxidation of a conjugating conducting polymer (Figure 1.6a) occurs, a radical and a positive charge are formed. These radical and positive charges are coupled to each other via local resonance along the polymer backbone. This combination of a charge site and a radical is known as polaron (Figure 1.6b). Polarons can also be defined as a radical cation (spin ½) which is partially delocalized over some of the polymer segment and is stabilized by polarizing the medium around it. A polaron can move over several double bonds by rearrangement along the conjugated backbone [44].

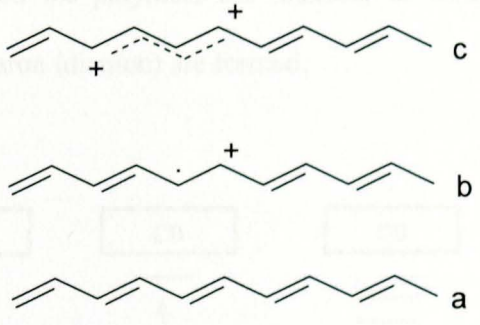

Figure 1.6. Structures of: (a) undisturbed conjugation, (b) polaron, and (c) bipolaron

The formation of a polaron creates new localized electronic energy states in the band gap between conduction and valence band. The lower energy state is occupied by a single unpaired electron (Figure 1.7). At low oxidation levels, two polarons are kept away from each other by coulombic repulsion. When the oxidation potential increases, the polarons become crowded and begin to interact along the conjugated backbones. A bipolaron is formed when two polarons are combined due to further oxidation (Figure 1.6c). It is defined as a pair of like charges (dication) associated with a strong local geometrical

distortion and it is spinless. The bipolaron has a lower energy level and is more stable in comparison to a polaron.

The bipolaron in non-degenerate conducting polymers may not be stable because of the coulombic repulsion of the two polarons which constitute the bipolaron. However, the presence of dopant ions in the neighborhood can stabilize the bipolaron [45]. At higher doping levels, bipolarons form a bipolaron band (Figure 1.7). It is possible for a heavily doped conducting polymer that the upper and lower bipolaron bands will combine with the CB and VB respectively, forming a partially filled band similar to a metal. The same phenomenon occurs when the polymers are reduced, in which the negative polaron (radical anion) and bipolaron (dianion) are formed.

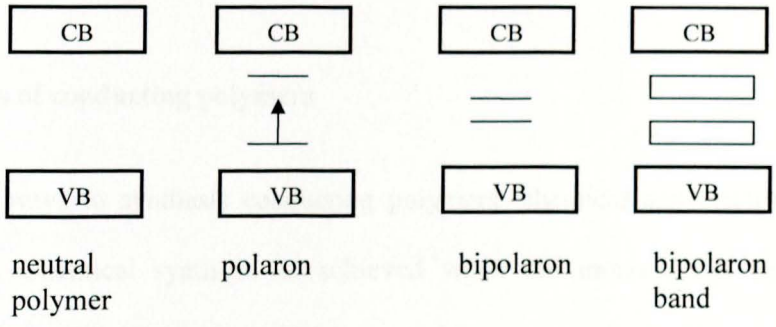

Figure 1.7. Schematic representation of polaron, bipolaron, and bipolaron band energy states between valence band (VB) and conduction band (CB)

The positive charges in the structure of a bipolaron are free to move along the conjugated backbones. Electronic conductivity arises from the mobility of the polaron and bipolaron charge carriers. As mentioned earlier, these charge carriers are stabilized by dopant ions

from the electrolyte solution. To further illustrate this phenomenon, the oxidation polymerization of a monomer (HMH) is considered (Eq. 1.1) [46].

$$(n + 2)\ HMH \rightarrow HM(M)_nMH^{(nx)+} + (2n + 2)H^+ + (2n + 2 + nx)e^- \qquad (1.1)$$

(2n + 2) electrons are used for the polymerization process itself, while the additional charging of the polymer film requires nx electrons. In general, x lies between 0.25 and 0.4 and represents the doping level of the polymer. This means that every third to fourth monomeric subunit is charged at the end of polymerization [46]. The conductivity of conducting polymers depends on the amount of anionic or cationic doping. The higher the level of doping, the more the conductivity of a conducting polymer would be due to the creation of more mobile charges. Therefore, the conductivity of the polymer is not only dependent on the redox state of the polymer but also on the level of doping.

1.2.1. Synthesis of conducting polymers

There are two ways to synthesis conducting polymers: chemical and electrochemical polymerization. Chemical synthesis is achieved when the monomer is exposed to relatively strong oxidizing agents such as ammonium peroxydisulfate, potassium dichromate or ferric chloride. This can be carried out in solution or directly on the surface of a substrate. Chemical synthesis on a surface of an electrode involves depositing the desired monomer solution on it and then subsequently treating the surface with the solution or vapor of the oxidizing agent. As a result, a polymer film is formed on the surface of the substrate.

The most common way of preparing conducting polymers is anodic electropolymerization. Here, the first step of polymerization involves oxidation of a monomer to its radical cations, $M^{+\cdot}$, followed by radical-radical coupling that leads to a radical dication. Then, the radical dication loses two protons to form a dimer. As this dimer is more easily oxidized than the monomer, because of its greater conjugation, it is immediately oxidized to its cation, undergoing a next coupling step with a monomeric radical cation and then from the resulting charged trimer again protons are eliminated. This series of reactions (like chain propagation reaction) results in the formation of a polymer (P) (see Scheme 1.1, considering: monomer, M; dimer, D; trimer, T; tetramer, Q) [47, 48].

$$2M \xrightarrow[Oxad]{-2e^-} 2M^{+\cdot}$$

$$M^{+\cdot} + M^{+\cdot} \rightarrow D + 2H^+$$

$$D \xrightarrow[Oxad]{-2e^-} D^{+\cdot}$$

$$D^{+\cdot} + M^{+\cdot} \rightarrow T + 2H^+$$

$$T \xrightarrow[Oxad]{-2e^-} T^{+\cdot}$$

$$T^{+\cdot} + M^{+\cdot} \rightarrow Q + 2H^+ \rightarrow\rightarrow\rightarrow [\text{--P--}]_n$$

Scheme 1.1: Chain propagation approach of electrochemical synthesis of conducting polymers

Even though the chain propagation reaction is widely accepted, a different mechanism (oligomer approach) has recently been proposed [46]. The reason behind this approach is that the very first step a radical ion dimerization of the monomeric starting molecules

took place and the coupling tendency between charged oligomers and a monomer radical cation decreased as a function of the oligomeric chain length. The electropolymerization deposition of the polymer occurring by coupling of oligomers is shown in Scheme 1.2.

$$2M \xrightarrow[Oxad]{-2e^-} 2M^{+\cdot}$$

$$M^{+\cdot} + M^{+\cdot} \rightarrow D + 2H^+$$

$$D \xrightarrow[Oxad]{-2e^-} D^{+\cdot}$$

$$D^{+\cdot} + D^{+\cdot} \rightarrow Q + 2H^+$$

$$Q \xrightarrow[Oxad]{-2e^-} Q^{+\cdot}$$

$$Q^{+\cdot} + Q^{+\cdot} \rightarrow \text{Octamer} + 2H^+ \rightarrow\rightarrow\rightarrow [\text{--P--}]_n$$

Scheme 1.2: Oligomer approach of electrochemical synthesis of conducting polymers [47]

When a suitable potential is applied to a conducting substrate that has been placed in a monomer solution, electropolymerization takes place. There are different techniques of electropolymerization: Potentiostatic (constat potential), galvanostatic (constant current) or potentiodynamic (multi-sweep cyclic voltammetry) techniques. The potentiodynamic experiment, in particular, provides simple information on the rate of growth of conducting polymers. The increase in current with each cycle of a multi-sweep cyclic voltammogram is a direct measure of the increase in accessible surface and the number of rechargeable redox sites (Figure 1.8). An adherent polymer film can be attached directly onto an electrode in one simple step. Reproducible films can be formed as the film thickness can be controlled by monitoring the number of cycles.

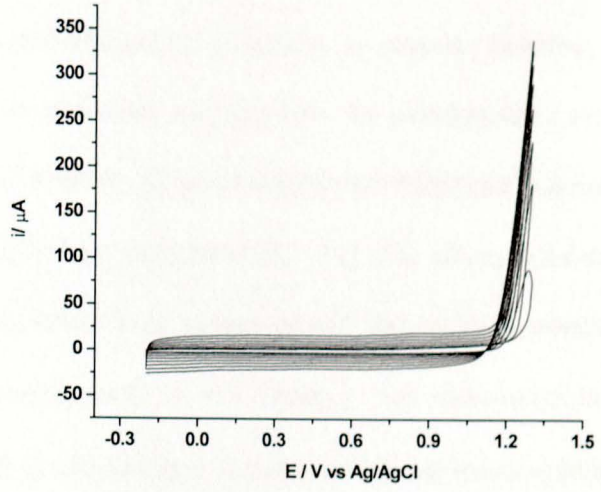

Figure 1.8. Potentiodynamic growth of a poly(3,4-ethylenedioxythiophene) film at GCE in acetonitrile (0.1 M Bu_4NBF_4, $\nu = 50$ mV s^{-1})

1.2.2. Poly(3,4-ethylenedioxythiophene)

Polythiophene (Figure 1.3 (**2**)) is formed from the polymerization of thiophene which has relatively high oxidation potential (+1.6 V vs. SCE) compared to pyrrole (+0.8 V vs. SCE) [49]. Polythiophene is relatively stable in air and moisture in both doped and undoped states [50]. Substitution at the 3- and 4-positions of thiophene by an electron withdrawing group results in an increase in the oxidation potential by approximately 0.5-0.7 V compared to the unsubstituted thiophene [51, 52]. This causes difficulty to electropolymerize the substituted thiophene with electron withdrawing groups and results in poor conductivity of the polymer due to degradation (over-oxidation). This difficulty has been attributed to the high reactivity of the corresponding radicals that undergo rapid reactions with the solvent or anions to form soluble products instead of promoting electropolymerization [51].

On the other hand, substitution of thiophene by electron donating groups results in a decrease in oxidation potentials and stabilizes the corresponding radicals. Conductivity and electrochemical stability of alkyl-substituted thiophene polymer are significantly lower than unsubstituted polythiophene [53, 54]. For alkoxy-substituted polythiophene, the electron donating effect from oxygen lowers the oxidation potential even more [55]. Considering this development, a new strategy was discovered in 1991 [56, 57] to electropolymerize β–β disubstituted thiophene (3,4-ethylenedioxythiophene) to produce more ordered polymers with longer conjugation. This new polymer is known as poly(3,4-ethylenedioxythiophene) (PEDOT).

The monomer 3,4-ethylenedioxythiophene (EDOT) has a boiling point of 225°C and slowly turns dark upon exposure to air and light because of partial oxidation. Substitution at the 3- and 4- position of thiophene (Figure 1.9 (**1**)) by an oxygen electron donor lowers the oxidation of EDOT compared to thiophene [58] and prevents the occurrence of α–β and β–β coupling during electropolymerization. These donating groups also stabilize the positive charge generated in doped PEDOT (Figure 1.9 (**2**)). Under milder preparation conditions, the resulting polymers are not as sensitive to nucleophilic attack as the corresponding unsubstituted materials are [59].

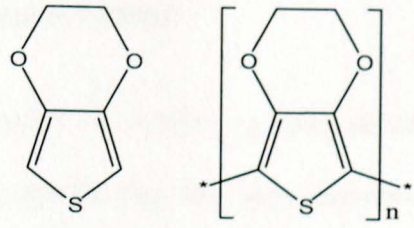

1 2

Figure 1.9. Chemical structures of EDOT (**1**) and PEDOT (**2**)

Because of its intrinsic features, PEDOT has become one of the most popular conducting polymers being studied by many scientific research groups [60, 61]. It also shows some advantages such as high conductivity (about 300 S cm^{-1}), environmental stability, high transparency [59], low oxidation potential, relatively low band gap [62], good chemical and electrochemical properties [58]. However, EDOT and PEDOT have the drawback of poor water solubility (2.1 g L^{-1} at 20°C), both in neutral and doped forms [49]. This problem has been overcome by introducing polystyrene sulfonate (PSS) during the polymerization to obtain EDOT/PSS. PSS is a water soluble polyelectrolyte that acts as a charge-balancing dopant [58, 61].

As a result of the aforementioned features, PEDOT is used for a number of applications [63] such as antistatic coatings for photographic films, electrode material in solid-state capacitors, substrates for electrodless metal deposition in printed circuit boards, indium tin oxide (ITO) electrode-replacement material in inorganic electroluminescent lamps and hole conducting material in organic/polymer-based light-emitting diodes and sensors [49, 64-66].

1.2.3. Electropolymerization of PEDOT

Electrochemical polymerization of PEDOT is achieved when an anodic potential is applied to a conducting substrate that has been immersed in a suitable electrolyte containing the monomer and the desired doping salt. Insoluble oligomers precipitate at the electrode surface forming a thin polymer film. The conductivity of these films changes by several orders of magnitude upon oxidation of the polymer backbone. Upon applying potential onto the film of the electrode, PEDOT can be switched from neutral, partially oxidized, and to fully oxidized states as depicted in Figure 1.10. A polaron is formed when a neutral polymer (Figure 1.10A) loses one electron and further oxidation of the polymers leads to formation a bipolaron (Figure 1.10C).

When PEDOT is synthesized through electrochemical method, the electropolymerization conditions such as solvent, electrode, supporting electrolyte, polymerization potential and mode of electropolymerization have important effects on the properties of the PEDOT films. PEDOT can be electropolymerized in water-solvent mixtures or pure water [67-70]. Electropolymerization in aqueous media is performed using surfactants such as sodium dodecylsulfate [67] or sodium dodecylbenzenesulfonate [69]. The surfactants form a micellar aqueous medium to induce a catalytic effect by lowering the oxidation potential. The polymerization of EDOT in the presence of a micellar medium produces well organized, compact, and adherent films on the electrode. However, due to low solubility of EDOT in water, it is usually electropolymerized in non-aqueous medium.

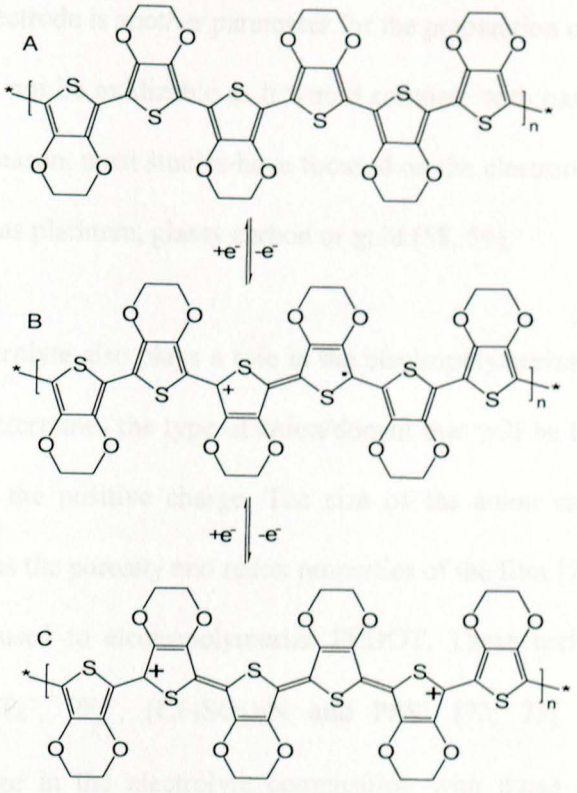

Figure 1.10. (A) Oxidation of PEDOT segments leading to formation of: (B) radical cations (polarons) and (C) dications (bipolarons)

PEDOT films have been prepared in organic media such as acetonitrile containing $LiClO_4$ [61], tetrabutylammonium perchlorate (TBAP) [71] and propylene carbonate containing tetra(n-butyl) ammonia hexafluorophosphate ($TBAPF_6$) [72]. In organic media, EDOT monomers are well dispersed and yield rough films without regularity. This is attributed to the better solubility of oligomers-EDOT which electrodeposits onto the electrode surface [58, 59]. Acetonitrile is found to be a more efficient medium for producing adherent films compared to other non-aqueous solvents such as propylene carbonate and dichloromethane [58].

The nature of the electrode is another parameter for the preparation of PEDOT films. The electrode used must not be oxidizable as it would compete with oxidation of the EDOT monomer. For this reason, most studies have focused on the electrodeposition of PEDOT at inert anodes such as platinum, glassy carbon or gold [58, 59].

The supporting electrolyte also plays a role in the electropolymerization process. This is because it usually determines the type of anion/dopant that will be incorporated into the polymer to balance the positive charge. The size of the anion can influence various characteristics such as the porosity and redox properties of the film [71]. A vast variety of dopants have been used to electropolymerize PEDOT. These include anions such as ClO_4^-, $CF_3SO_3^-$, BF_4^-, PF_6^-, $(CF_3SO_2)_2N$ and PSS^- [72, 73]. From conductivity investigations, change in the electrolyte composition with those of non-nucleophilic anions yield slight difference in conductivity [73], perchlorate and fluoroborate being the best performing anions [71].

The potential has also a significant role in the electropolymeristion of EDOT. The oxidation of EDOT occurs between 0.85 V and 1.50 V vs. SCE. Oxidation at potentials higher than this leads to a decrease in the conductivity of the polymer. This process, which is known to be an over-oxidation process, is irreversible and occurs gradually with increasing potential. A conductivity investigation was made and it was found that upon over-oxidation its conductivity decreases due to degradation of the polymer [74, 75]. The conductivity of the n-doped form was also measured and values approximately 100 times lower than that of p-doping was observed, even though degradation occurs in this highly negative potential range [74].

Finally, the mode of polymerization also has an effect on the polymerization of EDOT. PEDOT films are most commonly electropolymerized via galvanostatic, potentiostatic and poteniodynamic methods. The films formed from a constant current or constant potential mode of polymerization are usually more porous and uneven, while the films obtained using repetitive multi-sweep CV are generally smoother and compact [76].

1.3. Zeolite

Zeolites are microporous, aluminosilicate minerals commonly used as commercial adsorbents. The term zeolite was originally coined in 1756 by the Swedish mineralogist Axel Fredrik Cronstedt, who observed that upon rapidly heating the material, stilbite, it produced large amounts of steam from water that had been adsorbed by the material [77]. He called the material *zeolite*, from the Greek words "ζέω" (*zéo*) and λίθος (*líthos*), meaning "boiling stone".

The atomic structures of zeolites are based on three-dimensional frameworks of silica and alumina tetrahedra, that is, silicon or aluminum ions surrounded by four oxygen ions in a tetrahedral configuration. Each oxygen is bonded to two adjacent silicon or aluminum ions, linking them together which forms the primary building unit for zeolites. Clusters of tetrahedra form boxlike polyhedral units that are further linked to build up the entire framework. These polyhedral-unit arrangements are known to be the seconday building units (SBUs).

The wide variety of possible zeolite structures is due to the large number of ways in which the SBU can be linked to form various polyhedra. These polyhedra create

networks of regular channels and cavities. One of the simplest zeolite types is sodalite. Its structure consists of a body centered cubic arrangement of β-cage (see Figure 1.11). The spatial arrangements of the tetrahedral TO_4 (T = Si or Al) give rise to a continuous three-dimensional pattern made of voids and channels of discrete size. The pore or channel openings range from 3 Å to 15 Å depending on the structure.

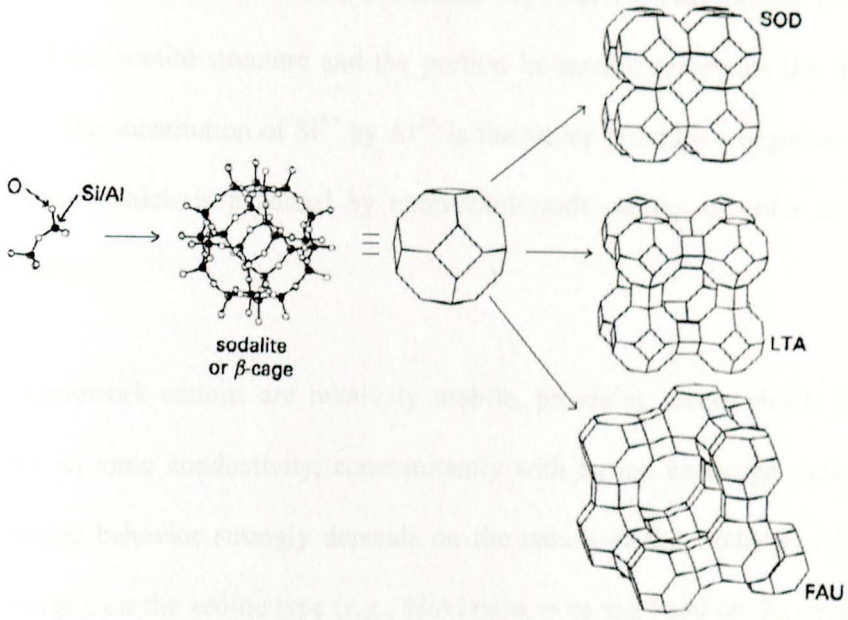

Figure 1.11. The soldalite or β-cage and the different structure of zeolite types formed from its β-cage such as sodalite (SOD), zeolyte A (LTA) and faujasite (FAU)

Figure 1.11 shows how the sodalite cage is formed by the three-dimensional arrangement of the TO_4 tetrahedra and it also displays the three-dimentional structures of two zeolite widely used at electrochemical interfaces, zeolite A (LTA) and zeolite type X or Y (faujasite, FAU), which are built from the same building unit: the sodalite cage, the same cage unit from which sodalite (SOD) is formed. The relative flexibility of the T-O-T bonds (Figure 1.11) allows the formation of supercages and pore apertures of different

sizes. As a result, zeolites provide unique molecular sieving properties, applied to both shape and size molecular discrimination.

The general chemical composition of zeolites is given by the following formula:

$$A_y[Al_nSi_{m-n}O_{2m}].xH_2O$$

where A is the extra-framework cation of valence +1, +2 or +3. This formula is applied to a unit cell of the zeolite structure and the portion in bracket represents the framework composition. The substitution of Si^{4+} by Al^{3+} in the lattice provides a negative charge in zeolite structure which is balanced by extra-framework cations in order to maintain electroneutrality.

The extra-framework cations are relatively mobile, providing electronically insulating zeolites with an ionic conductivity, concomitantly with an ion exchange capacity. The cation exchange behavior strongly depends on the nature of the exchangeable species (size and charge), on the zeolite type (e.g., Si/Al ratio, pore size) and on the experimental conditions (e.g., concentration, pH) [78].

1.3.1. Importance of zeolite for electroanalysis

The interest in aluminosilicate zeolites for the electroanalytical chemist relies on the intrinsic properties of these materials. Zeolites are stable at high temperatures, insoluble in most organic solvents and provide better resistance to extreme experimental conditions than numerous organic polymers commonly employed to modify electrode surfaces.

In addition, zeolites offer size, shape and charge selectivities due to their rigid, three-dimensional and negatively charged lattice structure. Under equilibrium conditions, only those cations with smaller size than the aperture of the host zeolite pores are able to diffuse freely into the zeolite framework [78]. Zeolites have been used as preconcentration media for various inorganic, organic and organometallic cations because of their ion exchange capacity [78, 79]. This property can be advantageously exploited to promote the selective preconcentration of analytes at an electrochemical interface and confine electron transfer mediators inside the large cavities of the zeolite.

1.3.2. Electron transfer at zeolite modified electrodes

The electrochemistry of zeolites relies on the mechanism responsible for electron transfer processes occurring at zeolite modified electrodes as zeolites are insulating materials. There are broadly two mechanisms to explain the electron transfer at the zeolite modified electrodes: intrazeolite and extrazeolite mechanisms [79].

The intrazeolite electron transfer mechanism takes place when an entrapped species in the zeolite lattice undergoes a redox reaction. As these entrapped species cannot carry out any ion exchange reaction, the electron transfer occurs within the zeolite matrix via electron hopping processes [80]. Here the charge balance is maintained by the electrolyte cation entering the zeolite lattice (Eq. 1.2). The mechanism does not differentiate species located deeply in the bulk zeolite and those situated at the surface of the zeolite. In contrast, extrazeolite electron transfer mechanism involves ion exchange of the

electroactive probes for the electrolyte cations (Eq. 1.3) prior to the electron transfer reaction at the electrode-solution interface (Eq. 1.4) [41].

Intrazeolite mechanism

$$E_{(z)}^{m+} + ne^- + nC_{(s)}^+ \rightleftharpoons E_{(z)}^{(m-n)+} + nC_{(z)}^+ \quad (1.2)$$

Extrazeolite mechanism

$$E_{(z)}^{m+} + mC_{(s)}^+ \rightleftharpoons E_{(i)}^{m+} + mC_{(z)}^+ \quad (1.3)$$

$$E_{(i)}^{m+} + ne^- \rightleftharpoons E_{(i)}^{(m-n)+} \quad (1.4)$$

where E is the electroactive species with charge C^+ representing the electrolyte cation (chosen as monovalent for convenience), the subscripts z, i, and s refer to the zeolite phase, the interface and the solution, respectively.

1.3.3. Preparation of zeolite modified electrodes

Since a zeolite material is electronically insulator, its use for electroanalysis requires a close contact to an electrode material. Different strategies have been employed to prepare suitable zeolite modified electrodes. Broadly, two approaches have been used: (1) the dispersion of solid particles in carbon-based composite matrices and (2) the deposition of thin films on solid electrode surfaces [41, 81-83].

Zeolite modified carbon paste electrodes can be prepared by thorough mixing of zeolite and carbon powder together with a mineral oil which acts as a binder. The mixture is then put into a holder equipped with an electrical contact and its surface is smoothed by mechanical polishing. As far as all components of the modified paste are uniformly

dispersed in the composite, the electrode can reach a good level of reproducibility after mechanical renewal of its surface. This has been widely applied to prepare zeolite modified electrodes which were used for electroanalysis [84-87]. To get more convenient modified electrode for practical applications, this carbon-based composite approach has been extended to the production of disposable electrodes by the thick-film technology (screen-printing) by using carbon inks doped with zeolites [88].

Another approach of preparing zeolite modified electrodes is film-base electrode. Zeolite has been deposited on solid electrodes by evaporation of an organic suspension containing the dispersed mineral particles. Mostly, a dissolved organic polymer (e.g., polystyrene, poly(vinyl alcohol)) was added to the suspension in order to increase the adhesion of the particles to the electrode surface and between them [89, 90]. Usually, carbon particles were added along with mineral powder to improve the conductivity of the modified electrode.

Both approaches, the bulk composites and the film-based zeolite modified electrodes, are of importance regarding the target application [41]. Film-based modified electrodes require mass and charge transfer reactions to occur across the material layer from the solution to the electrode surface while the bulk composite provide both the modified and the conductive part of the electrode in direct contact to the solution. The film-based configuration would thus be of interest for permselective detection where as the bulk composite configuration would be more appropriate for electrocatalysis.

2. Overview of the electroanalytical techniques used in the study

This thesis mainly focuses on the use of electroanalytical techniques for quantitative determination of various analytes. Electroanalytical techniques encompass a group of methods that are based upon the electrical properties of an electroactive species. The principal criterion for electroanalytical measurements is that the species, which is desired to be measured, should react directly (or indirectly through coupled reaction) at the electrode.

2.1. Electrode processes

An electrode reaction is a heterogeneous electrochemical process which involves the passage of an electron from an electrode to a chemical species in solution or *vise versa*. The electrode/solution interface can be partitioned roughly into four regions as shown in Figure 2.1. These are the electrode, the double layer, the diffusion layer and the bulk of the solution. The electrode/solution interface represents a plane with respect to the distribution of the electrical charge. This interface results in unequal charge distribution on the electrode side (negative charge on the electrode side, see Figure 2.1) and positive charge on solution, creating a double layer.

The diffusion layer is still a region dominated by unequal charge distribution due to the electron transfer processes occurring at the electrode surface. In fact, the electrode acts as an electrostatic pump for species of a certain charge, causing the flow of these charged systems from the bulk of the solution towards the electrode, or *vice versa*.

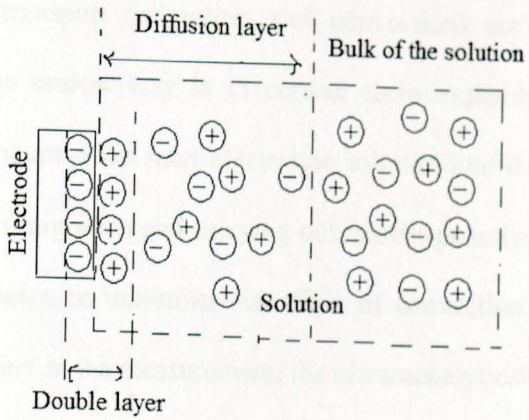

Figure 2.1. The schematic representation of the electrode/solution interface

A typical electrode reaction involves the transfer of charge between an electrode and a species in solution. The reaction involves a series of steps:

1. The reactant diffuses to the interface, this is known as mass transport,

2. Heterogeneous electron transfer between the electrode and the electroactive species at the electrode surface,

3. The product diffuses away from the electrode to allow fresh electroactive species to the surface.

An electrode can donate or accept electron(s) only to/from species present in a layer of solution that is immediately adjacent to the electrode. For this electrode process, the transport of electroactive species to the electrode surface can occur by any of the following processes: diffusion (transport of species due to concentration gradient), convection (movement due to mechanical motion of the solution as a result of stirring), and migration (transport of ions as a result of the electrostatic attraction between the oppositely charged electrode and ions.)

The two modes of transport (migration and convection) are difficult to describe mathematically, so the easiest way is to control them experimentally. To this end, introducing a large amount of an inert electrolyte solution into the electrochemical cell suppresses the effect of migration and carrying out current-potential measurements under quiescent conditions helps to minimize the effect of convection. Once migration and convection have no effect in the measurement, the electroanalytical techniques are purely diffusion controlled.

Diffusion controlled electrochemical techniques are powerful and versatile analytical techniques that offer high sensitivity, accuracy and precision as well as a wide linear range. Among the electrochemical techniques, voltammetry is the most commonly employed method for quantitative determination of various species.

2.2. Voltammetry

Voltammetry is an electrochemical technique in which current-potential behavior at an electrode surface is measured. The potential is varied in a systematic manner to cause a redox reaction of the electroactive chemical species at the electrode. The resulting peak current is proportional to the concentration of an analyte in the bulk of the solution.

Three electrodes in an electrochemical cell are employed to carry out voltammetric measurements. These are a working electrode, a reference electrode, and a counter electrode. The working electrode is the electrode at which the redox process of interest takes place. It is ideally polarizable, i.e., the electrode shows a large change in potential

when an infinitesimally small current passes through it. The reference electrode serves to control the potential of the working electrode. It is a nonpolarizable electrode where potential does not vary. The counter electrode is a current conducting electrode which carries the bulk of the current (instead of the reference electrode). Voltammetric measurements are usually performed in a quiescent solution in the presence of a large excess of a supporting electrolyte. Control and data acquisition of the response can be done by computer which is interfaced with potentiostat. The potentiostat is the electronic hardware required to control a three electrode cell and run most electroanalytical experiments.

Various types of voltammetric techniques such as cyclic voltammetry, differential pulse voltammetry, square wave voltammetry and stripping voltammetry have been used for the characterization and quantification of electroactive analytes investigated.

2.2.1. Cyclic voltammetry

Cyclic voltammetry (CV) belongs to the category of voltammetric techniques based on a linear potential sweep technique. It is widely used for the study of redox process, understanding reaction intermediates and obtaining stable reaction products. In this technique, the potential at the working electrode is linearly changed with time with a well-defined rate (scan rate), forward and reverse (cyclic) scan between a starting (E_{start}) and a "switching" (E_{λ}) potential value with respect to a reference electrode, and the resulting current is measured. A typical representation of the CV is depicted in Figure 2.2, where plots of: (A) potential vs. time and (B) current vs. potential are shown.

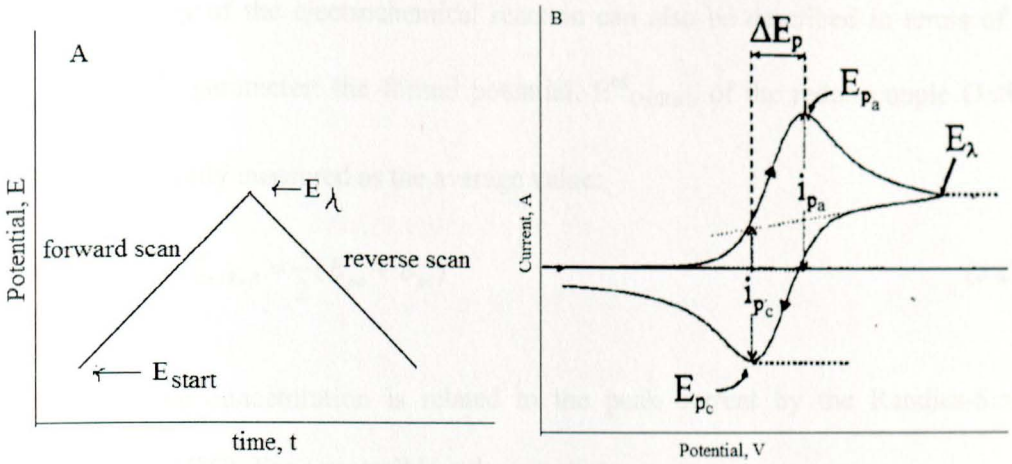

Figure 2.2. Representation CV plots of: (A) potential–time pulse and (B) current versus potential response

The important parameters in a cyclic voltammogram are peak potentials (E_{pc}, E_{pa}) and peak currents (i_{pc}, i_{pa}) of the cathodic and anodic peaks, respectively (see Figure 2.2B). If the electron transfer process is faster than other processes (such as mass transport), the reaction is said to be electrochemically reversible and the peak separation is

$$\Delta E_p = E_{pa} - E_{pc} = 2.303RT/nF \qquad (2.1)$$

Thus, for a reversible redox reaction at 25°C with n electrons, the peak-to-peak separation, ΔE_p, should be 0.059/n V or about 60 mV for one electron. In practice this value is difficult to attain because of different factors such as solution resistance. A departure of 10–20 mV from the theoretical ΔE_p value does not compromise the criterion of reversibility, because the solution resistance is not adequately compensated by the electrochemical instrumentation.

The reversibility of the electrochemical reaction can also be described in terms of the thermodynamic parameter: the formal potential, $E^{o\$}_{Ox/Red}$, of the redox couple Ox/Red which is commonly measured as the average value:

$$E^{o'}_{Ox/Red} = \frac{1}{2}(E_{pa} + E_{pc}) \qquad (2.2)$$

In addition, the concentration is related to the peak current by the Randles-Sevcik expression (at 25°C). For a reversible redox reaction:

$$i_p = 2.69x10^5 n^{3/2} Ac(Dv)^{1/2} \qquad (2.3)$$

where i_p is the peak current, A is the electrode area, D is the diffusion coefficient, v is the scan rate and c is the concentration of the electroactive species.

If the rate of the electron transfer is lower than that of the mass transport, the potential at which the reduction reaction takes place is much more cathodic than the formal potential of the Ox/Red couple. In addition, commonly the separation between the forward peak and the reverse peak is so large and the reverse peak is not detected. Under this circumstance the redox process behaves irreversibly. For this type of reaction, the peak current, i_p, is given by:

$$i_p = 2.99x10^5 n(\alpha n_a)^{1/2} Ac(Dv)^{1/2} \qquad (2.4)$$

is still proportional to the bulk concentration, but will be lower in peak height depending on the value of α. Assuming a value of α 0.5, the ratio of reversible-to-irreversible current peaks is 1.27 (that is, the peak current for irreversible process is about 80% of the peak for a reversible one) [15].

In electron transfer processes, one observes that at low scan rates the process behaves reversibly; whereas at high scan rates the process behaves irreversibly (such behavior is more easily seen for processes that are not complicated by coupled reactions). Processes occurring in the transition zone between reversible and irreversible behavior are known to be quasi-reversible. This process occurs when the rate of the electron transfer of a redox reaction is of the same order of magnitude as the mass transport. For this systems (with $10^{-1} > k^{o} > 10^{-5}$ cm s^{-1}) the current is controlled by both the charge transfer and mass transport. A quasi-reversible process is characterized by determining the formal potential, given that $0.3 < \alpha < 0.7$. In this case, the shift of the cathodic peak towards more negative potential values and the shift of the oxidation peak towards more positive values, both caused by the kinetic effects, essentially compensate each other.

CV can be also used to study the interfacial behavior of electrochemical active species. When the redox species are confined at the electrode surface, by physical or covalent attachment, the redox reaction becomes adsorption controlled and the shape of the voltammogram is mirror symmetric cyclic voltammetric peaks ($\Delta E_p = 0$). In this reversible adsorption reaction, the peak current is proportional to the surface coverage (Γ) and scan rate (ν) rather than $\nu^{1/2}$.

$$i_p = \frac{n^2 F^2 \Gamma A \nu}{4RT} \tag{2.5}$$

Similarly, i_p is also proportional to ν for irreversible adsorption process,

$$i_p = \frac{\alpha F^2 \Gamma A \nu}{2.718RT} \tag{2.6}$$

2.2.2. Pulse techniques

Pulse voltammetric techniques are employed to lower the detection limit of voltammetric measurements. The various pulse techniques are all based on a sampled current/potential-step experiment. A sequence of such potential steps, each with duration of about 50 ms, is applied onto the working electrode. After the potential is stepped, the charging (capacitive) current decays rapidly (exponentially) to a negligible value, while the faradaic current decays more slowly (square root of time). Thus by sampling the current late in the pulse life, the current becomes purely faradaic.

In this regard, two techniques are particularly useful for the determination of electroactive compounds investigated in this thesis: differential pulse voltammetry and square wave voltammetry.

2.2.2.1. Differential pulse voltammetry (DPV)

The potential waveform of pulses superimposed on a staircase during the DPV scan is shown in Figure 2.3A [91]. For the potential, typically the pulse height is about 50 mV and the step height of the staircase is about 10 mV or less. During a pulse period the current is periodically measured twice: before the pulse, i_1, and at the end of the pulse, i_2, respectively, as illustrated in Figure 2.3A. It is evident that after subtracting the two currents (i.e., $i_2 - i_1$) most of the capacitive current is eliminated. Thus a differential pulse voltammogram is a plot of the difference ($i_2 - i_1$) as a function of the base staircase potential.

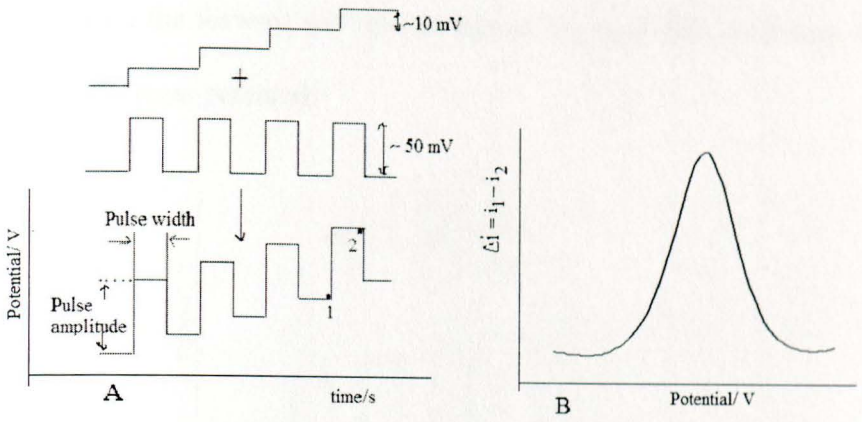

Figure 2.3. (A) Schematic waveform of pulse superimposed on a staircase for differential pulse voltammetry and (B) current versus potential response resulting from DPV scan

A differential curve (bell-shaped) with a peak is obtained as depicted in Figure 2.3B. The height of the peak is directly proportional to the concentration of the electroactive species as expressed in Equation 2.5. It means that the shape of the response function and the height of the peak can be treated quantitatively in a direct manner.

$$i_p = \frac{nFAD^{1/2}c}{\pi^{1/2}t^{1/2}}\left(\frac{1-\sigma}{1+\sigma}\right) \qquad \sigma = \exp\left(\frac{nF\Delta E}{2RT}\right) \tag{2.7}$$

2.2.2.2. Square pulse voltammetry (SWV)

The excitation signal in SWV consists of a symmetrical square-wave pulse of amplitude E_{sw} superimposed on a staircase waveform, where the forward pulse of the square wave coincides with the staircase step. The current is sampled twice during each square-wave cycle, once at the end of the forward pulse (at t_1) and once at the end of the reverse pulse (at t_2) as shown in Figure 2.4 [15]. The net current, i_{net}, is obtained by taking the

difference between the forward and reverse current (i_{for}–i_{rev}). This difference is plotted versus the base staircase potential.

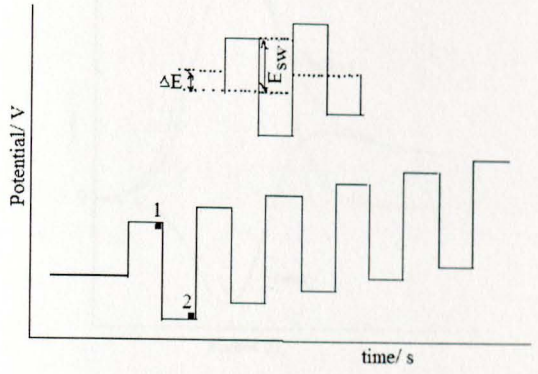

Figure 2.4. Square-wave waveform showing the amplitude, E_{sw}; step height, ΔE; and current measurements times, 1 and 2

As shown in Figure 2.5, the square wave voltammogram, like in DPV, is peak-shaped, but it is composed of a differential curve between the current recorded in the forward half-cycle and the current recorded in the reverse half cycles (it is noted that since the forward and the reverse currents have opposite signs, their difference corresponds in absolute to their sum).

The main advantage of SWV is its speed. The scan rate depends on the square-wave frequency and step height. For example, if the step potential and frequency of the square-wave are 10 mV and 50 Hz, respectively, then the effective scan rate is 0.5 V s^{-1}. Consequently, the analysis time is abruptly reduced; a complete voltammogram can be obtained within a few seconds, as compared to about 2–3 min in DPV.

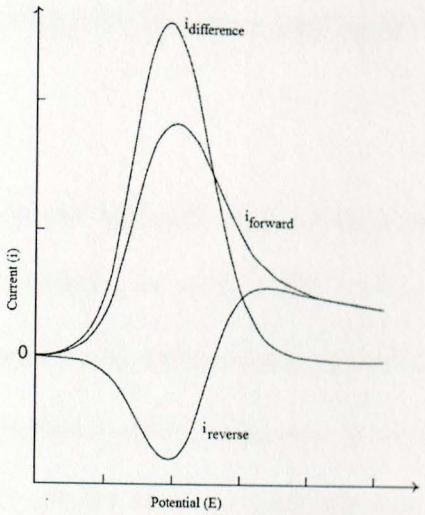

Figure 2.5. Square-wave voltammograms for reversible electron transfer

2.3. Stripping voltammetry

Stripping voltammetry is a sensitive electroanalytical technique for the determination of trace amounts of organic compounds and metal ions. The technique is carried out in three steps. First, an analyte is preconcentrated onto an electrode which is held at a suitable potential. The solution containing the analyte is stirred during this preconcentration step to enhance mass transport. Second, stirring is stopped so that the solution becomes in steady condition. Third, the preconcentrated analyte is stripped from the electrode by sweeping the potential. The observed current during the stripping step can be related to the concentration of the analyte.

The stripping step can be either a positive or a negative potential scan which creates an anodic or a cathodic current, respectively. Correspondingly, anodic stripping voltammetry (ASV) and cathodic stripping voltammetry (CSV) are two specific stripping techniques.

2.4. Electrochemical techniques for pharmaceutical active compounds and biological fluids

Pharmaceutical compounds and biological fluids analyses play vital roles in quality control and have significant impacts on public health. The establishment of simple, fast, sensitive and accurate method for the determination of biomedical substances is of great concern and interest. Electrochemical techniques are well suited for the determination of these analytes in various samples such as pharmaceutical and clinical media. The advantage of the modern electrochemical methods is that the analyte of interest is selectively detected in a sample matrix and generally sample preparation such as separation and extraction procedures are not required. Thus, it only requires easy sample preparation, usually consisting of dissolving the analyte of interest in a suitable solvent followed by performing direct analysis on an aliquot of this solution.

Increase in the number of pharmaceutical industries results in a wide variety of drugs with various structures and compositions, differing in their activity and therapeutic properties. This causes problems of controlling not only the quality of the therapeutic substances but also the content of drugs in various matrices including biological samples.

Voltammetric techniques are gaining importance for monitoring drugs and metabolites in biological and clinical samples. These techniques are sensitive, reliable and simple, and the redox reactions often provide selectivity for the compounds of interest even in the presence of their degradation products. Accordingly, the present study mainly focuses on voltammetric methods for the determination of pharmaceutical compounds and biological

fluids such as APAP (its degradation product, PAP), niclosamide, PAM-2 and uric acid, and their respective structures are shown in Figure 2.6.

General objective

The general objective of this study was to design and develop chemically modified electrodes based on modifiers namely PEDOT and activated iron(III) doped zeolite and to apply the proposed methods for the determination of pharmaceutical compounds and biological fluids.

Specific objectives include:

- To develop a voltammetric technique for the simultaneous determination of APAP and PAP at PEDOT-modified electrode
- To develop anodic stripping voltammetric technique for the determination of niclosamide at PEDOT-modified electrode
- To fabricate chemically modified electrodes based on activated $Fe^{3+}Y$ modified GCE for the determination of PAM-2
- To develop an electrochemical method for the determination of uric acid at $Fe^{3+}Y$ modified GCE

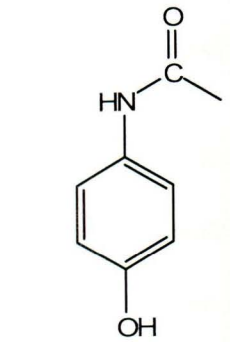

N-acetyl-p-aminophenol (APAP)

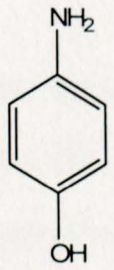

P-aminophenol (PAP)

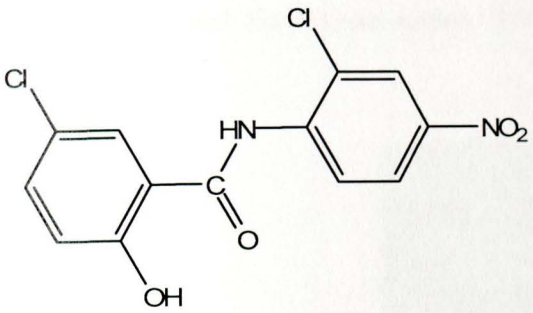

Niclosamide

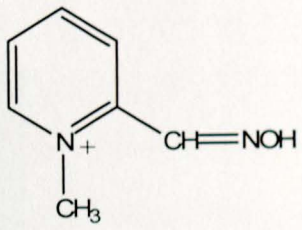

Pyridine-2-aldoxime methochloride (PAM-2)

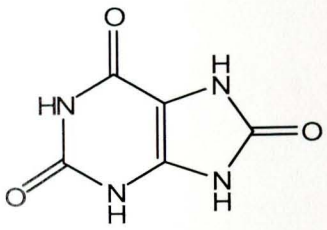

Uric acid (UA)

Figure 2.6. Structures of the analytes studied in the thesis

3. Experimental

3.1. Electrochemical cell

The electrochemical cell consists of a pair of electrodes of unequal size (a WE and a CE) and a reference electrode as shown in Figure 3.1. Three electrodes are usually necessary in order to avoid the passage of current through the reference electrode, which otherwise would alter its potential via changes in the activities of the various species. The electrical circuit, through which the current passes, is between the working electrode and a counter electrode.

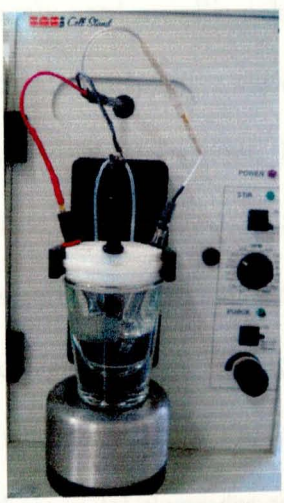

Figure 3.1. Electrochemical cell consisting of working electrode (black), counter electrode (red) and reference electrode (white)

3.1.1. Working electrode

The working electrode is the electrode in an electrochemical cell on which the analyte of interest undergoes a redox reaction. Common working electrodes are mercury, gold, platinum, and various forms carbon. Liquid mercury electrode was commonly used in the

earlier days of electroanalytical chemistry. It has the special advantage of providing renewed surface, which helps to minimize the effects from adsorption of solution impurities and fouling of the electrode surface by a film produced in the electrode reaction. However, mercury is readily oxidized, particularly in the presence of anions such as halides, cyanide and others. For this reason, it is seldom used to study anodic processes. In addition, mercury electrodes are not in use nowadays due to environmental reasons.

Platinum and gold are the commonly used metallic solid electrodes. These metals are obtained in high purity and fabricated readily into a variety of geometric configurations such as wires, rods, flat sheets and woven gauzes. Platinum has extremely small overpotentials for hydrogen evolution, which is the basis for its use in the construction of hydrogen electrodes. Gold has a significantly large overpotential, but it is much smaller than that of mercury. Gold does not significantly adsorb hydrogen and this factor together with its larger overpotential for hydrogen evolution makes gold the metal of choice to study cathodic processes. Hence these metal electrodes cannot be used for both cathodic and anodic process.

Carbon electrode is useful for both oxidation and reduction in both aqueous and non-aqueous solutions. Several different forms of carbon have been used to make successful electrodes including spectroscopic-grade graphite, carbon paste, or glassy carbon. The use of glassy carbon as an electrode material was reported in 1965 [92]. Glassy carbon is electrically conductive and a gas impermeable material, highly resistant to chemical attack and obtainable in pure state. The advantage of glassy carbon over gold or platinum

are: low cost, easy polishing, wide potential window and electrocatalytic activity for a variety of redox reactions [93]. Due to these advantages, this thesis work is mainly based on GCE.

3.1.2 Reference electrode

A reference electrode is an electrode whose potential is known and constant. The electrode potential has to be stable (with time and temperature) and independent of the properties of the solution because it is used to control the potential of the working electrode by the application of a voltage between them. This means that the electrode must be unaffected by the passage of the small amounts of current required in making potentiometric measurements. The high stability of the electrode potential is usually reached by employing a redox system with constant (buffered or saturated) concentrations of each of the participants of the redox reaction. There are two common reference electrodes in use, i.e., silver-silver chloride (Ag/AgCl) and saturated calomel electrode (SCE).

3.1.3. Counter electrode

In voltammetric studies the current flows between the working electrode and the counter electrode. If a two electrode system containing only the reference and the working electrodes is used, then the current flows through the reference electrode causing a change in its potential. So a three electrode system, incorporating a third electrode called the counter electrode is used. The main condition for an electrode to act as a counter electrode is that it should not dissolve in the medium of the electrochemical cell and the

reaction product at this electrode should not react at the working electrode. The electrode surface area of the counter electrode must also be larger than that of the working electrode to ensure that the area of the electrode does not control the limiting current. Platinum electrodes in the form of coils or thin wires are the most widely used as counter electrodes in aqueous and non-aqueous media.

3.2. Supporting electrolytes

A supporting electrolyte is a solution of an inert soluble salt added to the solvent, generally in 10-fold or 100-fold excess over the concentration of the species being studied. There are three functions of the supporting electrolytes.

First, it carries most of the ionic current of the cell since its concentration is much larger than that of the other species in solution. Thus, it serves to complete the circuit of the electrochemical cell and lower the cell resistance. The second purpose of the supporting electrolyte is that it maintains a constant ionic strength. This is necessary because the structure of the interface region should not change significantly if a reaction occurs there. A stable structure is created on the electrolyte side by adding a large concentration of an inert salt. The third purpose of the supporting electrolyte is to suppress the effect of the migration current. Migration current is the current that arises as a result of the movement of ions caused by an electric field. The net migration current observed is reduced by the presence of a large excess of ions that are not electrochemically active.

In our experiments, the supporting electrolytes are inorganic salts or buffer solutions. The buffer in most cases was made from phosphate solution (0.1 M NaH_2PO_4, 0.1 M Na_2HPO_4, 0.1 M KH_2PO_4, and 0.1 M K_2HPO_4 in aqueous media). In non-aqueous media, particularly for the modification of PEDOT on to the electrode surface, tetrabutylammonium tetrafluoroborate (Bu_4NBF_4) in acetonitrile solvent was used.

3.3. Modification of electrode

The glassy carbon electrode is modified by using two kinds of modifiers, these are: PEDOT and activated iron(III) doped zeolite.

3.3.1. PEDOT modified electrode

Prior to modification, a GCE was polished with 0.05 μm alumina on polishing cloth and cleaned with deionized water followed by immersing the polished electrode into a 0.1 M EDOT monomer containing 0.1 M Bu_4NBF_4 in acetonitrile. The EDOT was electropolymerized on the GCE by running cyclic voltammetry from −0.2 to 1.3 V for ten cycles. Then, the modified electrode was cycled 15 times in 0.1 M Bu_4NBF_4/acetonitrile solution for stabilization. After electropolymerization, the PEDOT modified GCE was carefully washed with acetonitrile. Finally, the modified electrode was conditioned by running CV in phosphate buffer solution (pH 7.0) between 0.0 V and 0.8 V for a number of cycles until a stable CV was obtained.

3.3.2. $Fe^{3+}Y$ modified electrode

2 g of sodium-zeolite type Y was added to 250 mL 0.01 M $FeCl_3$ solution and stirred for 6 h. After filtration, the prepared zeolite was washed with HCl (pH = 3.0) and then with pure water to remove adsorbed species and was left to dry in air. From chemical analysis, iron(III) in the doped zeolite was found to be 0.6 % and 0.8 % (w/w) in the faujasite and natural zeolites, respectively. Equal amounts graphite powder and $Fe^{3+}Y$ (50 mg) were taken and ground together for 15 min. This mixture was dispersed in a solution of 200 μL tetrahydrofuran, 300 μL dichloromethane and 10 mg polystyrene. Zeolite free carbon paste modified GCE (CPGCE) was prepared in the same way as $Fe^{3+}Y$ modified electrode but without zeolite. Then 10 μL of this suspension was applied to a previously cleaned GCE and dried in air for 20 min. The electrode cleansing step was done by polishing it with 0.1 μm alumina powder and rinsing with pure water in an ultrasonic bath.

3.4. Sample preparation

3.4.1. APAP and PAP

Five tablets (500 mg APAP per tablet) of pharmaceutical formulations were accurately weighed and finely powdered in a porcelain mortar. An adequate amount of the powder was weighed and transferred to a 100 mL flask containing 30 mL of 0.1 M phosphate buffer (pH 7.0). The flask was thoroughly shaken until most of the sample dissolved and the mixture was centrifuged. Finally, the clear solution was filtered through a Whatman

41 filter paper and the pH of the supernatant was adjusted to 7.0. The recovery of the tablet sample solutions was obtained by using standard addition method.

A urine sample was collected from a healthy person 4 h after intake of two tablets of 500 mg APAP per tablet. The extraction of the urine sample was carried out according to the literature recently reported [94]. A mixture of 0.2 M NaOH and urine sample was manually swirled for 2 min followed by adding ethyl acetate. After centrifugation at 4500 rpm for 5 min, the organic phase was separated from the aqueous. The ethyl acetate was removed using a Rotavapor under low pressure and reduced temperature (50°C). The dried samples were reconstituted with phosphate buffer solution (pH 7.0).

3.4.2. Niclosamide

Five tablets (500 mg niclosamide/tablet) of pharmaceutical formulations were accurately weighed and finely powdered in a porcelain mortar. An adequate amount of the powder was taken and dissolved in 25 mL DMF in order to obtain 0.5 mM niclosamide which was diluted to 0.75 μM with pbs. The recovery of the tablet solutions was made using standard addition method.

3.5. Electrochemical measurements

3.5.1. APAP, PAP and niclosamide at PEDOT-modified electrode

The voltammetric investigations were carried out using BASi Epsilon-EC USB, controlled by a Dell computer with a conventional three-electrode configuration. The PEDOT-modified GCE was used as the working electrode, a platinum wire electrode

served as the counter electrode with Ag/AgCl/saturated KCl as the reference electrode. The pH of the buffer solutions was measured with a Jenway model 3510 pH meter.

The electrochemical experiments of APAP and PAP at the PEDOT-modified GCE were done by using CV and differential pulse voltammetry (DPV). A potential window between +0 mV and +500 mV together with the optimized pulse amplitude (25 mV) and pulse width (75 ms) was used to obtain the differential pulse voltammograms. Prior to each experiment, the modified electrode was regenerated by running cyclic voltammetry between −100 mV and 700 mV in the phosphate buffer solution until the peak for APAP and PAP disappeared.

The electrochemical behavior of niclosamide at the PEDOT modified GCE was investigated by using CV. For cyclic voltammetric experiments, the potential was scanned from −0.3 V to −0.8 V, and then swept anodically to 0.5 V and back to −0.3 V. For experiments using anodic stripping voltammetry with an accumulation potential of −0.55 V, the modified electrode was left in the solution containing the desired concentration of niclosamide with stirring for 80 s. Then, the potential was swept from −0.20 V to 0.10 V using an optimized pulse amplitude (25 mV) and pulse width (75 ms). The differential pulse voltammograms were obtained under quiescent conditions. Prior to each experiment, the modified electrode was regenerated by immersing it into DMF for 2 min and running CV between −0.20 V and 0.70 V in the phosphate buffer solution till a stabilized cyclic voltammogram was obtained.

3.5.2. PAM-2 and uric acid at $Fe^{3+}Y$ modified electrode

Electrochemical measurements were carried out using an Ecochemie BV Autolab PGSTAT 12. The experiments were controlled with General Purpose Electrochemical System (GPES) software. All electrochemical studies were performed at room temperature with a conventional three-electrode system with a saturated calomel reference electrode (SCE), platinum gauze counter electrode, and $Fe^{3+}Y$ modified or zeolite-free carbon paste modified GCE working electrode. The pH of the buffer solutions was measured with a BASIC 20 pH meter.

The electrochemical behavior of PAM-2 at the $Fe^{3+}Y$ modified GCE was investigated by using CV. In square wave anodic stripping measurements, the modified electrode was left in the solution containing the desired concentration of PAM-2 with stirring for 5 min followed by a potential sweep from 0.20 V to 1.0 V. The square wave voltammograms were recorded under quiescent conditions using an optimized step potential 10 mV, amplitude 20 mV and frequency 10 Hz. Prior to each experiment, the modified electrode was regenerated by scanning SWV from 0.20 V to 1.0 V in phosphate buffer solution until the peak current for the analyte disappears. The modified electrode was kept in 0.3 M K_2SO_4 solution when it was not in use.

The electrochemical behavior of uric acid (UA) at the $Fe^{3+}Y$ modified GCE was investigated by using CV. During preconcentration, the modified electrode was put in the solution containing the desired concentration of UA with stirring for 90 s at open-circuit potential of 0.2 V. Then the square wave voltammograms were recorded under quiescent

conditions using an optimized step potential 5 mV, amplitude 20 mV and frequency 10 Hz. Prior to each experiment, the modified electrode was regenerated by scanning SWV from 0.20 V to 0.9 V in pbs (pH 4.6) until the peak current for the analyte disappears.

3.6. Chemicals and reagents

APAP (Sigma), PAP (Sigma–Aldrich), Niclosamide (Sigma), Bu_4NBF_4 (Sigma–Aldrich), acetonitrile (Scharlau Chemie), disodium hydrogen phosphate (Techno Pharmchem), sodium dihydrogen phosphate (BDH), hydrochloric acid (Riedel-deHaen), and sodium hydroxide (BDH) were used without further purification. 3,4-Ethyleneoxythiophene (EDOT) was distilled repeatedly under vacuum until a colorless liquid was obtained and was kept in the dark.

Stock solutions of APAP and PAP in phosphate buffer solutions (0.1 M NaH_2PO_4 and 0.1 M Na_2HPO_4) were prepared by using deionized water. The pH of the phosphate buffer solution was adjusted by adding drops of concentrated hydrochloric acid and sodium hydroxide. A stock solution of niclosamide (0.5 mM) was prepared in dimethylformamide (DMF) and was kept in the dark. The serial dilution of the niclosamide was made using aqueous phosphate buffer (0.1 M).

Zeolite (CBV100:SiO_2/Al_2O_3 ratio 5:1, Na_2O %wt 13.0, and surface area 900 $m^2\ g^{-1}$) was purchased from Zeolyst, and natural zeolite (Stilbite: ratio of Si/Al 3:3 and Ca/Na 4:2) was obtained from Ethiopia. Pyridine-2-aldoxime methochloride, iron(III) chloride, uric acid, dichloromethane, ascorbic acid and potassium sulphate were from Sigma-Aldrich, while graphite powder, potassium dihydrogen phosphate, dipotassium hydrogen

phosphate, and tetrahydrofuran were from Fluka. All chemicals were of analytical grade and were used without further purification. Glucose (Sigma) solutions were left to reach mutarotational equilibrium at room temperature for 24 h before use. Stock solutions of PAM-2 (pbs, pH 7.0) and UA (pbs, pH 4.6) were prepared and ultrapure water was used for the preparation of the buffers and standards.

4. Results and discussion

4.1. Simultaneous determination of APAP and PAP at PEDOT-modified GCE

4.1.1. Background

APAP also known as paracetamol or acetaminophen, is one of the most commonly used drugs in the world. It is the preferred alternative to aspirin, to patients who cannot tolerate aspirin [95]. APAP is an acylated aromatic amide that was first introduced in medicine by Von Mering in 1893 and had been in use as an analgesic for home medication for over 50 years [96]. It has been accepted as an effective drug for the relief of pain and fever in adults and children [97]. PAP, the primary hydrolytic degradation product of APAP, can exist as a synthetic intermediate in pharmaceutical preparations or as a degradation product of APAP. PAP is considered as an impurity for APAP by European Pharmacopoeia (Ph. Eur. 2000) and numerous specifications of manufacturers [98].

Standard usage of APAP has no detrimental effect on the human body but overusage of the drug could lead to some serious side effects such as kidney damage [99] and liver failure [100], while PAP is a substance of modest toxicity and can cause nephrotoxocity and tetragenic effects [101, 102]. Availability of APAP without prescription has increased the use of the compound for self-poisoning [94]. Consequently, it is vital to develop a simple, selective and reliable technique for the determination of APAP and its impurities.

The various methods reported for the determination of APAP and PAP in body fluids and pharmaceutical formulations include spectrophotometry [103, 104], liquid chromatography [105, 106], capillary electrophoresis [107–109], and chemiluminescence [110]. Spectrophotometric and chemiluminescence methods use extraction of the analytes prior to detection, while liquid chromatography and capillary electrophoresis take longer time that hampers the suitability of the methods for routine analysis.

Electrochemical techniques based on chemically modified electrodes have attracted much attention because of their fast response, high sensitivity and selectivity in the determination of trace level of analytes [17]. The use of bare electrode, such as GCE for the electrochemical determination of APAP and its impurities is limited because of the sluggish electron transfer and fouling which result in poor sensitivity, selectivity and reproducibility [111]. Owing to these limitations, various types of chemically modified electrodes have been used for the electrochemical studies of APAP, for example, graphene-modified GCE [112], carbon film resistor electrode [113], carbon-coated nickel magnetic nanoparticles modified electrodes [114], C60-modified GCE [115], multi-walled carbon nanotube (MWCNT) modified basal plane pyrolytic graphite electrode [116], boron-doped diamond electrode [117], carbon ionic liquid electrode [118], carbon–ceramic modified electrodes [119], and polyaniline–MWCNT composite modified electrode [120]. Although these modified electrodes demonstrated good sensitivity, selectivity and low detection limit, none of them has been applied for the simultaneous determination of APAP and its impurities.

The PEDOT-modified electrode has gained interest in a wide range of areas such as the determination of pesticides [121] and phenolic compounds [122]. The modified electrode has been found to show much better results compared to bare GCE and has a lot of potential applications for electroanalytical investigations.

Here the preparation of PEDOT-modified GCE and its application for the simultaneous determination of APAP and PAP are presented [123, 124]. The method offers well-resolved voltammetric responses for APAP and PAP. The response for APAP in the presence of other interferents, such as ascorbic acid, p-nitrophenol and uric acid has also been investigated. The PEDOT-modified electrode was applied for the determination of APAP in tablets and biological samples.

4.1.2. Electropolymerization of EDOT on GCE

The electropolymerization of the EDOT monomer on a GCE was made by running successive cycles between –0.2 V and 1.3 V versus Ag/AgCl/saturated Cl^- at a scan rate of 50 mV s^{-1} as shown in Figure 4.1. The polymerization was carried out from a non-aqueous solution containing 0.1 M Bu_4NBF_4 in acetonitrile. The cyclic voltammograms show the redox peaks that are characteristic for polymer formation [125] and the current increases with each successive cycling, which indicate an enhancement in the film thickness of PEDOT polymer on GC with each cycle. The inset in Figure 4.1 demonstrates the cyclic voltammogram of the PEDOT modified electrode in the phosphate buffer solution without APAP and PAP.

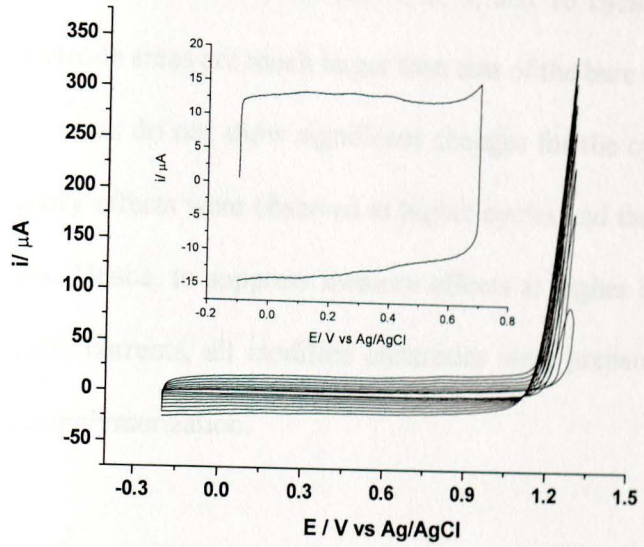

Figure 4.1. Electropolymerization of EDOT at GCE at scan rate 50 mV s^{-1}. Inset: CV of the PEDOT-modified electrode in pbs (pH 7.0)

The redox behavior of $[Fe(CN)_6]^{3-/4-}$ was taken as a molecular probe to obtain the optimum film thickness of PEDOT/GC electrodes. The anodic peak currents for 1.0 mM of $Fe(CN)_6^{3-}$ as a function of the square root of the scan rate is shown in Figure 4.2. Linear responses of the anodic peak currents as function of the square-root of scan rate for both the bare and PEDOT-modified GCEs indicate that the reaction is diffusion-controlled. Hence, the active electrode area was determined based on the expression given in Equation 4.1 for diffusion controlled reactions [3]:

$$i_{pa} = 0.446nFcA(\frac{DnF}{RT})^{\frac{1}{2}}v^{\frac{1}{2}} \qquad (4.1)$$

where n is the number of electron(s) involved in the redox reaction, D is the diffusion coefficient, c is the molar concentration, A is the active electrode area, ν is the scan rate and F, R, and T have their usual meanings.

The active electrode areas of the PEDOT-modified electrode from Eq. (4.1) were found to be 0.111, 0.114, 0.116 and 0.119 cm^2 for 7, 8, 9, and 10 cycles, respectively. The modified active electrode areas are much larger than that of the bare GCE (0.068 cm^2). In addition, the active areas do not show significant changes for the cycles between 7 and 10. However, memory effects were observed at higher cycles and the peak currents were low at lower cycles. Hence, to suppress memory effects at higher cycles and to obtain reasonably high peak currents, all modified electrodes were prepared by running eight cycles during electropolymerization.

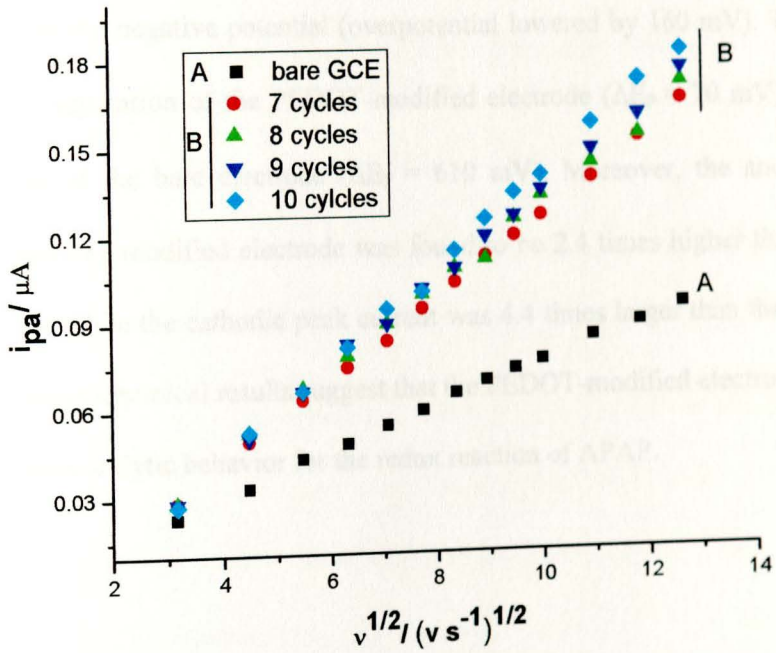

Figure 4.2. Plots of anodic peak current of $Fe(CN)_6^{3-/4-}$ versus square root of scan rates for: A) bare GCE; B) PEDOT-modified electrode for 7, 8, 9, 10 cycle numbers of CV during electropolymerization

4.1.3. Electrochemical behavior of APAP at bare and PEDOT-modified electrodes

The electrochemical response for 1.0 mM APAP at bare and PEDOT-modified GC electrodes was investigated by running cyclic voltammetry at a scan rate of 100 mV s^{-1} (see, Figure 4.3). The E_{pa} and E_{pc} for APAP at bare GC electrode were found to be 574 mV and -34.5 mV, respectively, as depicted in Figure 4.3b. On the other hand, the E_{pa} and E_{pc} values for the PEDOT-modified electrode were 414 mV and 335 mV respectively (see Figure 4.3c). The anodic potential of APAP at the modified electrode shows a substantial shift to the negative potential (overpotential lowered by 160 mV). The peak-to-peak potential separation of the PEDOT-modified electrode (ΔE_p = 70 mV) is much smaller than that of the bare electrode (ΔE_p = 610 mV). Moreover, the anodic peak current of the PEDOT-modified electrode was found to be 2.4 times higher than that of the bare electrode while the cathodic peak current was 4.4 times larger than the bare GC electrode. The electrochemical results suggest that the PEDOT-modified electrode exhibit an excellent electrocatalytic behavior for the redox reaction of APAP.

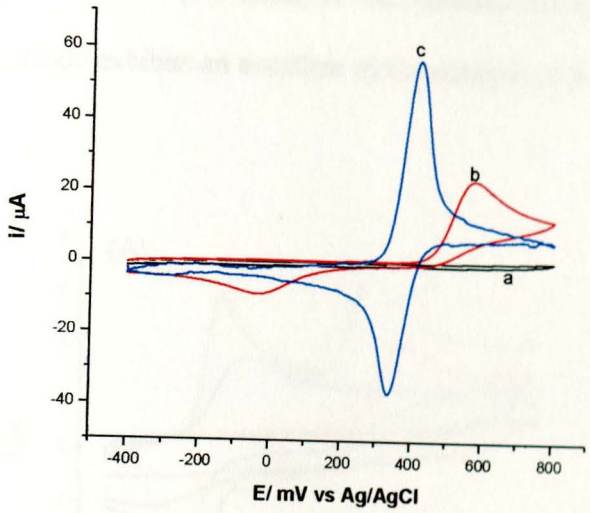

Figure 4.3. CVs obtained at: (a) GC electrode for 0.1 M pbs (pH 7), (b) bare GC for 1 mM APAP (c) PEDOT modified GC electrode with for 1 mM APAP, scan rate 100 mV s^{-1} (background subtracted)

4.1.4. Electrochemical behaviors of APAP and PAP at bare and PEDOT-modified electrodes

In order to investigate the electrocatalytic activity of the PEDOT-modified GCE, CV experiments for APAP and PAP were performed in phosphate buffer pH 7.0. Figure 4.4(A) and (B) depict the cyclic voltammograms of APAP and PAP at bare GCE and PEDOT-modified GCE, respectively. The modified electrode has shown a large capacitive current which could be caused by higher active electrode area of the PEDOT polymer film on the GCE [112]. At the bare GCE, 0.2 mM APAP gives an irreversible behavior with an anodic peak at 540 mV and a small cathodic peak at -10 mV vs. Ag/AgCl (sat'd KCl) while the PEDOT-modified electrode shows a quasireversible reaction. The substantial reduction of overpotential (about 200 mV) and the considerable

enhancement in the peak currents (4-5 times) of the modified electrode suggest that the PEDOT-modified electrode exhibits an excellent electrocatalytic activity (Figure 4.4 and Table 4.1.)

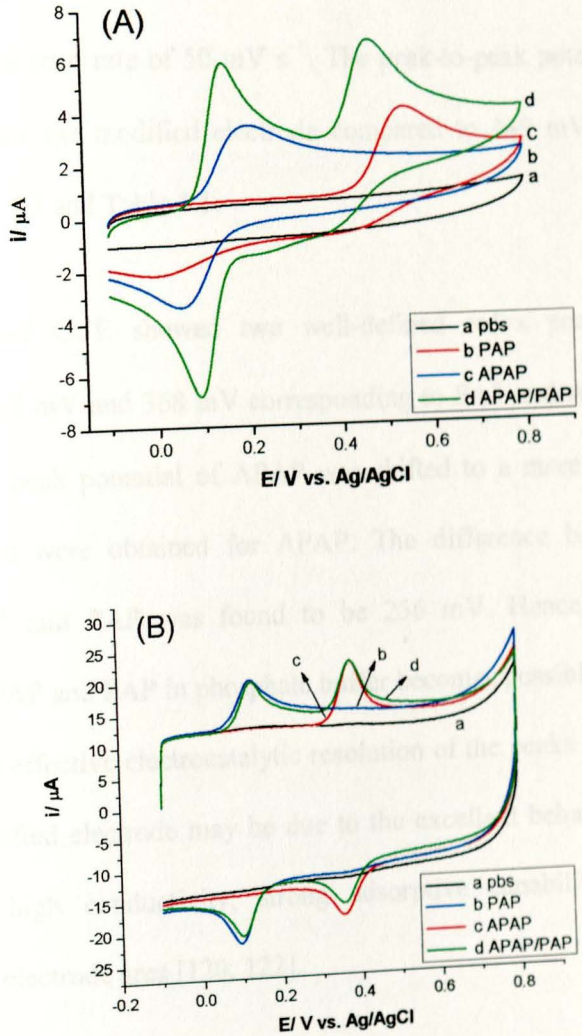

Figure 4.4. CV of (A) bare GCE and (B) PEDOT-modified GCE in a solution containing APAP (0.2 mM) and PAP (0.2 mM), at pH 7.0 pbs with a scan rate of 50 mV s^{-1}. In both CVs: a) pbs, b) PAP, c) APAP, and d) mixture of APAP and PAP

On the other hand, 0.2 mM PAP demonstrates irreversible behavior at the bare GC electrode and shows almost reversible peaks at the PEDOT-modified GCE. The oxidation and reduction peak potentials of PAP at the modified electrode appeared at 129 and 102 mV, respectively, at a scan rate of 50 mV s^{-1}. The peak-to-peak potential separation is lowered to 27 mV for the modified electrode compared to 149 mV for the bare GC electrode; see Figure 4.4 and Table 4.1.

The PEDOT-modified GCE showed two well-defined redox peaks at the formal potentials ($E^{o'}$) of 112 mV and 368 mV corresponding to PAP and APAP, respectively. Since the reduction peak potential of APAP was shifted to a more positive potential, distinct redox peaks were obtained for APAP. The difference between the formal potentials of APAP and PAP was found to be 256 mV. Hence, the simultaneous determination of APAP and PAP in phosphate buffer becomes possible with the PEDOT-modified GCE. The effective electrocatalytic resolution of the peaks for APAP and PAP at the PEDOT modified electrode may be due to the excellent behavior of the PEDOT polymer such as high conductivity, strong adsorptive capability, and significant increment in active electrode area [120, 122].

Table 4.1. The cyclic voltammetric results for APAP and PAP at bare GC and PEDOT-modified GCE.

Parameter	APAP		PAP		Mixture			
					APAP		PAP	
	GC	PEDOT/GC	GC	PEDOT/GC	GC	PEDOT/ GC	GC	PEDOT/ GC
i_{pa} (μA)	4.14	22.5	3.51	19.9	6.76	22.5	5.94	20.2
i_{pc} (μA)	-2.19	-18.1	-3.41	20.1	-	-16.3	-6.82	-22.0
E_{pa} (mV)	543	382	198	129	468	382	151	130
E_{pc} (mV)	-10	354	49	102	-	354	90	93
ΔE_p (mV)	553	28	149	27	-	28	61	37
$E^{o'}$ (mV)	267	368	123	116	-	368	121	112

The effect of scan rate on the electrochemical responses for APAP and PAP was assessed by cyclic voltammetry as shown in Figure 4.5A. The redox peak currents at the modified GCE for APAP and PAP increased linearly with the scan rate in the range 10 to 500 mV s^{-1} (see Figure 4.5B; linear regression equations for APAP: $i_{pa} = 5.201 + 197.59\nu$, R = 0.9968; $i_{pc} = -1.851 - 108.38\nu$, R = 0.9976 and Figure 4.5C; linear regression for PAP: $i_{pa} = 3.772 + 81.64\nu$, R = 0.9952; $i_{pc} = -3.888 - 95.95\nu$, R = 0.9971). The results suggest that the reactions at the modified electrode for both APAP and PAP are surface-confined processes.

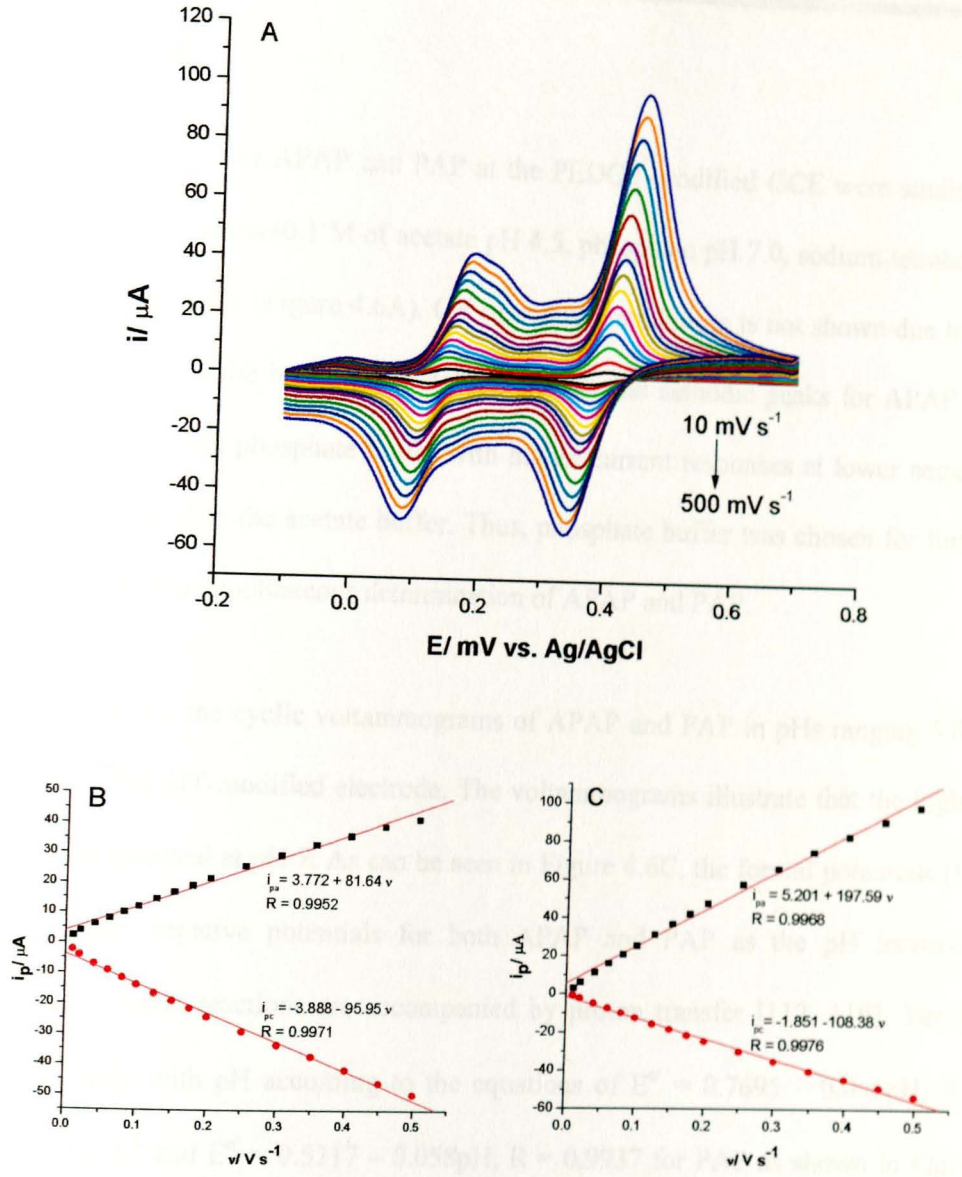

Figure 4.5. (A) CVs of the PEDOT modified GCE for APAP (0.2 mM) and PAP (0.2 mM) in pbs (0.1 M pH 7.0) at scan rates of 10 to 500 mV s^{-1}. The peak currents of (B) PAP and (C) APAP versus scan rates (background subtracted)

4.1.5. Effect of pH

The redox responses for APAP and PAP at the PEDOT-modified GCE were studied in different buffer solutions (0.1 M of acetate pH 4.5, phosphate pH 7.0, sodium tetraborate pH 9.5) by running CV (Figure 4.6A). CV of sodium tetraborate is not shown due to the instability of PAP in the buffer. Well-defined anodic and cathodic peaks for APAP and PAP were obtained in phosphate buffer with higher current responses at lower negative potentials compared to the acetate buffer. Thus, phosphate buffer was chosen for further experiments and the simultaneous determination of APAP and PAP.

Figure 4.6B shows the cyclic voltammograms of APAP and PAP in pHs ranging 5.0 to 9.0 using the PEDOT-modified electrode. The voltammograms illustrate that the highest response was obtained at pH 7. As can be seen in Figure 4.6C, the formal potentials ($E^{o'}$) shifted towards negative potentials for both APAP and PAP as the pH increased, indicating the redox reactions are accompanied by proton transfer [112, 119]. The $E^{o'}$ changed linearly with pH according to the equations of $E^{o'} = 0.7695 - 0.056pH$, $R = 0.9926$ for APAP and $E^{o'} = 0.5317 - 0.058pH$, $R = 0.9937$ for PAP as shown in Figure 4.6C. The slopes of the linear regression equations are close to the ideal 59 mV (Nernstian process: $E = E^{o'} - \frac{0.059m}{n} pH$, where m is number of proton and n is number of electron) for each unit pH change suggesting the same numbers of electrons and protons are involved in the redox reactions for both APAP and PAP. The oxidation of APAP involves the formation of *N*-acetyl-*p*-quinone-imine and a loss of two electrons and two protons as reported previously [126, 127]. Similarly, the oxidation reaction of

PAP proceeds with the formation of *p*-quinone-imine and releasing two electrons and two protons as shown in Eq. 4.2. [127, 128].

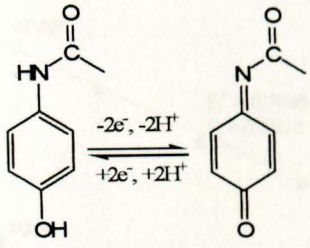

(4.2)

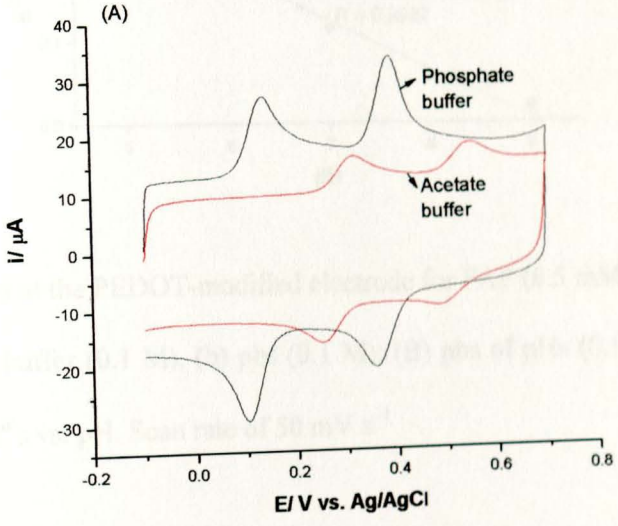

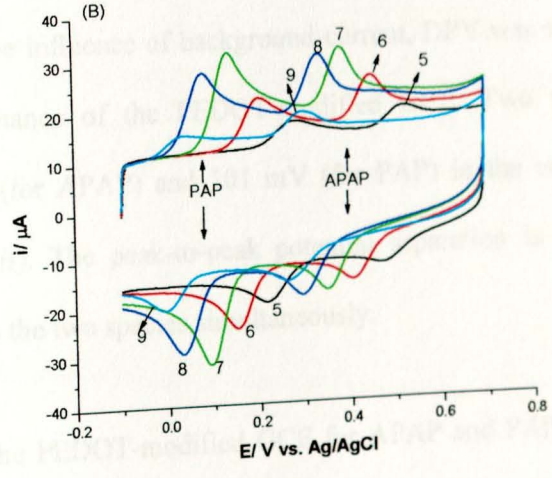

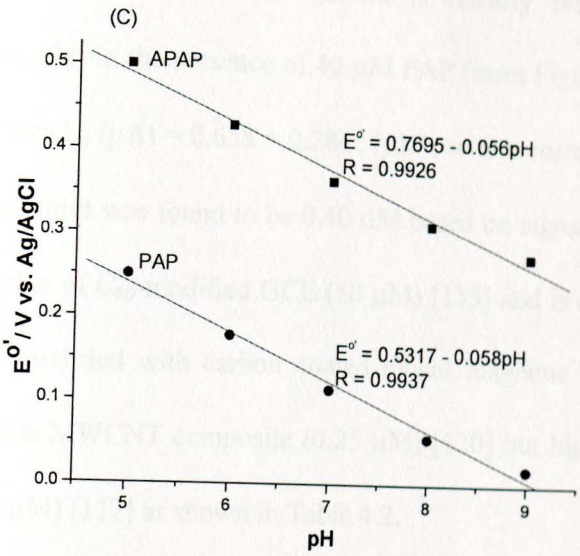

Figure 4.6. (A) CVs at the PEDOT-modified electrode for PAP (0.5 mM) and APAP (0.5 mM) in (a) acetate buffer (0.1 M), (b) pbs (0.1 M); (B) pbs of pHs (0.1 M) of 5, 6, 7, 8 and 9. (C) Plot of $E^{o'}$s vs. pH. Scan rate of 50 mV s^{-1}

4.1.6. Analytical performances of the modified electrode

In order to suppress the influence of background current, DPV was selected to examine the analytical performance of the PEDOT-modified GCE. Two well-defined peaks appeared at 367 mV (for APAP) and 101 mV (for PAP) in the voltammograms; see Figure 4.7 (A) and (B). The peak-to-peak potential separation is 266 mV, which is sufficient to determine the two species simultaneously.

The performance of the PEDOT-modified GCE for APAP and PAP was studied under the optimized conditions. Figure 4.7(A) and (B) show the DPV responses for the APAP and PAP mixture prepared by varying the concentration of either of the analyte while

keeping the other constant. The anodic current is linearly related to the APAP concentration (1–100 μM) in the presence of 40 μM PAP (inset Figure 4.7A). The linear regression equation was i_{pa} (μA) = 0.658 + 0.284c (μM), with a correlation coefficient of 0.9936. The detection limit was found to be 0.40 μM based on signal to noise ratio of 3, which is lower than that of C_{60}-modified GCE (50 μM) [115] and is comparable to those obtained with GCE modified with carbon coated nickel magnetic nanoparticles (0.60 μM) [114], polyaniline-MWCNT composite (0.25 μM) [120] but higher than graphene-modified GCE (0.03 μM) [112] as shown in Table 4.2.

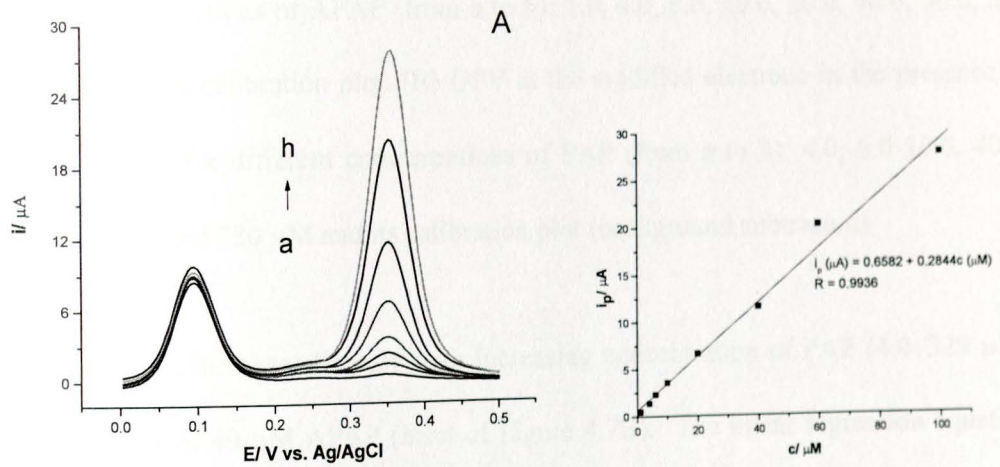

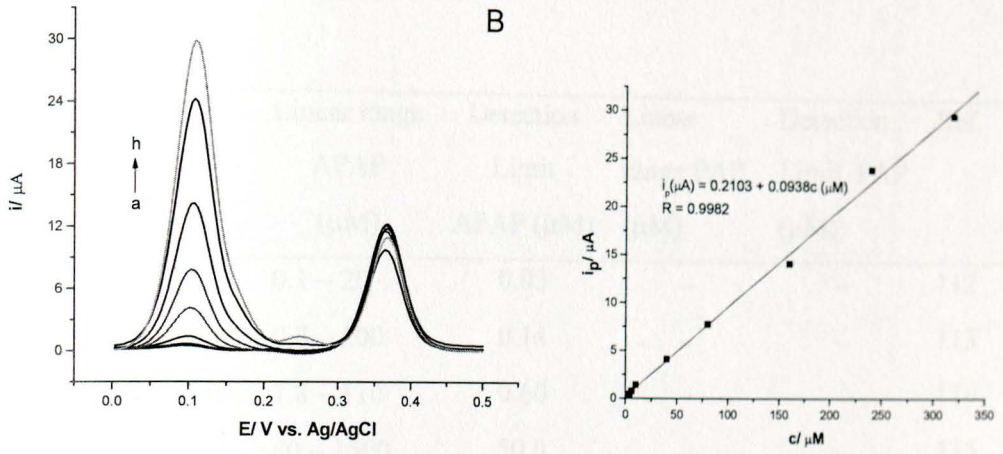

Figure 4.7. A) DPV at the PEDOT-modified GCE in the presence of PAP (40 μM) for different concentrations of APAP (from a to h): 1.0, 4.0, 6.0, 10.0, 20.0, 40.0, 60.0, and 100.0 μM and its calibration plot. (B) DPV at the modified electrode in the presence of APAP (40 μM) for different concentrations of PAP (from a to h): 4.0, 6.0 10.0, 40.0, 80.0, 160, 240, and 320 μM and its calibration plot (background subtracted)

Similarly, the i_{pa} increases linearly with increasing concentration of PAP (4.0–320 μM) in the presence of 40 μM APAP (inset of Figure 4.7B). The linear regression equation was i_{pa} (μA) = 0.210 + 0.094c (μM), with a correlation coefficient of 0.9982. The detection limit was 1.2 μM based on signal to noise ratio of 3. The calibration plots of the modified electrode for PAP with and without APAP show similar sensitivity, indicating the two species do not interfere in the electrochemical response of each other.

Table 4.2. Comparison of some CMEs reported for simultaneous determination of APAP and PAP

Modifier used	Linear range APAP (μM)	Detection Limit APAP (μM)	Linear range PAP (μM)	Detection Limit PAP (μM)	Ref.
Graphene/GCE	0.1 – 20	0.03	–	–	112
Carbon-film resistor	0.8 – 500	0.14	–	–	113
Carbon nickel/GCE	7.8 – 110	0.60	–	–	114
C_{60}/GCE	50 – 1500	50.0	–	–	115
Carbon ionic liquid	1.0 – 200	0.30	–	–	118
Carbon paste ionic liquid electrode	2.0 – 220	0.50	0.3 – 100	0.10	126
Polyaniline-MWCNT/GCE	1.0 – 100	0.25	–	–	120
PEDOT-modified GCE	1.0 – 100	0.40	4.0 – 320	1.2	This work

The reproducibility of four individual PEDOT-modified GCEs for the responses of 40 μM APAP and 40 μM PAP was evaluated and the relative standard deviations (RSD) obtained were 4.8% and 4.3%, respectively. The RSD for five successive determinations of 40 μM APAP and 40 μM PAP with a modified electrode were 2.1% and 1.9%, respectively, which demonstrate a very good repeatability of the performance of the modified electrode.

The inter-day stability of the PEDOT-modified electrode was tested by preparing three modified electrodes and keeping them at 4°C when not in use. The response current for

40 μM APAP was recorded for four consecutive days. The average response was found to be 87 ± 6.4% of the original one at the end of the investigation period.

4.1.7. Interference study

The selectivity of the PEDOT-modified GCE was studied in the presence of different interfering species. Possible interfering substances such as acetylsalicylic acid, saccharine, ascorbic acid, citric acid, sodium carbonate that can exist in pharmaceutical formulations did not interfere in APAP determination.

The interferences of uric acid and *p*-nitrophenol in the determination of APAP and PAP with the modified electrode were investigated by running CV. p-Nitrophenol did not exhibit any peak in the working potential window while uric acid (UA) showed interference as depicted in Figure 4.8. The cyclic voltammograms of a mixture of UA (0.5 mM) and APAP (0.5 mM) exhibited an enhanced peak with a shoulder (Figure 4.8d) by merging the peaks of UA and APAP that appeared at 320 mV (Figure 4.8b) and 390 mV (Figure 4.8c), respectively. The results indicate that the electrochemical response of the modified electrode for APAP and PAP in biological samples is free of interference from p-nitrophenol but suffers from uric acid. However, the interference of uric acid from biological samples can be avoided with ethyl acetate extraction as demonstrated in the urine sample recovery test.

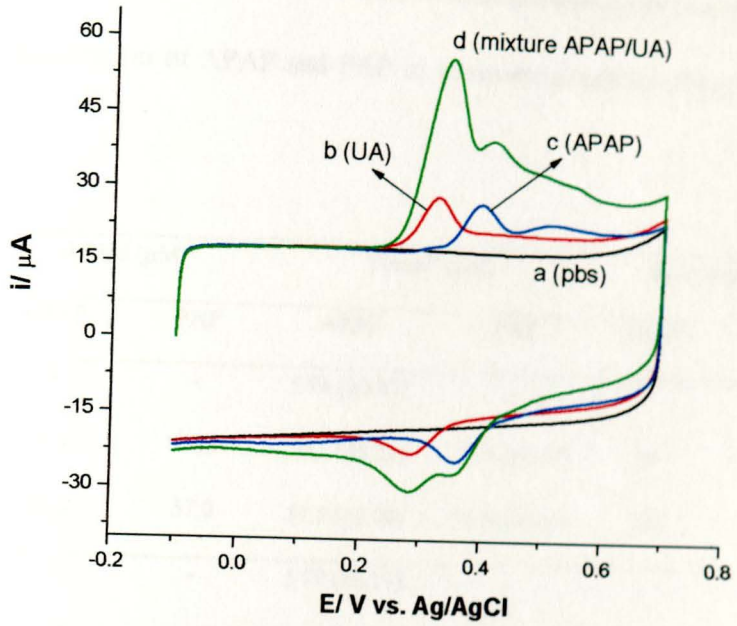

Figure 4.8. CVs at the PEDOT-modified GCE for: a) pbs (pH = 7.0), b) UA (0.5 mM), c) APAP (0.5 mM), d) mixture of UA (0.5 mM) and APAP (0.5 mM), scan rate 50 mV s^{-1}

4.1.8. Analytical application

The method developed was applied for the determination of APAP (500 mg per tablet) and PAP in the tablets to evaluate the validity of the PEDOT-modified GCE. Aliquots obtained by dissolution of APAP tablets were subsequently diluted to get a specified concentration of APAP that lies in the range of the calibration plot and the standard addition method was then employed for recovery tests. The results for APAP and PAP are summarized in Table 4.3.

Table 4.3. Determination of APAP and PAP in commercial tablets using the PEDOT-modified GCE.

Matrix	Added (μM)		Found[a] (μM)		Recovery (%)	
	APAP	PAP	APAP	PAP	APAP	PAP
	-	-	5.94 (±0.07)	-	-	-
Tablet 1	25.0	24.0	30.1 (±0.21)	25.4 (±0.17)	97	106
(EPHARM)	42.0	57.0	51.5 (±0.28)	54.5 (±0.24)	109	96
	-	-	5.79 (±0.11)	-	-	-
Tablet 2	34.0	54.0	41.1 (±0.27)	54.9 (±0.22)	104	102
(PANDOL)	49.0	66.0	58.6 (±0.23)	63.6 (±0.26)	108	96

[a] mean value ± standard deviation (n = 3)

Recovery tests are in the ranges 97% to 109% for APAP and 96% to 106% for PAP. The results show that tablet matrix does not have any interference on the simultaneous determination of the analytes. The amount of APAP in pharmaceutical formulations was found to be 492.0 mg per tablet with 1.6% error, showing a good agreement with the content of APAP given by the manufacturer.

Recovery studies were also carried out for urine sample after intake of APAP. The DPVs of phosphate buffer and urine samples are shown in Figure 4.9. The blank urine samples after dilution with the buffer solution reveal double broad peaks (Figure 4.9b), due to interference from uric acid. Extraction of urine samples with ethyl acetate removes the interferent from the urine sample (Figure 4.9c). A linear calibration plot was obtained for 0-68 μM spiked with APAP with a slope of 0.234 μA μM^{-1}, close to the slope obtained

for standard APAP solutions (0.224 μA μM^{-1}) as depicted in Figure 4.9B. Similar magnitudes in their sensitivity suggest that there is no significant matrix effect in urine sample. The percent recoveries for 26, 47 and 68 μM spiked with APAP into the extracted urine samples were found to be 88%, 109% and 103%, respectively.

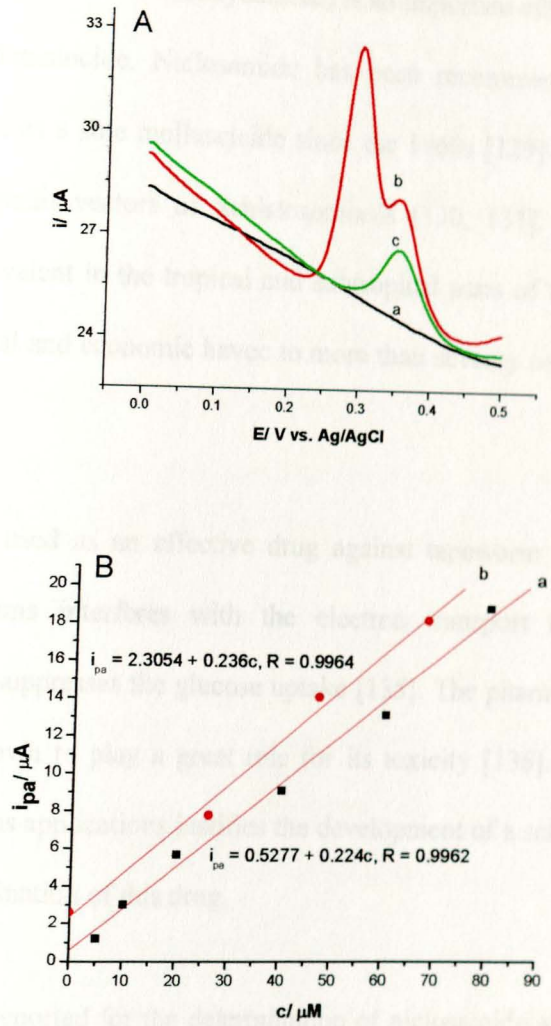

Figure 4.9. (A) DPV for a) pbs, b) unextracted urine sample, and c) extracted urine sample with a scan rate 20 mV s^{-1}. (B) The calibration plots for a) standard APAP and b) spiked urine sample

4.2. Determination of niclosamide at PEDOT-modified GCE

4.2.1. Background

Niclosamide (2′,5-dicloro-4′-nitrosalicylanilide) is an important ethanolamine salt used as molluscicide and nematocide. Niclosamide has been recommended by world health organization (WHO) as a sole molluscicide since the 1960s [129] and is still the choice for the control of snail vectors of Schistosomiasis [130, 131]. Schistosomiasis is a parasitic disease prevalent in the tropical and subtropical parts of the world and next to malaria causing social and economic havoc to more than seventy countries located in the regions [132, 133].

Niclosamide is also used as an effective drug against tapeworm infections [134]. Its activity against worms interferes with the electron transport linked to oxidative phosphorylation and suppresses the glucose uptake [135]. The pharmacokinetic behavior of niclosamide is known to play a great role for its toxicity [136]. The importance of niclosamide for various applications justifies the development of a sensitive and selective method for the determination of this drug.

The various methods reported for the determination of niclosamide are mainly based on high performance liquid chromatography [137, 138] and spectrophotometric methods [139-141]. The chromatographic methods involve laborious and slow derivatization procedures for the modification of niclosamide by various reagents. Prior to spectroscopic detection, the analyte must be complexed to enhance the sensitivity and selectivity of the techniques which hamper the suitability of the method for routine

analysis. Owing to these limitations, the search of an alternative methodology is very essential.

Much attention has currently been paid to electrochemical techniques because of their simplicity, accuracy and sensitivity. Voltammetric methods based on the electrochemical determination of niclosamide at bare GCE [142, 143] have been reported. However, the use of unmodified electrodes suffers from sluggish electron transfer and fouling which result in poor sensitivity and selectivity. In an attempt to improve the sensitivity and to avoid fouling, a method based on the electrochemical reduction of niclosamide at a chemically modified electrode using carbon nanoparticle/chitosan composite has recently been reported [144]. Although this modified electrode demonstrated a very good sensitivity and a low detection limit, a much simpler fabrication method of modified electrode is needed for routine analysis.

A GCE modified with PEDOT for the determination of APAP and its impurities was described in the previous section. It was found that the PEDOT-modified GCE demonstrated a very good electrocatalytic effect with a lower detection limit and improved sensitivity. This important electrochemical behavior of the PEDOT modified electrode is attributed to the high conductivity of the PEDOT and the larger electrode active area as described in section 4.1.2. The electrochemical investigation of niclosamide at the PEDOT-modified GCE using anodic stripping voltammetric technique is here presented [145]. The modified electrode was finally applied to pharmaceutical tablets and urine sample.

4.2.2. Electrochemical behavior of niclosamide at PEDOT-modified electrode

The electrochemical behavior of 0.05 mM niclosamide was investigated at bare and PEDOT-modified GCE in phosphate buffer pH 7.0 at a scan rate of 50 mV s^{-1} (Figure 4.10). The cyclic voltammogram of niclosamide at the modified GCE showed a characteristic irreversible reduction peak (iii_c) at a potential of –0.54 V with no reverse peak. This reduction peak corresponds to a four electron/four proton reaction, producing hydroxylamine (Eq. 4.3), typical of an aromatic nitro-reduction in aqueous solution [142,146]. Then the produced hydroxylamine undergoes a redox reaction with a formal potential of –0.07 V, corresponding to the N-phenylhydroxylamine/nitroso derivative pair (Eq. 4.4) [143,144].

$$R\text{-}NO_2 + 4e^- + 4H^+ \rightarrow R\text{-}NHOH + H_2O \quad (4.3)$$

$$R\text{-}NHOH \leftrightarrows R\text{-}NO + 2e^- + 2H^+ \quad (4.4)$$

where R =

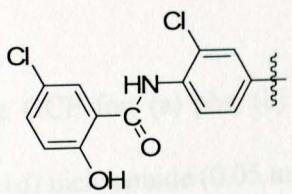

The responses of the PEDOT-modified and bare GCE for redox reaction of niclosamide are compared (Figure 4.10). The cathodic peak at the modified electrode corresponding to the irreversible reduction of the nitrophenyl group of the niclosamide is positively shifted from –0.61 V to –0.54 V, lowering the overvoltage by 70 mV. This peak current at the PEDOT-modified electrode (iii_c) is four times higher than that of the unmodified electrode (i_c). Furthermore, the anodic (iv_a) and cathodic (iv_c) peaks appearing at –0.06 V and –0.08 V, respectively, on the voltammogram (curve d of Figure 4.10) illustrate a

significant increment of the peak currents and more like a reversible behavior of the redox couple compared to the bare GCE. The observed enhancement in the electrochemical behavior of the modified electrode over the bare electrode can be attributed to the increase in the electrode active surface and the high conductivity of the PEDOT film [147,148].

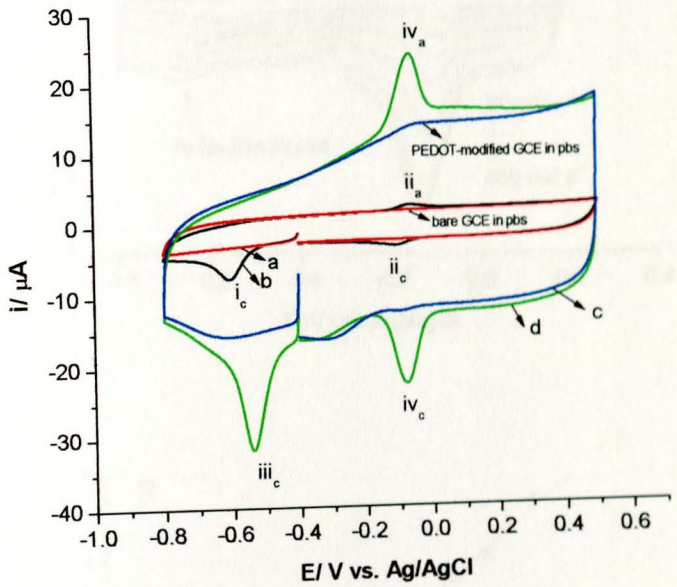

Figure 4.10. CVs at bare GCE for: (a) pbs, (b) niclosamide (0.05 mM), and PEDOT-modified GCE in (c) pbs, (d) niclosamide (0.05 mM) at scan rate of 50 mV s^{-1}

The influence of scan rate on the electrochemical responses for niclosamide was studied by running cyclic voltammetry (Figure 4.11). The logarithm of the irreversible reduction peak currents (log i_p) shown in the cyclic voltammograms (arrow indicated in Figure 4.11) linearly increased with the logarithm of scan rate (log ν) in the range 20–200 mV s^{-1} with a linear regression equation: $\log i_{pc} = -0.255 + 0.765 \log \nu$ and $R^2 = 0.9977$.

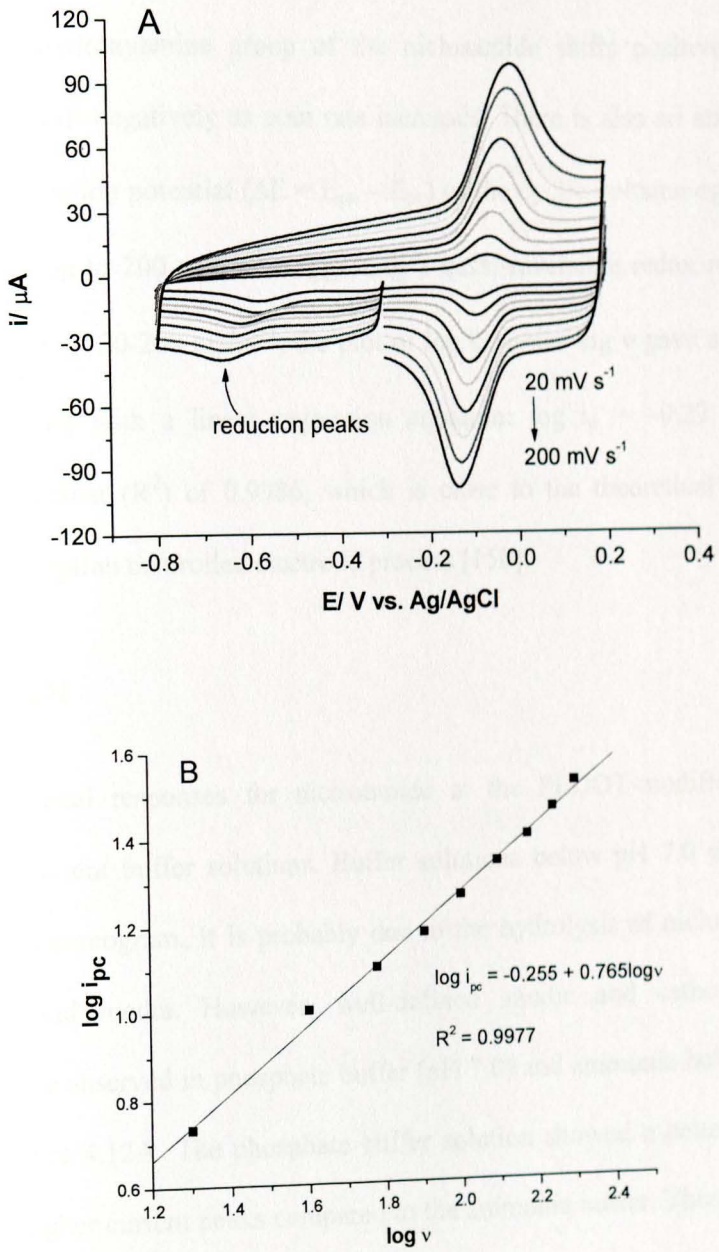

Figure 4.11. (A) CVs of niclosamide (0.05 mM) in pbs of pH 7.0 at the PEDOT-modified GCE for different scan rates: 20, 40, 60, 80, 100, 125, 150, 175 and 200 mV s^{-1}. (B) Plot of log i_p *versus* log ν

The cyclic voltammograms (on the right side of Figure 4.11) demonstrates that the oxidation phenylhydroxyamine group of the niclosamide shifts positively while the reduction peaks shift negatively as scan rate increases. There is also an enhancement of peak-to-peak separation potential ($\Delta E = E_{pa} - E_{pc}$) of the cyclic voltammogram recorded for the scan rate up to 200 mV s^{-1}, suggesting a quasi-reversible redox reaction [149]. With the scan rate of 20-200 mV s^{-1}, the plot of log i_p *versus* log ν gave a slope of 0.99 (see Figure 4.11B) with a linear regression equation: log i_p = –0.27 + 0.99log ν, correlation coefficient (R^2) of 0.9986, which is close to the theoretical value of 1.0, expected for adsorption controlled electrode process [150].

4.2.3. Effect of pH

The electrochemical responses for niclosamide at the PEDOT-modified GCE were examined in different buffer solutions. Buffer solutions below pH 7.0 did not show a good cyclic voltammogram. It is probably due to the hydrolysis of niclosamide and its instability in acid media. However, well-defined anodic and cathodic peaks for niclosamide were observed in phosphate buffer (pH 7.0) and ammonia buffer (pH 9.2) as depicted in Figure 4.12A. The phosphate buffer solution showed a better voltammetric response with higher current peaks compared to the ammonia buffer. Thus, the phosphate buffer was chosen for further studies.

The effect of pH on the anodic stripping peak current for 5 μM niclosamide at the PEDOT-modified GCE was investigated. Figure 4.12B exhibits the differential pulse anodic stripping voltammetric (DPASV) peak current for niclosamide at different pH in

the range 6.2–8.6. Lower anodic stripping peak currents were observed in acidic media due to the instability of niclosamide in the medium. The anodic stripping peak current of niclosamide decreased with increasing pH in basic media. The optimum voltammetric response was observed at pH 7.0, and hence, pH 7.0 was chosen for subsequent experiments.

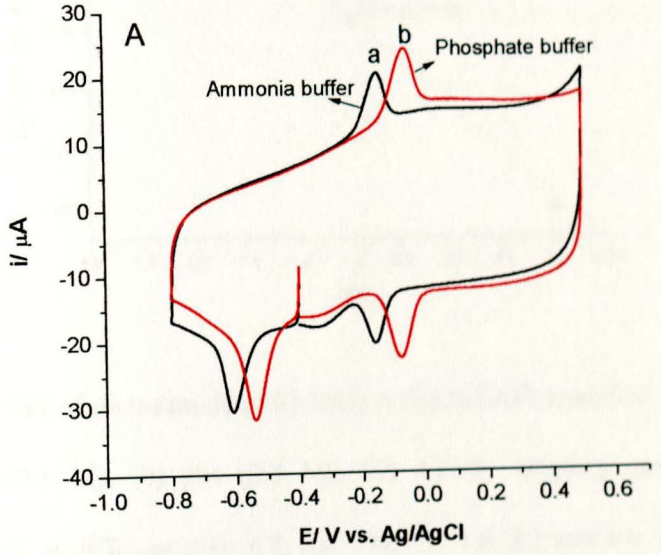

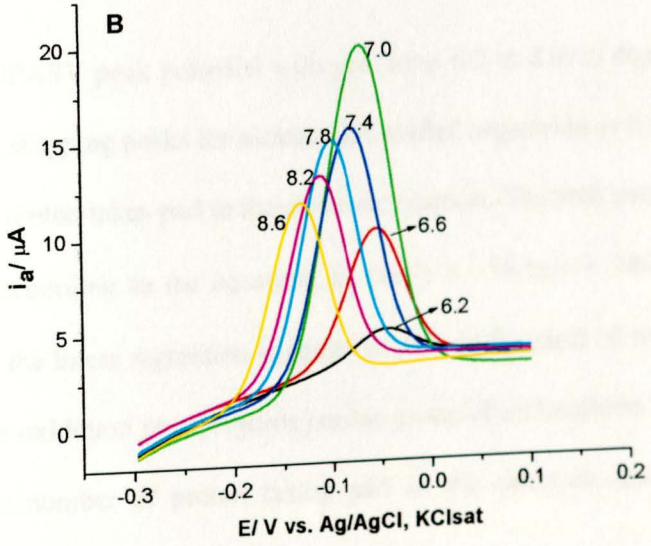

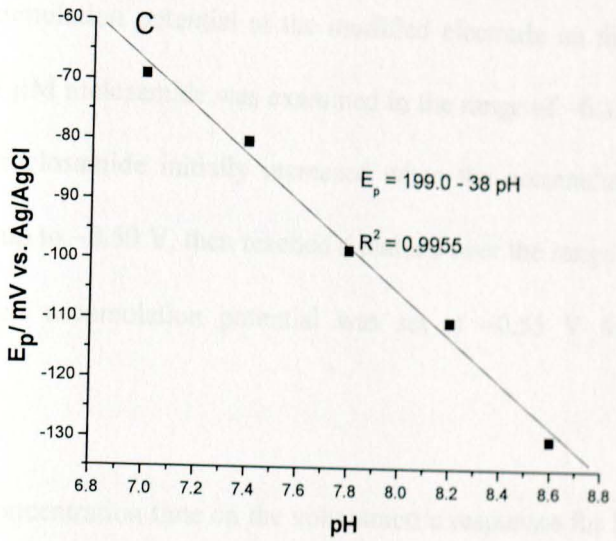

Figure 4.12. (A) CVs of niclosamide (0.05 mM) at the PEDOT-modified electrode in (a) ammonia buffer (0.1 M), (b) pbs (0.1 M); (B) Anodic stripping peak currents of niclosamide (5 μM) at different pHs: 6.2, 6.6, 7.0, 7.4, 7.8, 8.2 and 8.6. (C) The plot of Ep versus pH. Scan rate: 50 mV s^{-1}

The variation of DPASV peak potential with pH (from 6.2 to 8.6) is depicted in Figure 4.12C. The anodic stripping peaks for niclosamide shifted negatively as the pH increased, indicating that the proton takes part in the electrode reaction. The peak potentials changed linearly with pH according to the equation: E_p (mV) = –36.3pH + 185; R^2 = 0.9955. Since the slope of the linear regression equation is close to the ideal 30 mV for each unit pH change and the oxidation phenylhydroxyamine group of niclosamide involves loss of two electrons, the number of proton taking part in the electrode reaction is one as reported previously [143].

4.2.4. Accumulation potential and preconcentration time

The effect of accumulation potential at the modified electrode on the anodic stripping peak current for 5 μM niclosamide was examined in the range of –0.35 to –0.70 V. The peak current for niclosamide initially increased when the accumulation potential was increased sharply up to –0.50 V, then reached a plateau over the range –0.55 to –0.70 V. Thus, the optimum accumulation potential was set at –0.55 V for the subsequent experiments.

The effect of preconcentration time on the voltammetric responses for 5 μM niclosamide at a potential of –0.55 V was also investigated. The peak currents increased up to 80 s and then after the preconcentration time showed no significant change in the peak current. Hence, for all subsequent measurements, a preconcentration time of 80 s was employed.

4.2.5. Analytical performance of the modified electrode

To verify the linear relationship between the anodic stripping peak current and niclosamide concentration, a calibration curve was constructed under the optimum conditions in 0.1 M phosphate buffer solution (pH 7.0). Figure 4.13 shows differential pulse anodic stripping voltammograms obtained at the PEDOT-modified GCE for various concentrations of niclosamide. A linear range from 0.075 to 7.5 μM was obtained, with a linear regression equation of i_p (μA) = 5.04c (μM) + 1.76; R^2 = 0.9942 (see Figure 4.13B). The sensitivity of the PEDOT-modified GCE was 5.04 μA μM^{-1} which is lower

than the composite modified electrode 48.8 μA μM^{-1} [144] but better than that of the bare GCE 0.286 μA μM^{-1} [142]. Moreover, the detection limit was found to be 0.01 μM based on signal to noise ratio of 3, which is much better than that of bare GCE (4.5 μM) [142] and is comparable to that obtained with carbon nanoparticles/chitosan modified GCE (7.7 nM) [144].

The reproducibility of three individual PEDOT-modified GCEs for the responses of 2 μM niclosamide was evaluated and the relative standard deviation (RSD) obtained was 4.1%. The RSD for five successive determinations of 2 μM niclosamide with a modified electrode was 1.7%, which indicates a very good repeatability. In addition, the inter-day stability of the PEDOT-modified electrode was tested by preparing three modified electrodes and keeping them at ambient condition when not in use. The response current for 2 μM niclosamide was recorded for four consecutive days. The average response was found to be 93±3.8% of the original one at the end of the investigation period.

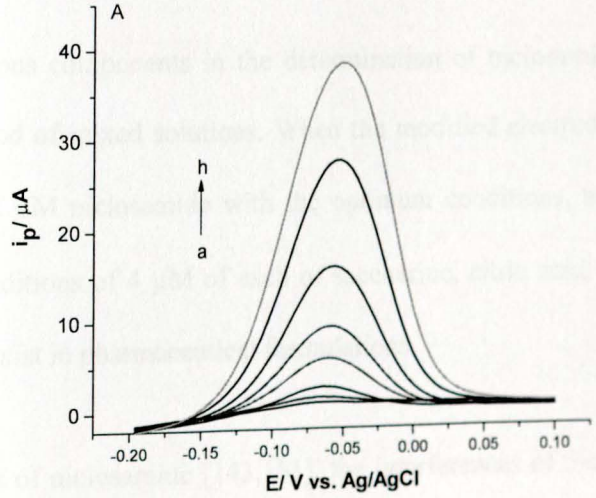

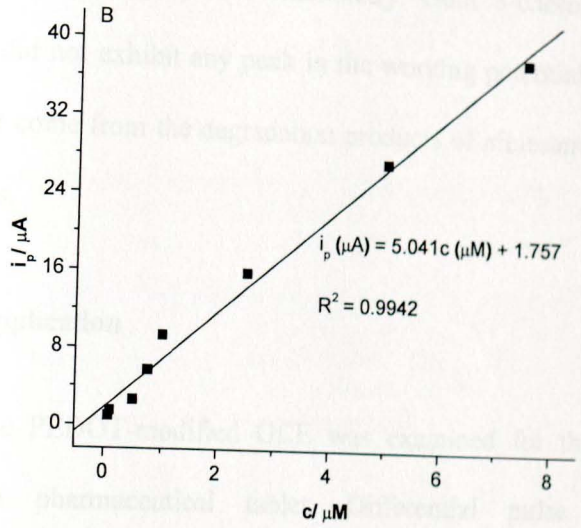

Figure 4.13. (A) Anodic stripping curves of niclosamide at PEDOT-modified GCE in phosphate buffer (pH = 7.0) by DPASV for different concentrations of analyte: (a) 0.075, (b) 0.1, (c) 0.5, (d) 0.75, (e) 1.0, (f) 2.5, (g) 5.0, and (h) 7.5 μM, background current subtracted. (B) Calibration plot for niclosamide using DPASV technique

4.2.6. Interference study

The effect of various components in the determination of niclosamide was studied by applying the method of mixed solutions. When the modified electrode was used for the determination of 2 μM niclosamide with the optimum conditions, no interference was encountered for additions of 4 μM of each of saccharine, citric acid, starch and sodium carbonate that co-exist in pharmaceutical formulations.

Due to degradation of niclosamide [143,151], the interferences of 5-cholorsalicylic acid and aminoniclosamide in the determination of niclosamide with the modified electrode

were investigated by running cyclic voltammetry. Both 5-cholorsalicyclic acid and aminoniclosamide did not exhibit any peak in the working potential window, indicating no interference that come from the degradation products of niclosamide as demonstrated in the recovery tests.

4.2.7. Analytical application

Applicability of the PEDOT-modified GCE was examined for the determination of niclosamide in a pharmaceutical tablet. Differential pulse anodic stripping voltammograms were obtained by adding appropriate standard solutions to diluted solutions under the optimized conditions as described earlier. The recovery results for niclosamide are summarized in Table 4.4. The recoveries were acceptable, indicating that the modified electrode could be effectively used for the determination of trace amounts of niclosamide in pharmaceutical formulations. Besides, the mean value of niclosamide in pharmaceutical formulations was found to be 493.6 mg/tablet with 1.3% error, showing a good agreement with the content of niclosamide declared by the manufacturer (500 mg/tablet).

Recovery tests were also carried out for urine sample to ensure the reliability of the electrochemical method. An aliquot of urine sample from a healthy person was collected. A certain amount of niclosamide was added into 25 mL of the urine (the concentration is 15 μM) and then 2.5 mL of this urine sample was diluted to 100 mL with phosphate buffer solution (pH 7.0). The procedure was repeated for pure phosphate buffer solution containing the same amount of niclosamide (0.38 μM) as that of the urine. Then, the

niclosamide concentration in the urine was determined using the proposed method by multiple standard additions.

Table 4.4. Determination of niclosamide in commercial tablets using the PEDOT-modified GCE

Sample	Added (μM)	Found[a] (μM)	Recovery (%)
Tablet (AFP)	-	0.8 (±0.1)	-
	1.2	1.9 (±0.2)	95
	3.0	3.9 (±0.2)	105
	4.8	5.5 (±0.2)	99

[a] mean value ± standard deviation (n = 3)

Differential pulse anodic stripping voltammograms were obtained by spiking 100, 200 and 300 μL of 300 μM niclosamide to the 25 mL of urine sample and 25 mL of phosphate buffer solution (pH 7.0), see Figure 4.14(A) and (B). In these investigations, the slopes of the plots for the variation of the anodic stripping peak current *versus* volume standard added were 39.2 μA mL^{-1} (R^2 = 0.9914) in phosphate buffer solution (inset Figure 4.14A) and 39.3 μA mL^{-1} (R^2 = 0.9901) in the urine sample (inset Figure 4.14B). The results provided a very good recovery for the niclosamide added to the urine sample (94%) indicating the complex matrix in urine did not interfere with the voltammetric determination of niclosamide.

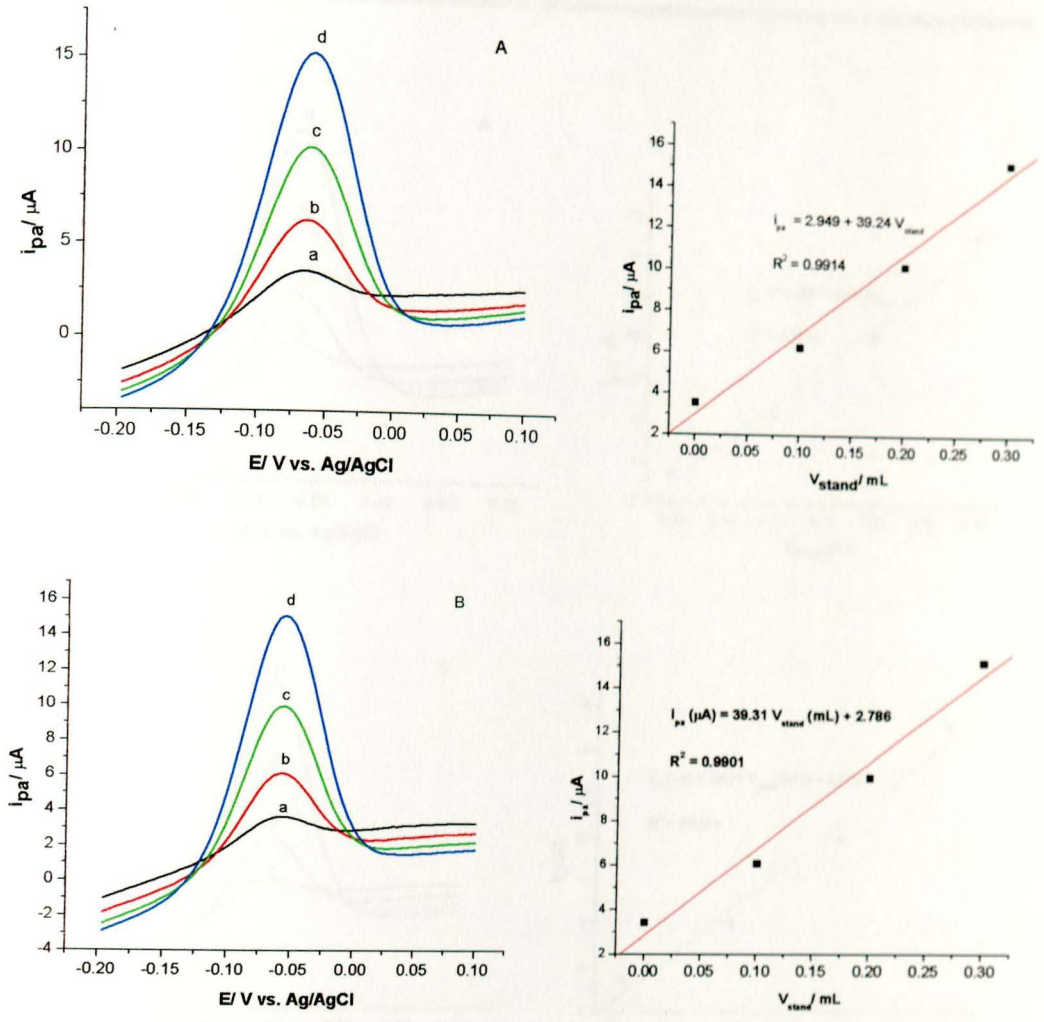

Figure 4.14. Anodic stripping voltammetric responses for 0.38 µM niclosamide in 25 mL of (A) pbs and (B) urine sample; spiked with 300 µM niclosamide of (a) 0, b) 100 µL, (c) 200 µL and (d) 300 µL

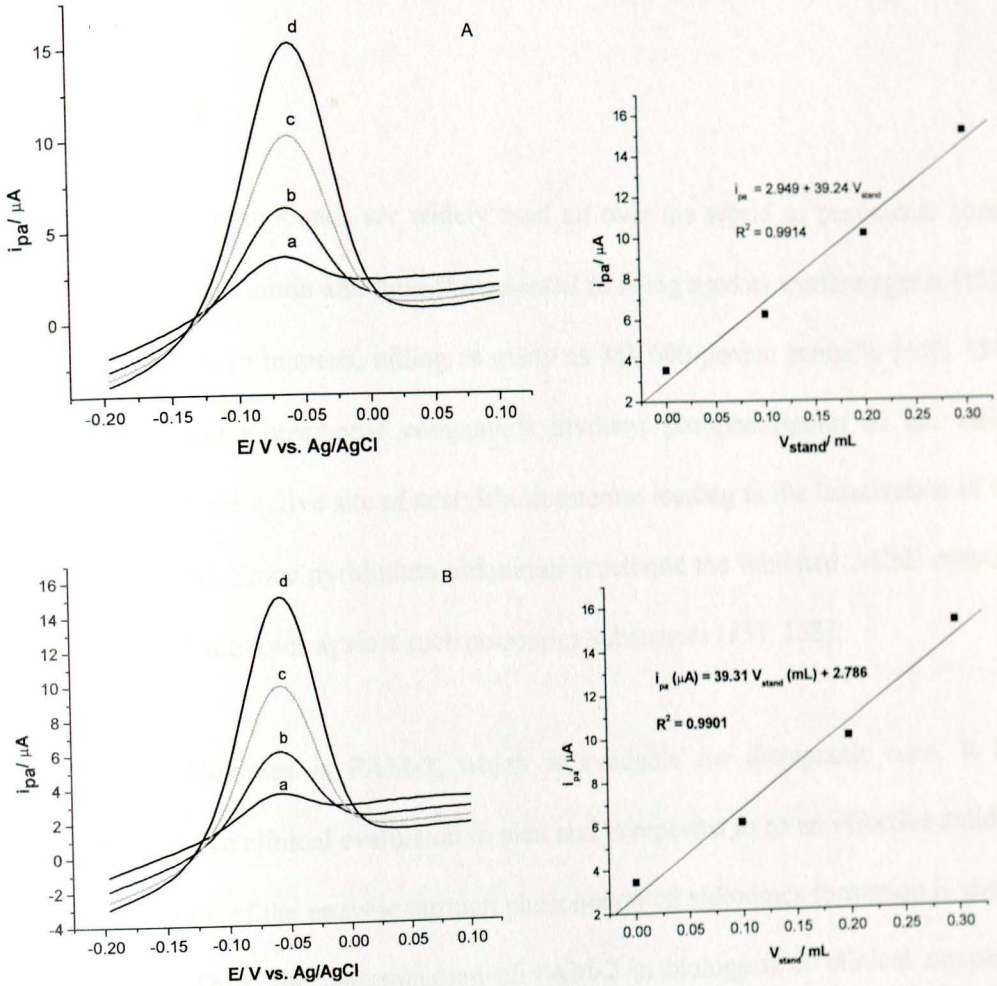

Figure 4.14. Anodic stripping voltammetric responses for 0.38 µM niclosamide in 25 mL of (A) pbs and (B) urine sample; spiked with 300 µM niclosamide of (a) 0, b) 100 µL, (c) 200 µL and (d) 300 µL

4.3. Stripping voltammetric determination of PAM-2 at $Fe^{3+}Y$ modified GCE

4.3.1. Background

Organophosphorus compounds are widely used all over the world as pesticides. Some, like sarin, soman, and tabun also have the potential of being used as warfare agents [152]. They are poisonous to humans, killing as many as 350,000 people annually [153, 154]. Poisoning by organophosphorus compounds involves phosphorylation of the serine hydroxyl group in the active site of acetylcholinesterase leading to the inactivation of the enzyme [155, 156]. Since pyridinium aldoximes reactivate the inhibited AChE enzyme, they are potential antidotes against such poisonous substances [157, 158].

One of these aldoximes is PAM-2, which is available for therapeutic uses. It has undergone extensive clinical evaluation in men and is reported to be an effective antidote [157]. Reactivation of the enzyme through phosphorylated aldoximes formation is shown in Scheme 4.1. Thus, the determination of PAM-2 in biological or clinical sample is indispensable for monitoring its pharmaceutical use to those patients who suffer from self-poisoning of organophosphorus compounds or from poisoning of nerve gases.

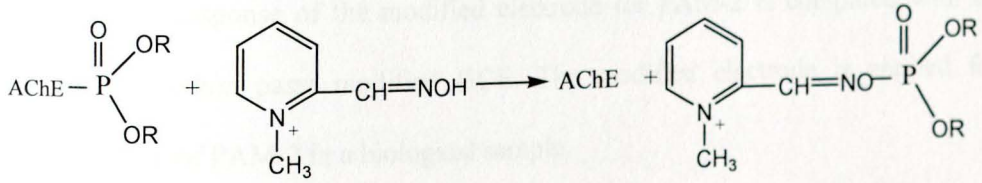

Scheme 4.1. Reactivation of phosphorylated AChE by PAM-2 through phosphorylated aldoxime formation

Various methods have been reported for the determination of PAM-2, including high performance liquid chromatography [159-161] and spectrophotometric methods [162]. Chromatographic methods involve laborious and sophisticated procedures. Similarly, spectroscopic detection requires complex formation to enhance the sensitivity and selectivity of the technique which hamper its suitability for routine analysis. Hence, the development of a simple, sensitive and selective technique for the determination of PAM-2 is of enormous importance. In this regard, electrochemical method is one choice to address such issue.

Only few voltammetric methods based on poly(*p*-toluene sulfonic acid) modified GCE [163] and multiwalled carbon nanotube modified platinum electrode [164] have recently been reported for the determination of PAM-2. Although these modified electrodes showed good linear range, important analytical parameters such as stability and sensitivity of the methods were not reported.

In this section, the development of stripping voltammetric method for the determination of PAM-2 at $Fe^{3+}Y$ modified GCE is presented [165]. The electrochemical behavior of the modified electrode was studied under different conditions. In addition, the voltammetric response of the modified electrode for PAM-2 is compared with that of zeolite-free carbon paste modified GCE. The modified electrode is applied for the determination of PAM-2 in a biological sample.

4.3.2. Electrochemical behavior of PAM-2 at the modified electrode

Cyclic voltammetry was run between 1.0 V and −0.2 V for five cycles in 0.25 M H_2SO_4 solution followed by rinsing the modified electrode with pure water. After a potential scan was made in the same potential window for several cycles in 0.3 M K_2SO_4 solution, the acid treated modified electrode was stabilized by running CV in 0.3 M KH_2PO_4 solution.

When CV of the modified electrode was successively run in sulfuric acid for five cycles at scan rate of 50 mV s^{-1}, increments in peak currents of ferric/ferrous redox couple and narrower peak-to-peak separations were observed as shown in Figure 4.15 (broken lines). Solid line in Figure 4.15 shows the cyclic voltammogram of the $Fe^{3+}Y$ modified electrode in 0.3 M K_2SO_4 at a scan rate 50 mV s^{-1}.

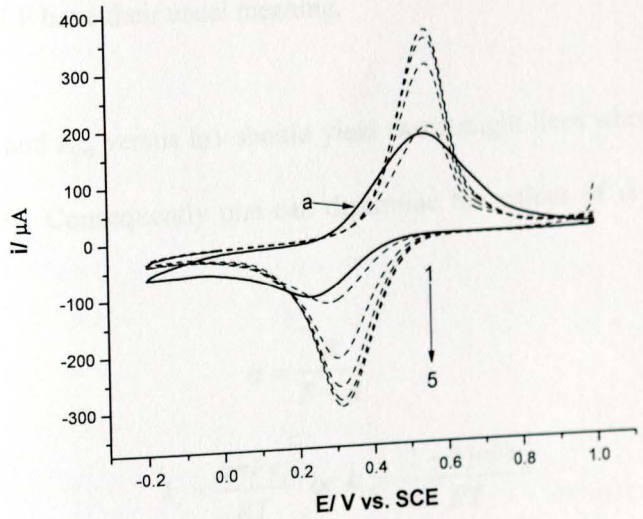

Figure 4.15. CVs of the $Fe^{3+}Y$ modified electrode without acid treatment (solid line) and with acid treatment for five successive cycles (broken line)

In order to demonstrate the difference in the electrochemical behavior of the sulfuric acid treated and untreated $Fe^{3+}Y$ modified electrode, the electrode kinetics was investigated by Laviron's approach [166, 167] which attempts to determine the electron-transfer coefficient (α) and the heterogeneous electron transfer kinetics constant (k_s). In this approach, the cathodic (E_{pc}) and anodic (E_{pa}) peak positions at different scan rate (ν) are expressed as

$$E_{pc} = E^{o'} - A\ln\frac{\alpha}{m} - A\ln\nu \tag{4.5}$$

$$E_{pa} = E^{o'} + B\ln\frac{1-\alpha}{m} + B\ln\nu \tag{4.6}$$

where $E^{o'}$ is the formal potential and

$$A = \frac{RT}{\alpha nF}, \qquad B = \frac{RT}{(1-\alpha)nF} \qquad \text{and } m = \frac{nF}{k_s RT}$$

where R, T, n and F have their usual meaning.

Thus, plot of E_{pc} and E_{pa} versus $\ln\nu$ should yield two straight lines whose slopes are –A and B respectively. Consequently one can determine the values of α and k_s from the equation:

$$\alpha = \frac{B}{B-A} \tag{4.7}$$

$$k_s = \frac{\alpha nF\nu_c}{RT} \text{ or } k_s = \frac{(1-\alpha)nF\nu_a}{RT} \tag{4.8}$$

where ν_c and ν_a are the cathodic and anodic scan rates at $E_p = E^{o'}$, respectively.

The above approach is valid only for irreversible reactions of electroactive species. This can be approximated experimentally when the peak-to-peak potential separation (ΔE_p) is greater than or equal to 200/n mV. Figure 4.16 (A) and (B) show the linear relationship between peak potentials of the untreated and the H_2SO_4 treated modified electrode and the natural logarithm of scan rates (ln v). The linear regression equations for the untreated modified electrode are: $E_{pa} = 230 + 78.7 \ln v$; $R^2 = 0.9987$ and $E_{pc} = 596 - 94.9 \ln v$; $R^2 = 0.9980$ (Figure 4.16A), and for the treated one are: $E_{pa} = 146 + 55.6 \ln v$; $R^2 = 0.9959$ and $E_{pc} = 596 - 79.1 \ln v$; $R^2 = 0.9975$ (Figure 4.16B). Using the above equations, α and k_s values were found to be 0.44 and 0.62 s^{-1} for the untreated $Fe^{3+}Y$ modified GCE, respectively. In contrast, α and k_s were 0.42 and 2.36 s^{-1}, respectively, for the acid treated modified electrode. This rapid response of the modified electrode after acid treatment can be attributed to the lower hydrophobic character of the polymer binder at the modified film which causes sluggish electrochemical behavior [41,168].

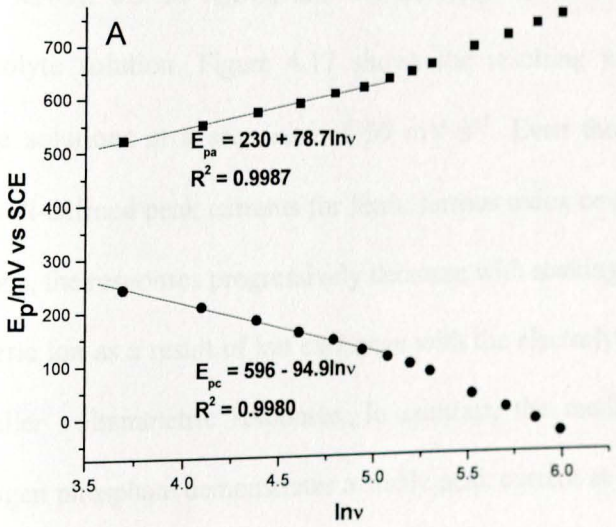

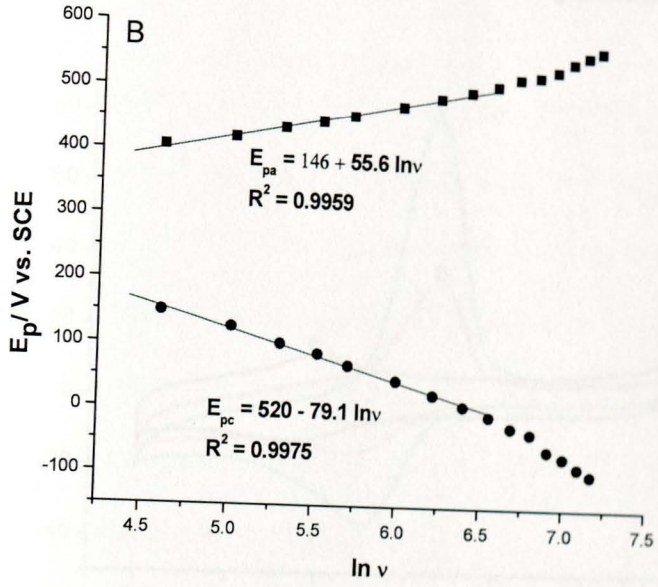

Figure 4.16. Plot of peak potentials versus ln ν for: (A) acid untreated $Fe^{3+}Y$ modified GCE and (B) acid treated $Fe^{3+}Y$ modified GCE

Voltammetric responses of the $Fe^{3+}Y$ modified electrode were tested in different solutions (0.3 M KNO_3, 0.3 M K_2SO_4 and 0.3 M KH_2PO_4) in order to obtain the appropriate electrolyte solution. Figure 4.17 shows the resulting voltammograms of various electrolyte solutions at a scan rate of 50 mV s^{-1}. Even though the modified electrode shows well-defined peak currents for ferric/ferrous redox couple in both KNO_3 and K_2SO_4 solutions, the responses progressively decrease with soaking time. Continuous leaching out of ferric ion as a result of ion exchange with the electrolyte cations leads to unstable and smaller voltammetric responses. In contrast, the modified electrode in potassium dihydrogen phosphate demonstrates a stable peak current at a formal potential of 160 mV, see curve a in Figure 4.17. In addition, there was no continuous depletion of ferric/ferrous ions at the electrode surface with soaking time, probably due to the

coordination of the metal ions with phosphate ion. For this reason potassium dihydrogen phosphate electrolyte solution was selected for subsequent experiments.

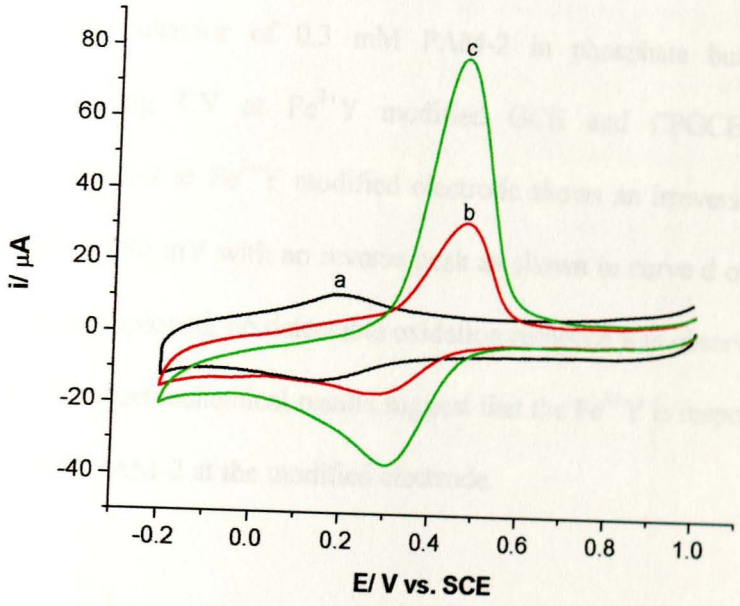

Figure 4.17. Cyclic voltammetric responses of $Fe^{3+}Y$ modified electrode in 0.3 M electrolyte solutions: a) KH_2PO_4, b) KNO_3 and c) K_2SO_4

4.3.3. Electrochemical behavior of PAM-2 at the modified electrode

Two types of zeolite such as faujasite (NaY) and natural zeolite were screened to find the best modifier for the determination of PAM-2. A voltammetric peak for 0.3 mM PAM-2 was observed at $Fe^{3+}Y$ modified electrode (curve d in Figure 4.18). In contrast, no voltammetric peak current appeared on the cyclic voltammogram for the same solution at the iron doped natural zeolite modified GCE. This might be due to the larger pore aperture of faujasite Y type of zeolite to incorporate PAM-2 into its structure and preconcentrate it at the modified layer and give a voltammetric response where as the

smaller pore size of the natural zeolite prevents the preconcentration of the PAM-2 molecule.

The electrochemical behavior of 0.3 mM PAM-2 in phosphate buffer was also investigated by running CV at $Fe^{3+}Y$ modified GCE and CPGCE. The cyclic voltammogram of PAM-2 at $Fe^{3+}Y$ modified electrode shows an irreversible oxidation peak at a potential of 686 mV with no reverse peak as shown in curve d of Figure 4.18. When the CPGCE is employed, no detectable oxidation response was observed, see curve b in Figure 4.18. The electrochemical results suggest that the $Fe^{3+}Y$ is responsible for the catalytic oxidation of PAM-2 at the modified electrode.

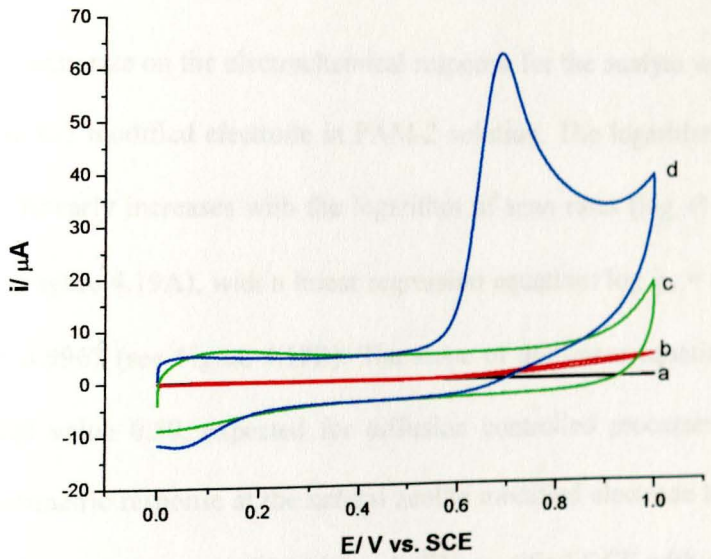

Figure 4.18. CVs at: a) CPGCE without PAM-2, b) CPGCE with 0.3 mM PAM-2, c) $Fe^{3+}Y$ modified GCE without PAM-2 and d) $Fe^{3+}Y$ modified GCE with 0.3 mM PAM-2

This can be explained by considering two kinds of mechanisms [41,169-173]: the first is intrazeolitic in which electroactive species carry out electron transfer inside the zeolite structure, and the second is extrazeolitic that involves the exchange of ions of the electroactive species for the electrolytic cations prior to electron transfer reaction. PAM-2 is a salt which exist as cationic form in phosphate buffer solution pH 7.0. The incorporation of cationic PAM^+ into the faujasite Y zeolite results in preconcentration of the PAM^+ prior to voltammetric determination. This leads to an enhanced electrochemical response when the soaking time of the $Fe^{3+}Y$ modified GCE in the PAM-2 solution increases.

The influence of scan rate on the electrochemical response for the analyte was studied by CV after soaking the modified electrode in PAM-2 solution. The logarithm of the peak currents ($\log i_p$) linearly increases with the logarithm of scan rates ($\log \nu$) in the range 20–200 mV s^{-1} (Figure 4.19A), with a linear regression equation: $\log i_{pa} = 0.64 + 0.538 \log \nu$, and $R^2 = 0.9967$ (see Figure 4.19B). The slope of the linear equation (0.538) is close to the ideal value 0.50, expected for diffusion controlled processes [150]. The absence of voltammetric response at the natural zeolite modified electrode together with enhancement of the peak currents of PAM-2 at $Fe^{3+}Y$ modified GCE with soaking time suggests that the electron transfer reaction be an intrazeolitic mechanism [41].

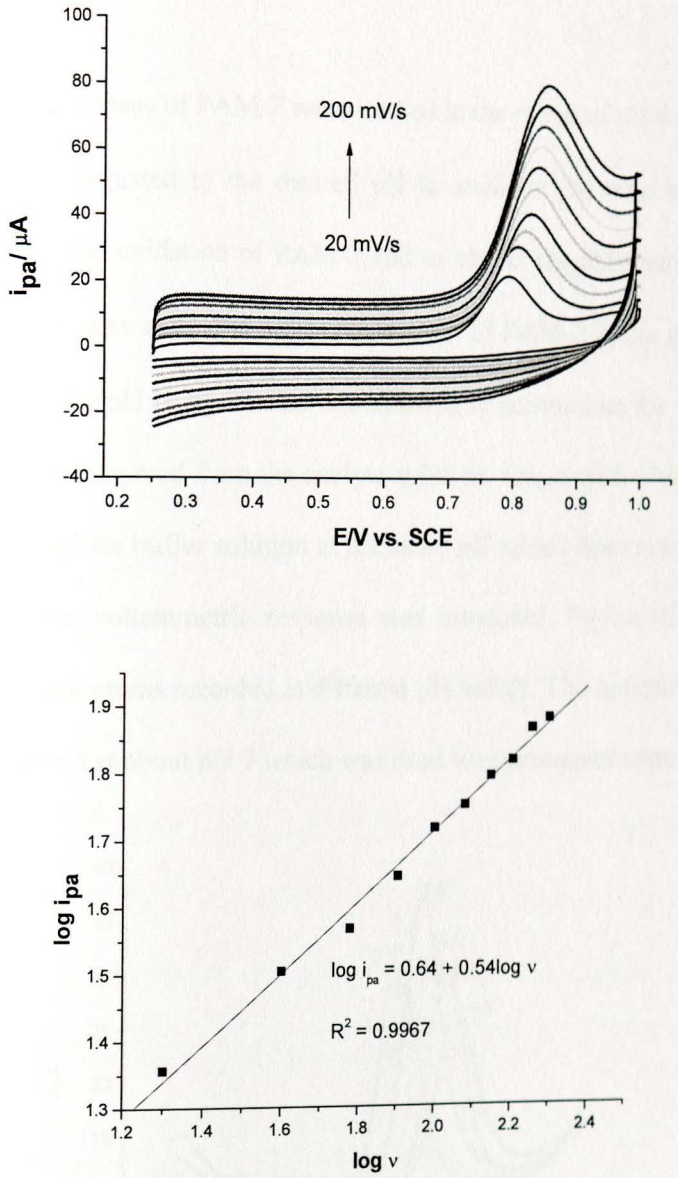

Figure 4.19. (A) CVs of PAM-2 (50 μM) in phosphate buffer solution pH 7.0 at $Fe^{3+}Y$ modified electrode for scan rates: 20, 40, 60, 80, 100, 120, 140, 160, 180, and 200 mV s^{-1}. (B) Plot of log i_p *versus* log ν

4.3.4. Effect of pH

The voltammetric responses of PAM-2 were studied in the range of pH 4.6–8.6, using 0.1 M phosphate buffer adjusted to the desired pH to evaluate the ratio of electrons and protons involved in the oxidation of PAM-2 and to obtain the optimum pH value. The $Fe^{3+}Y$ modified GCE was soaked in a 50 μM solution of PAM-2 in the phosphate buffer solution adjusted to the pH being studied and allowed to accumulate for 5 min. Then the soaked electrode was removed from the analyte solution, rinsed with ultrapure water and placed in fresh phosphate buffer solution at the same pH which does not contain PAM-2 and the square wave voltammetric response was measured. Figure 4.20A shows the square wave voltammograms recorded at different pH values. The optimum voltammetric response was observed at about pH 7 which was used for subsequent experiments.

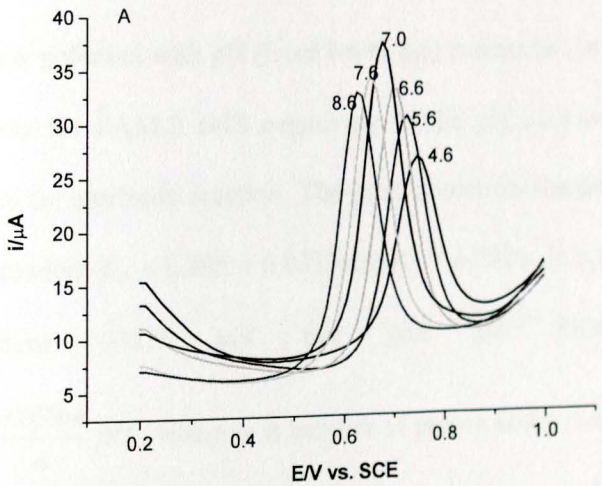

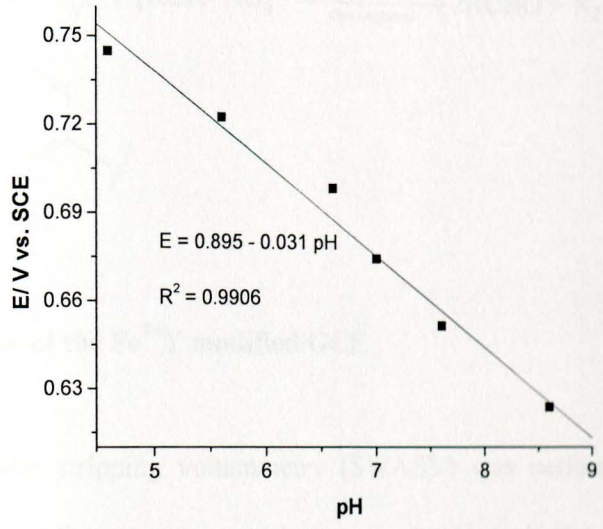

Figure 4.20. (A) Anodic stripping SWVs for 50 μM PAM-2 at $Fe^{3+}Y$ modified electrode in 0.1 M PBS with pH 4.6, 5.6, 6.6, 7.0, 7.6, and 8.6. (B) Plot of peak currents versus pH values at a scan rate 50 mV s^{-1}

The variation of peak potential with pH (from 4.6 to 8.6) is depicted in Figure 4.20B. The anodic peak currents for PAM-2 shift negatively as the pH increases, indicating that proton takes part in the electrode reaction. The peak potentials linearly change with pH according to the equation: $E_p = 0.895 - 0.0313$pH; $R^2 = 0.9906$. It is clear from the plot that the gradient –31.3 mV per unit pH increase (Nernstian process: $E = E^{o'} - \frac{0.059m}{n} pH$, where m is number of proton and n is number of electron) corresponds to a two-electron, one-proton process. The result is consistent with the literature report [163] and the reaction of PAM-2 at the modified electrode is likely to be [172]:

$$RCH{=}NOH \xrightarrow[-H^+]{-2e^-} [RCH{=}NO]^+ \xrightarrow[\text{dimerization}]{+RCH=NOH} 2RCHO + N_2 \qquad (4.9)$$

where R is 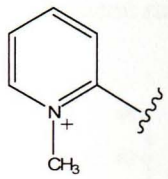

4.3.5. Performance of the $Fe^{3+}Y$ modified GCE

Square wave anodic stripping voltammetry (SWASV) was performed for analytical purpose. Prior to anodic stripping experiments in phosphate buffer (pH 7), the $Fe^{3+}Y$ modified GCE was soaked in the analyte solution containing 25 μM PAM-2 in phosphate buffer solution (pH 7.0) and rinsed with pure water. Then the SWVs with increasing soaking times were recorded. The peak current increased up to 5.0 min and then after there was no significant change in the voltammetric peak up to 10 min. Hence, 5.0 min soaking time was used as the optimum time for subsequent experiments.

To demonstrate the linear relationship between the anodic stripping peak current and PAM-2 concentration, a calibration curve was constructed under the optimum conditions. Figure 4.21A shows the SWASVs obtained at the $Fe^{3+}Y$ modified GCE for different concentrations of PAM-2. A concentration range from 0.5 to 100.0 μM was measured with a linear regression equation of i_p (μA) = 8.08 + 0.36c (μM); R^2 = 0.9984 (Figure 4.21B). The sensitivity of the modified electrode was 0.36 μA μM^{-1} and the detection limit was found to be 0.16 μM based on signal-to-noise ratio of 3, which is comparable to

that obtained with carbon nanotube modified GCE (0.30 μM) [161] and larger than the result at the poly(*p*-toluene sulfonic acid) (*p*-TSA) modified GCE (0.03 μM) [163].

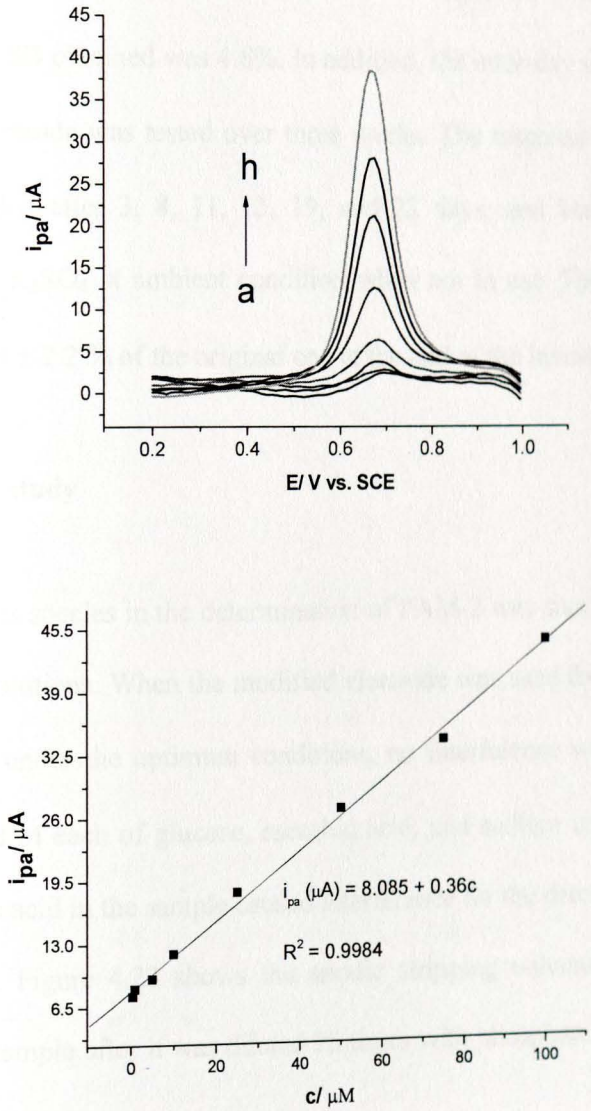

Figure 4.21. (A) Anodic stripping SWV peaks for PAM-2 at Fe^{3+}Y modified GCE in phosphate buffer (pH = 7.0) for different concentrations of analyte: (a) 0.5, (b) 1, (c) 5, (d) 10, (e) 25, (f) 50, (g) 75 and (h) 100 μM, background current subtracted. (B) Calibration plot i_{pa} versus different concentrations of PAM-2

The relative standard deviation (RSD) for five successive determinations of 25 μM PAM-2 at the modified electrode was 1.5%, which indicates a very good repeatability. The reproducibility of three $Fe^{3+}Y$ modified GCEs for the responses of 25 μM PAM-2 was evaluated and the RSD obtained was 4.6%. In addition, the inter-day stability of the three $Fe^{3+}Y$ modified electrode was tested over three weeks. The response current for 25 μM PAM-2 was recorded after 3, 8, 11, 15, 19, and 22 days, and keeping the modified electrode in 0.3 M K_2SO_4 at ambient condition when not in use. The average response was found to be 104 ± 2.2 % of the original one at the end of the investigation period.

4.3.6. Interference study

The effect of various species in the determination of PAM-2 was studied by applying the method of mixed solutions. When the modified electrode was used for the determination of 25 μM PAM-2 under the optimum conditions, no interference was encountered for additions of 50 μM of each of glucose, ascorbic acid, and sodium carbonate. However, the presence of uric acid in the sample caused interference for the determination of PAM-2 in urine sample. Figure 4.22 shows the anodic stripping voltammetric response of PAM-2 in a urine sample after it was diluted 25 times with phosphate buffer solution pH 7.0.

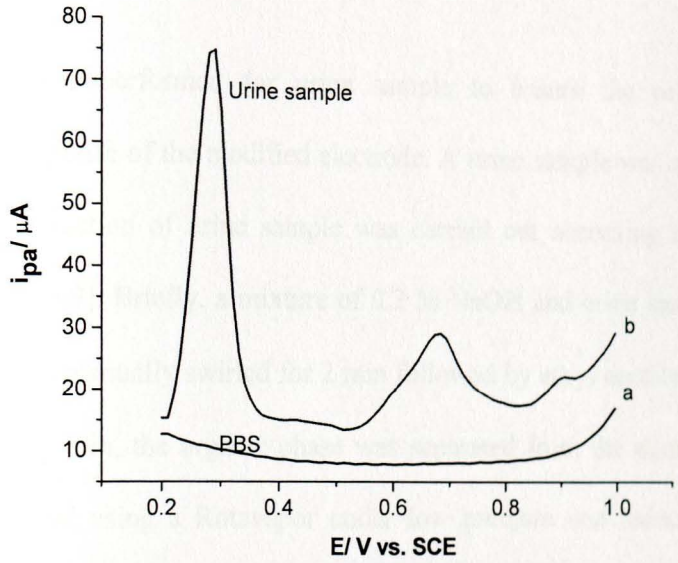

Figure 4.22. Anodic stripping voltammograms for: a) phosphate buffer solution (pbs) and b) urine sample diluted with pbs in the presence of PAM-2 (8 μM)

Even though the peak potential of the uric acid appeared at a different potential (300 mV) from that of PAM-2 (670 mV), the interference of uric acid was still observed. To illustrate its interference, higher concentrations of PAM-2 (20, 40 and 60 μM) were added to the urine sample. The voltammetric peak current of PAM-2 did not increase, indicating the host zeolite lattice on the modified electrode was already occupied by uric acid. For the determination of PAM-2 in urine sample, extraction of uric acid was performed as demonstrated in the recovery test.

4.3.7. Application of the modified electrode

Recovery tests were performed for urine sample to ensure the reliability of the electrochemical response of the modified electrode. A urine sample was collected from a person and the extraction of urine sample was carried out according to the literature recently reported [169]. Briefly, a mixture of 0.2 M NaOH and urine sample containing PAM-2 (8 μM) was manually swirled for 2 min followed by ethyl acetate addition. After centrifugation for 5 min, the organic phase was separated from the aqueous. The ethyl acetate was removed using a Rotavapor under low pressure and reduced temperature (50°C). The dried urine samples were reconstituted using phosphate buffer solution (pH 7.0) to make 25 mL urine sample. Then, the PAM-2 concentration in the urine was determined using the proposed method by multiple standard additions.

Anodic stripping voltammograms were obtained by spiking 75, 150 and 225 μL of 3.0 mM PAM-2 to the 25 mL of urine sample and 25 mL of phosphate buffer solution (pH 7.0), see Figure 4.23 A and B. In these investigations, the slopes of the plots for the variation of the anodic stripping peak current versus the volume of standard added were 4.29 μA mL^{-1} (R^2 = 0.9978) in phosphate buffer solution (Figure 4.23A) and 4.15 μA mL^{-1} (R^2 = 0.9973) in the urine sample (Figure 4.23B). The results provided a very good recovery for the PAM-2 added to the urine sample (99.5%) indicating the complex matrix in urine sample after the removal of uric acid did not interfere in the voltammetric determination of PAM-2.

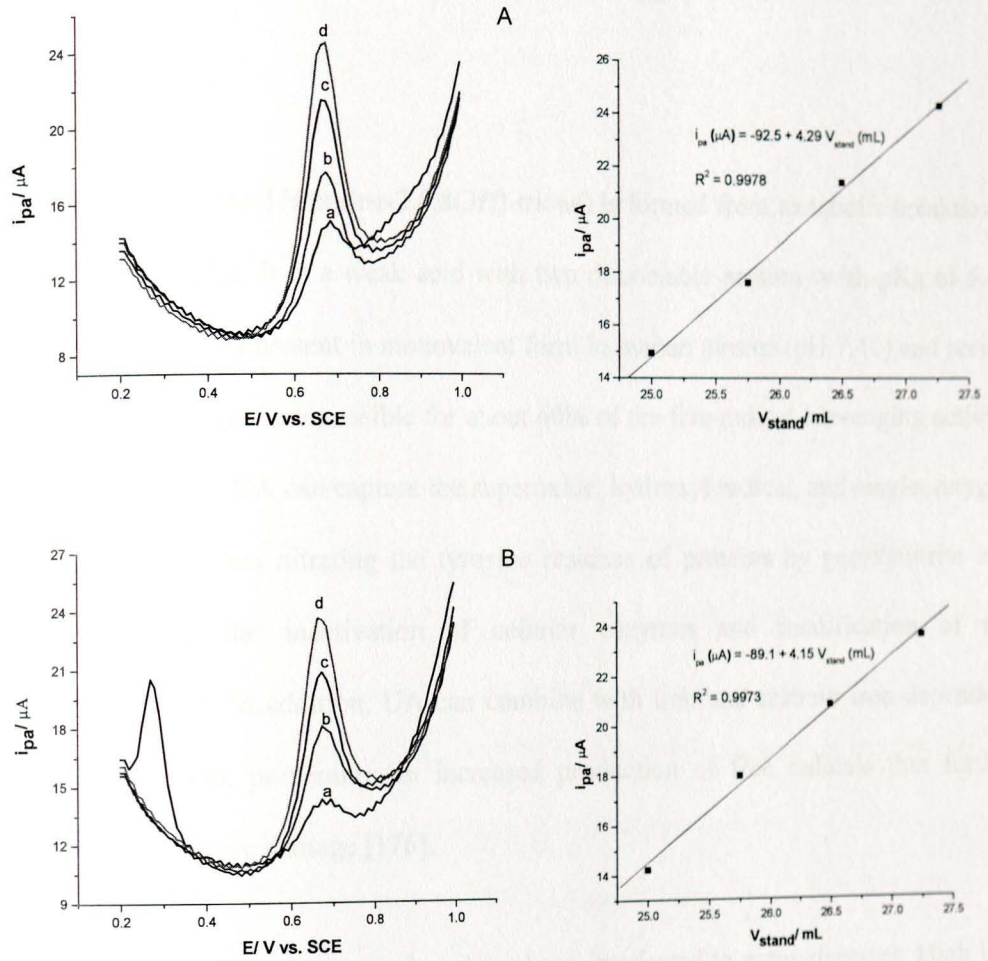

Figure 4.23. Anodic stripping voltammetric responses for 8 µM PAM-2 in 25 mL of (A) pbs and (B) urine sample: a) sample, sample spiked with: b) 75 µL, c) 150 µL and (d) 225 µL of 3.0 mM PAM-2

4.4. Determination of uric acid at $Fe^{3+}Y$ modified GCE

4.4.1. Background

Uric acid (7,9-dihydro-1*H*-purine-2,6,8(3*H*)-trione) is formed from metabolic breakdown of purine nucleotides. It is a weak acid with two dissociable protons, with pKa of 5.40 and 10.3 [174]. UA is present in monovalent form in human plasma (pH 7.40) and serves as a natural antioxidant, responsible for about 60% of the free radical scavenging activity in the plasma [175]. UA can capture the superoxide, hydroxyl radical, and singlet oxygen [176]. It also prevents nitrating the tyrosine residues of proteins by peroxynitrite and thereby avoiding the inactivation of cellular enzymes and modification of the cytoskeleton [177]. In addition, UA can combine with iron and restrain iron-dependent ascorbate oxidation, preventing an increased production of free radicals that further contribute to oxidative damage [176].

However, abnormal UA concentrations have been implicated to many diseases. High UA level (hyperuricemia) has been linked to gout, hypertension, cardiovascular and renal diseases [178-181], while a lower UA level (hypouricemia) has been related to neurodegenerative diseases such as multiple sclerosis, Parkinson's disease and Alzheimer's disease [182, 183]. Hyperuricemia has been defined when serum UA concentration is greater than 380 μM where as hypouricemia manifests for less than 120 μM serum UA, vary slightly depending on gender [176].

The common method for the determination UA in clinical laboratories uses uricase enzyme to oxidize UA to hydrogen peroxide, carbondioxide and allantoin [184]. Other

alterative methods for UA determination include the reduction of phosphotungstic acid by UA to give tungsten blue followed by spectrophotometric determination [185] and HPLC on reversed phase columns with UV absorbance or mass spectrometry [186]. These methods involve several step-wise reactions and enzymatic techniques to determine the concentration of the H_2O_2 intermediate which results in time consuming procedures and use of sophisticated instrument. Hence, there is a great interest to develop a simple and sensitive method for UA determination.

Electrochemical techniques have attracted much attention due to their advantages of rapid analysis, simple experimental procedures, and relatively cheaper instrumentals with high sensitivity and selectivity [187]. Since UA is an electrochemically active compound, a non-enzymatic electrochemical approach appears to be the best alternative technique for its determination [188]. The use of bare electrode, such as GCE for the electrochemical determination of UA is limited because of the sluggish electron transfer and interference from other electrochemically active species [189]. In order to address these limitations, most electrochemical methods rely on chemically modified electrodes such as graphene modified graphite electrode [190], methylene blue modified zirconia–silica composite electrode [191], platinum and gold nanoparticles modified GCE [192], poly (Evans Blue) modified GCE [193], palladium nanoparticle-loaded carbon nanofibers modified electrode [194], dopamine modified pyrolytic graphite electrode [195], polymerized luminol modified GCE [196], poly (vinyl alcohol) modified GCE [197], nanostructured polymer film modified electrode [198] and carbon paste iron(III) doped zeolite modified electrode [199]. However, because of the paramount importance of UA determination for clinical analysis, many researchers look for at better chemically modified electrodes.

In this section, the development of a voltammetric method for the determination of UA at activated $Fe^{3+}Y$ modified GCE is presented. The voltammetric response for UA at modified GCE is compared with that of the bare GCE. The performance of the modified electrode is evaluated in terms of sensitivity, detection limit and linear range. Finally, the developed modified electrode is applied for the determination of UA in a biological sample.

4.4.2. Electrochemical behavior of UA at $Fe^{3+}Y$ modified GCE

The $Fe^{3+}Y$ modified electrode was initially treated with sulfuric acid as described in section 4.3.2. The treatment was done by running CV for five cycles, and the treated modified electrode was stabilized by sweeping the potential between 1.0 V and –0.2 V in 0.3 M KH_2PO_4 solution. It was shown that the acid treated modified electrode showed better electrochemical response compared to the untreated one and hence, this treated modified electrode was employed to develop an electrochemical method for the determination uric acid.

The influence of the modification of the GCE on the intensity of the peak current was investigated by running CV in 0.25 mM UA dissolved in phosphate buffer solution (pH 4.6) at a scan rate of 50 mV s^{-1} and evaluating the intensity of the electrochemical signal before and after the modification of the electrode. Oxidation peaks of UA were observed at a potential around 460 mV (vs. SCE) as shown in Figure 4.24. It was verified that the electrochemical response increased approximately four times after the modification of the electrode (curve d Figure 4.24), in comparison with the response in the absence of

modification (curve b Figure 4.24). The remarkable peak current enhancement by the modified electrode can be attributed to the catalytic property of $Fe^{3+}Y$ zeolite structure as described in section 4.3.2.

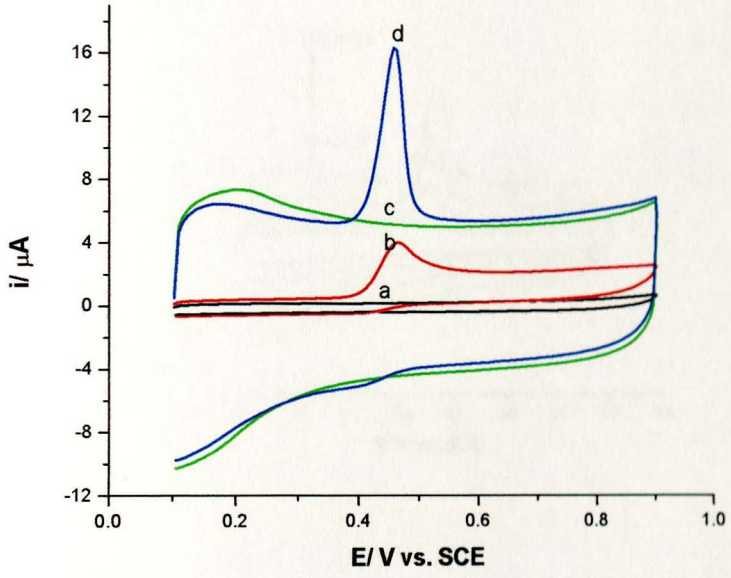

Figure 4.24. The electrochemical responses of the bare GCE in: a) pbs and b) 25 mM UA, and the $Fe^{3+}Y$ modified GCE in: c) pbs and d) 0.25 mM UA

In order to further study the electrochemical response for UA at the modified electrode, the effect of scan rate on the peak currents for UA was examined. Figure 4.25A shows the cyclic voltammograms of 20 μM UA obtained at the $Fe^{3+}Y$ modified electrode in the range of 20 to 200 mV s^{-1}. The anodic peak currents of UA exhibit a linear relationship with increasing scan rate (Figure 4.25B), indicating that UA is adsorbed onto the modified electrode surface. The linear relationship between the logarithm of the peak currents (log i_p) and the logarithm of scan rates (log ν) in the range 20–200 mV s^{-1} and its slope (0.99) obtained from the linear equation: log i_p = –0.433 + 0.99 log ν, and R^2 =

0.9966 (Figure 4.25C) confirm that adsorbed UA is oxidized in a totally irreversible process [3].

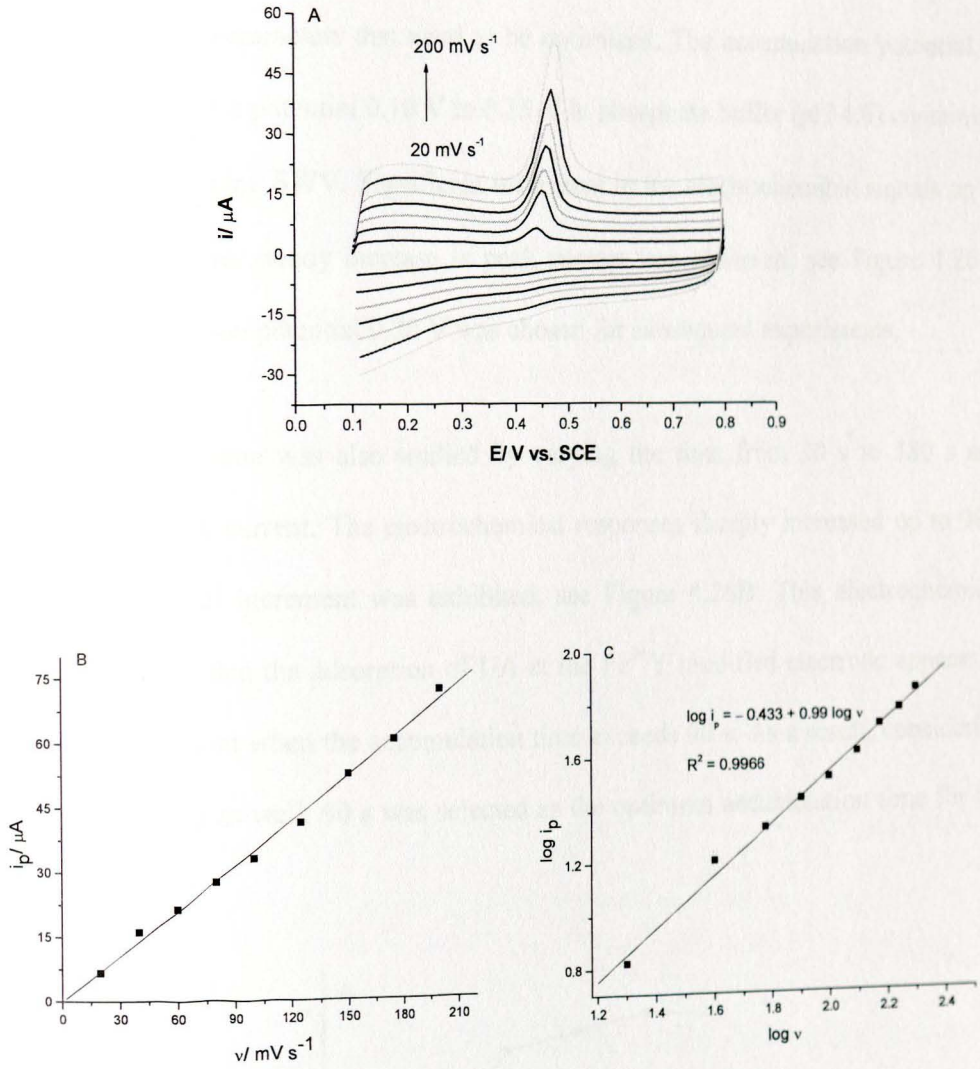

Figure 4.25. (A) CVs for 25 µM UA at $Fe^{3+}Y$ modified GCE in 0.1 M pbs pH 4.6 at different scan rates of 20 mV s^{-1} to 200 mV s^{-1}. (B) The plot of peak current of UA versus scan rate for 20 mV s^{-1} to 200 mV s^{-1}. (C) The plot of log i_p versus log v for 20 mV s^{-1} to 200 mV s^{-1}

4.4.3. Effect of accumulation potential and time

Because of adsorption of UA at the $Fe^{3+}Y$ modified electrode, accumulation potential and time are important parameters that need to be optimized. The accumulation potential of UA was varied from a potential 0.10 V to 0.35 V in phosphate buffer (pH 4.6) containing 20 μM UA and running SWV. Significant increment in the electrochemical signals up to 0.20 V and then after steady increase in peak current was observed, see Figure 4.26A. Thus, an accumulation potential 0.20 V was chosen for subsequent experiments.

The accumulation time was also studied by varying the time from 30 s to 180 s and measuring the peak current. The electrochemical responses sharply increased up to 90 s and a steady signal increment was exhibited, see Figure 4.26B. This electrochemical response indicates that the adsorption of UA at the $Fe^{3+}Y$ modified electrode appears to reach saturation point when the accumulation time exceeds 90 s. As a result, considering working efficiency as well, 90 s was selected as the optimum accumulation time for the rest of the study.

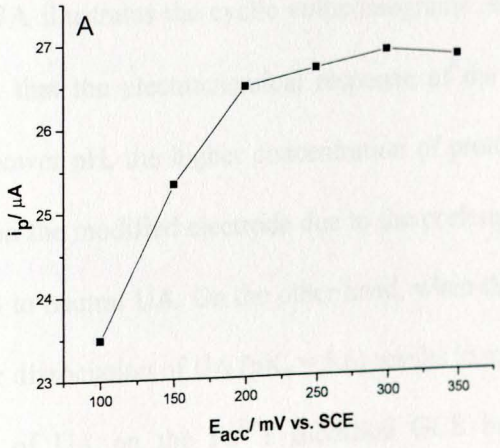

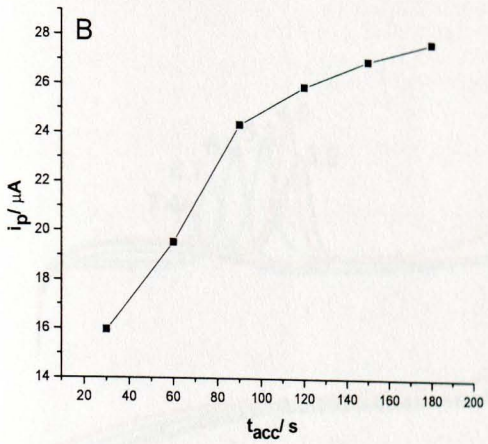

Figure 4.26. The effect of accumulation (A) potential and (B) time on the peak current for 20 µM UA at $Fe^{3+}Y$ modified electrode

4.4.4. Effect of pH

The influence of pH on the cyclic voltammetric response for 20 µM UA was examined between pH 3.9 and 7.4. The $Fe^{3+}Y$ modified GCE was kept in a 20 µM solution of UA in phosphate buffer solution adjusted to the pH being studied and allowed to accumulate for 90 s at a potential 0.2 V. Then CV was run between 0.0 V and 1.0 V at a scan rate of 50 mV s^{-1}. Figure 4.27A illustrates the cyclic voltammograms recorded at different pH values. It can be seen that the electrochemical response of the modified electrode is highest at pH 4.6. At lower pH, the higher concentration of proton could compete with the adsorption of UA on the modified electrode due to the preference of negative zeolite structure for the proton to neutral UA. On the other hand, when the pH of the solution is greater than pH 4.6, the dissociation of UA ($pK_a = 5.6$) results in more urate anions which hinder the adsorption of UA on the $Fe^{3+}Y$ modified GCE because of electrostatic repulsion. Thus pH 4.6 was chosen as the optimum pH for this study.

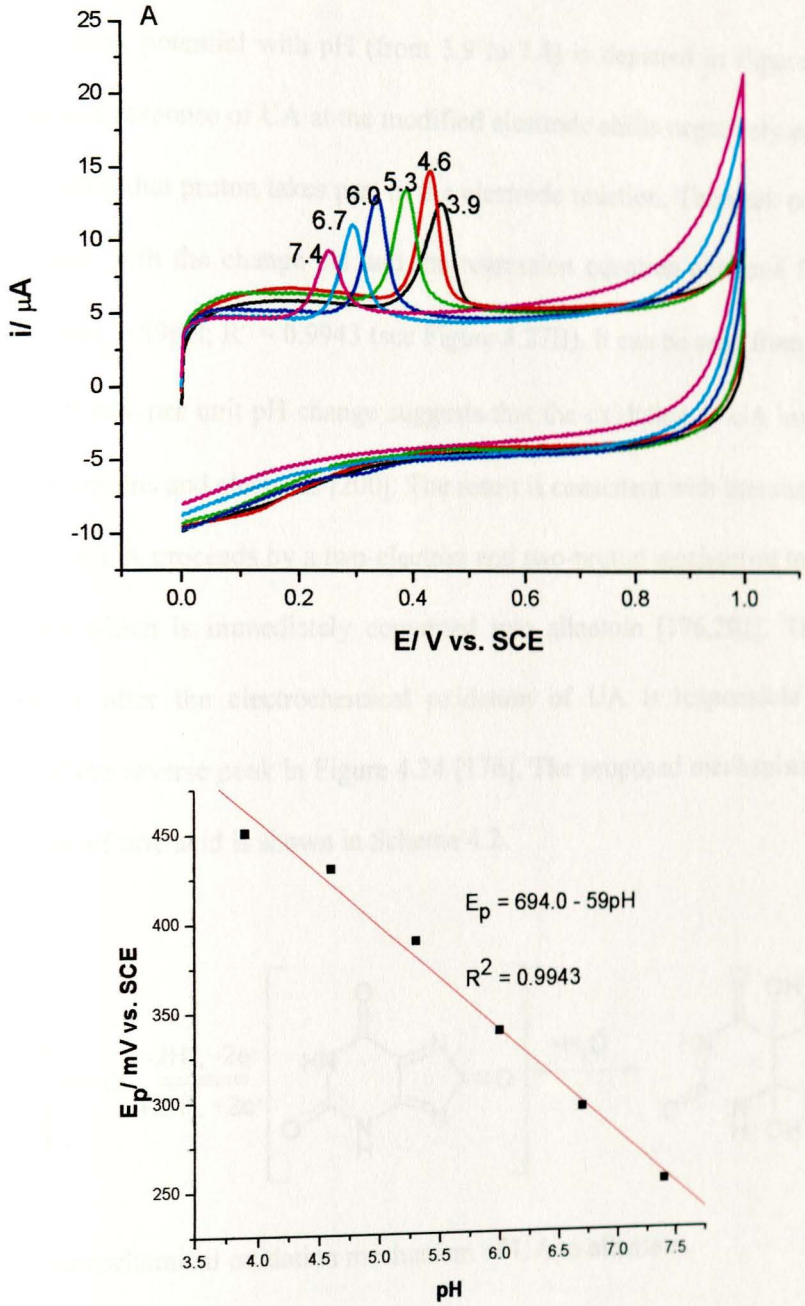

Figure 4.27. (A) CVs for 20 μM UA at Fe^{3+}Y modified GCE in 0.1 M pbs with pH 3.9, 4.6, 5.3, 6.0, 6.7, and 7.4. (B) Plot of peak currents versus pH values, 50 mV s^{-1}

The variation of peak potential with pH (from 3.9 to 7.4) is depicted in Figure 4.27A. The electrochemical response of UA at the modified electrode shifts negatively as the pH increases, suggesting that proton takes part in the electrode reaction. The peak potentials are linearly related with the change pH and the regression equation obtained from the linear fit is $E_p = 694 - 59pH$; $R^2 = 0.9943$ (see Figure 4.27B). It can be seen from the plot that the slope −59 mV per unit pH change suggests that the oxidation of UA involve an equal number of protons and electrons [200]. The result is consistent with literature report where oxidation of UA proceeds by a two-electron and two-proton mechanism to give an unstable diimine which is immediately converted into allantoin [176,201]. The latter chemical reaction after the electrochemical oxidation of UA is responsible for the disappearance of the reverse peak in Figure 4.24 [176]. The proposed mechanism for the electrode reaction of uric acid is shown in Scheme 4.2.

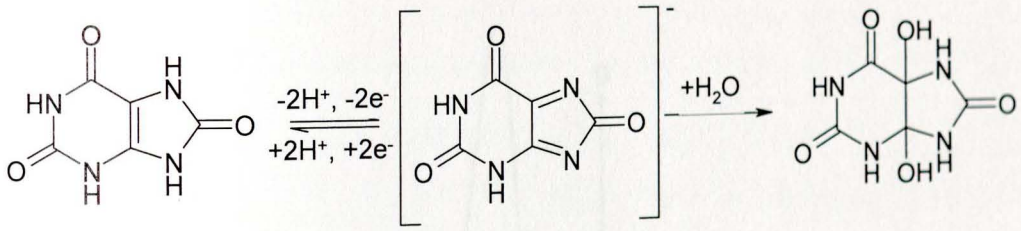

Scheme 4.2: Electrochemical oxidation mechanism of UA to allantoin.

4.4.5. Performance of the $Fe^{3+}Y$ modified GCE for UA

The applicability of the proposed method for the determination of UA was examined by recording the anodic peak current as a function of the concentration of the analyte under the optimized condition. The electrochemical responses increase with increasing

concentration of UA as demonstrated in Figure 4.28A. It can be seen from Figure 4.28B that a linear calibration plot in the range from 0.6 to 60.0 μM is attained with a regression equation of i_p (μA) = 5.43 + 0.64c (μM); R^2 = 0.9995. A very good sensitivity of 0.64 μA μM^{-1} was obtained at the $Fe^{3+}Y$ modified GCE and the detection limit was found to be 0.09 μM (s/n = 3), compared to other chemically modified electrodes as demonstrated in Table 4.5. The film based modified electrode prepared here has the same order of magnitude as that of the bulk zeolite modified electrode [199] in terms of the detection limit but the simplicity in the preparation and regeneration of the modified electrode in our work make it very useful for routine analysis of uric acid.

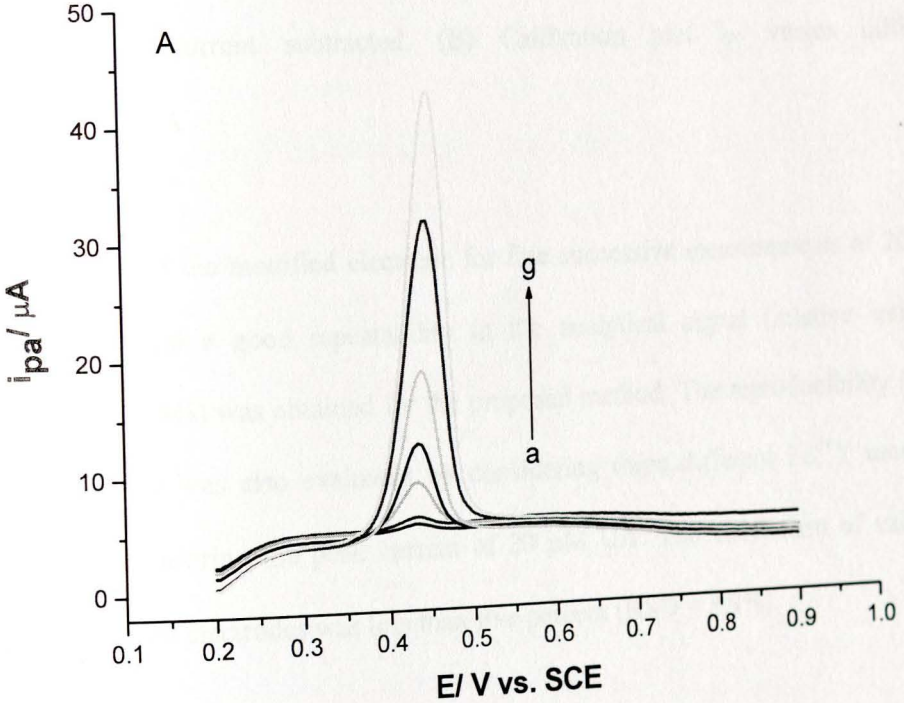

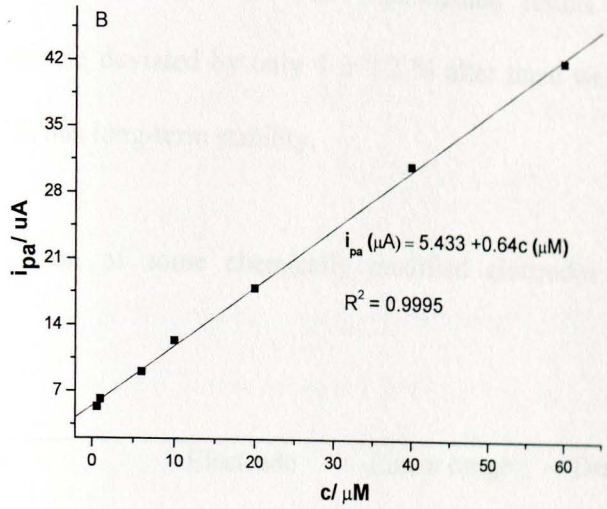

Figure 4.28. (A) SWV responses of UA at $Fe^{3+}Y$ modified GCE in pbs (pH = 4.6) for various concentrations of analyte: (a) 0.6, (b) 1, (c) 6, (d) 10, (e) 20, (f) 40, and (g) 60 μM, background current subtracted. (B) Calibration plot i_{pa} versus different concentrations of UA

The repeatability of the modified electrode for five successive measurements of 20 μM UA was tested and a good repeatability in the analytical signal (relative standard deviation, RSD, 1.8%) was obtained for the proposed method. The reproducibility of the modified electrode was also evaluated by considering three different $Fe^{3+}Y$ modified electrodes and measuring the peak current of 20 μM UA. The coefficient of variance among the modified electrodes was less than five percent (RSD = 3.9%).

The long-term stability of the $Fe^{3+}Y$ modified GCE was examined by measuring the current response at a fixed concentration of UA (20 μM) over a period of three weeks. The modified electrode was used every four-day and kept in 0.3 M K_2SO_4 solution at

ambient condition when not in use. The experimental results showed that the electrochemical response deviated by only 4 ± 2.2 % after three weeks, revealing that $Fe^{3+}Y$ modified GCE has long-term stability.

Table 4.5. Comparison of some chemically modified electrodes reported for UA determination

Modifier used	Electrode	Linear range (μM)	Detection limit (μM)	Reference
Graphene	Graphite	1.8 – 90	0.45	190
Methylene blue	Zirconia-silica composite	22 – 350	3.7	191
Pt Au nanoparticles	GCE	21 – 330	–	192
Poly (evans blue)	GCE	30– 110	2.0	193
Palladium nanoparticle-loaded carbon fibers	Carbon paste	2.0 – 200	0.7	194
Dopamine	Pyrolytic graphite	2.5 – 30	1.4	195
Polymerized luminol	GCE	30.0 – 1000	2.0	196
Poly (vinyl alcohol)	GCE	2.0 – 50	0.6	197
2-Amino-1,3,4-thiodiazole	GCE	10.0 – 100	0.2	198
Zeolite doped with Fe(III) without acid treatment	Carbon paste electrode	0.3–700	0.08	199
Fe(III) doped zeolite with acid treatment	GCE	0.6 – 60	0.09	this work

4.4.6. Interference study

One of the greatest problems in UA determination is the interference caused by some electrochemically active compounds in biological samples, which can be oxidized under the same condition, particularly with most usual interference coming from ascorbic acid and dopamine [197, 198]. In this regard, mixed solution technique was employed in order to study the effect of interfering substances on the electrochemical response of UA. When the peak current of 20 μM UA was compared to those of 20 μM UA in the presence of 40 μM of each of glucose, caffeine or ascorbic acid, the anodic peak current did not change, suggesting that no interference comes from those possibly interfering substances. Even though dopamine shows an electrochemical signal in the working potential window, its peak potential is negatively shifted by 150 mV from that of the UA as depicted in Figure 4.29. When the modified electrode was subjected to more amount of dopamine (30 or 40 μM) containing the same amount uric acid (20 μM), no change in the peak current of UA was observed. The result indicates that dopamine does not interfere in the determination UA, and the $Fe^{3+}Y$ modified has some selectivity towards UA.

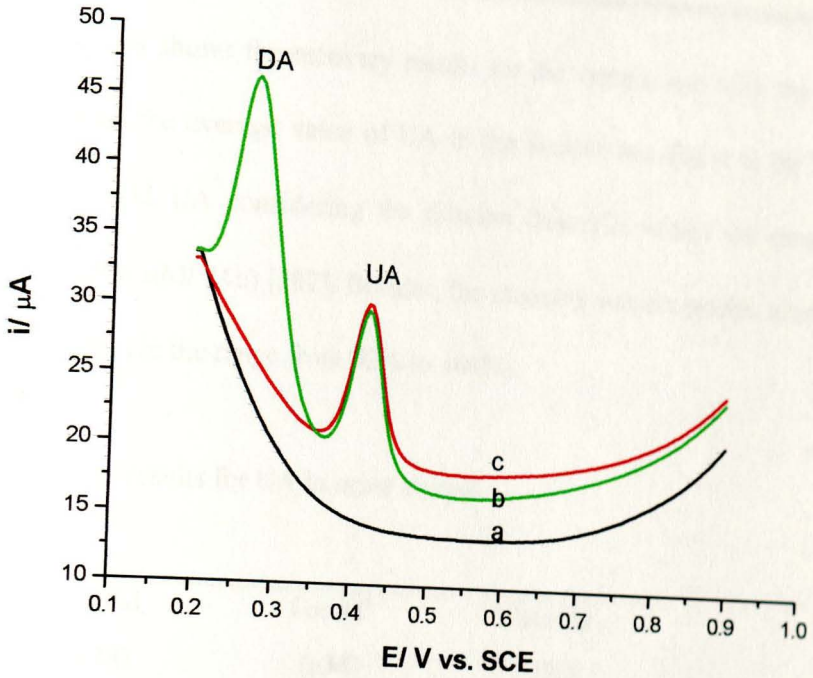

Figure 4.29. SWVs for: (a) pbs (pH 4.6), (b) 20 μM UA in the presence of 20 μM dopamine (DA) and (c) 20 μM UA only

4.4.7. Application of the modified electrode

Recovery tests were performed for urine sample to ensure the reliability of the electrochemical response of the $Fe^{3+}Y$ modified GCE. A urine sample was collected from a person and was subjected to a 1000-time dilution, in the supporting electrolyte (0.1 M PBS), in such a way that the concentration of UA present was kept in the concentration range of the calibration curve. With no further additional sample treatment, it was found that the urine sample exhibited only one peak at about 0.42 V (vs. SCE), which is due to the oxidation of UA. The electrochemical response clearly indicates that the modified electrode has some selectivity towards UA in human urine sample under the optimized

conditions. Table 4.6 shows the recovery results for the sample and from the standard addition experiment the average value of UA in the sample was found to be 3.04 μM. This result (3040 μM UA considering the dilution factor) is within the range in the literature (1500-4400 μM/ 24h) [202]. Besides, the recovery was acceptable after spiking UA into the samples (in the range from 92% to 104%).

Table 4.6. Recovery results for UA in urine sample

No.	Added (μM)	Found[a] (μM)	Recovery (%)
1	–	3.0 (±0.22)	–
2	3.8	6.6 (±0.33)	92
3	7.4	10.6 (±0.18)	103
4	10.7	14.2 (±0.26)	104

[a] Mean value ± standard deviation (n = 3).

5. Conclusions

This thesis has shown the development of various modifications of glassy carbon electrodes for the determination of different analytes. PEDOT and activated $Fe^{3+}Y$ modified electrodes were successfully employed for the determination of APAP (its degradation product, PAP), niclosamide, PAM-2, and UA in real samples.

A PEDOT-modified GCE was fabricated for the simultaneous determination of APAP and PAP using DPV technique. The results confirm that the presence of the PEDOT film on the surface of the electrode significantly affects the kinetics and sensitivity of the electrochemical responses for APAP and PAP. The significant peak separation of the two analytes offers the technique for the selective determination of APAP in the presence of PAP. The proposed method was applied for the determination of APAP and PAP in tablets with recovery ranging 96.6–108.5% and 95.6–105.8%, respectively. The PEDOT-modified GCE was successfully used for the determination of APAP in biological samples with a good percent recovery (88.4–109.1%).

An easy-to-make and low cost fabrication of PEDOT-modified GCE was also employed to determine niclosamide selectively. The PEDOT-modified GCE is capable of enhancing the electrochemical monitoring of niclosamide due to increase in the electrode active surface area. The high sensitivity, selectivity and very low detection limit (1.09×10^{-8} M) together with the very easy preparation and surface regeneration of the modified electrode make the PEDOT-modified electrode very useful in the construction

of simple electrochemical sensors for the determination of niclosamide in clinical and pharmaceutical formulations.

A simple electroanalytical method was also developed based on a stable $Fe^{3+}Y$ zeolite modified GCE for the selective determination of PAM-2. The modified electrode takes advantage of the acid treatment of the $Fe^{3+}Y$ zeolite which enables incorporation of the electroactive species and preconcentration of PAM-2 in its structure. As a result, the $Fe^{3+}Y$ modified electrode exhibits a better electrochemical response with a wider linear range, higher sensitivity and lower detection limit compared to the untreated modified electrode. The proposed method was successfully applied for the determination of PAM-2 in a biological sample with a very good recovery (99.5%) without interference from coexisting species.

The $Fe^{3+}Y$ modified GCE also provides good adsorption characteristics and exhibits high electrocatalytic activity towards the oxidation of UA. The modified electrode is sensitive, stable and selective for interferences from potentially interfering compounds such as ascorbic acid and dopamine. The $Fe^{3+}Y$ modified GCE offers the advantages of simple fabrication, easy surface regeneration and very low detection limit, which are suitable for routine determination of UA in clinical samples.

References

1. C.M.A. Brett, A.M.O. Brett, *Electrochemistry: Principles, Methods and Applications*, Oxford University press, Oxford, **1993**.

2. J. Heyrovskey, *Chem. Listy* **1922**, 16, 256 (from: M. Heyrovsky, *Chem. Rec.* **2012**, 12, 14.)

3. J.A. Bard, L.R. Faulkner, *Electrochemical Methods*, 2nd ed., Wiley, New York **2000**.

4. H.A. Lintent, I.M. Kolthoff, *J. Phys. Chem.* **1941**, 45, 1079.

5. L.A. Matheson, N. Nicholas, *Trans. Electrochem. Soc.* **1938**, 73, 193 (from: M. Heyrovsky, *Chem. Rec.* **2012**, 12, 14.)

6. J.E.B. Randles, *Trans. Faraday Soc.* **1948**, 44, 327.

7. R. Brdicka, K. Wiesner, *Collect. Czech. Chem. Commun.* **1947**, 12, 138, (from: M. Heyrovsky, *Chem. Rec.* **2012**, 12, 14.)

8. R. Seeber, F. Terzi, *J. Solid State Electrochem.* **2011**, 15, 1523.

9. J.W. Ross, R.D. DeMars, I. Shain, *Anal. Chem.* **1956**, 28, 1768.

10. R. Adams, *Electrochemistry at Solid Electrodes* M. Dekker, New York **1969.**

11. R.S. Nicholson, I. Shain, *Anal. Chem.* **1964**, 36, 706.

12. R.F. Lane, A.T. Hubbard *J. Phys. Chem.* **1973**, 77, 1411.

13. P.R. Moses, R.W. Murray *J. Am. Chem. Soc.* **1976**, 98, 7435.

14. R.W. Murray, *Chemically modified electrodes,* in: A.J. Bard (ed.) *Electroanalytical Chemistry*, Vol 13. M. Dekker, New York **1984**, pp 191–368.

15. J. Wang, *Analytical Electrochemistry*, 3rd ed., Wiley, New Jersey **2006**.

16. J. Zen, A.S. Kumar, D. Tsai, *Electroanalysis* **2003**, 15, 1073.

17. R.P. Baldwin, K.N. Thomsen, *Talanta* **1991**, 38, 1.

18. R.W. Murray, A.G. Ewing, R.A. Durst, *Anal. Chem.* **1987**, 59, 379A.

19. S. Flink, F. C. J. M. van Veggel, D. N. Reinhoudt, *Adv. Mat.* **2000**, 12, 1315.

20. A.N.J. Moore, E. Katz, I. Willner, *Electroanalysis*, **1996**, 8, 1092.

21. A. Ulman, Chem. Rev. **1996**, 96, 1533.

22. D. Mandler, I. Turyan, *Electroanalysis* **1996**, 8, 207.

23. M.M. Walczak, C. Chung, S.M. Stole, C.A. Widrig, M.D. Porter, *J. Am. Chem.* Soc. **1991**, 113, 2370.

24. R.W. Murray *Acc. Chem. Res.* **1980**, 13, 135.

25. A.J. Downard, *Electroanalysis* **2000**, 12, 1085.

26. M.W. Espenscheid, A.R. Ghatak-Roy, R.B. Moore, R.M. Penner, M.N. Szentirmay C.R. Martin, *J. Chem. Soc. Faraday Trans.1* **1986**, 82, 1051

27. U. Lange, N.V. Roznyatovskaya, V.M. Mirsky, *Anal. Chim. Acta* **2008**, 614, 1.

28. D. Bouchta, N. Izaoumen, H. Zejli, M.E. Kaoutit, K.R.Temsamani, *Biosens. Bioelectron.* **2005**, 20, 2228.

29. S. Lupu, F. Parenti, L. Pigani, R. Seeber, C. Zanardi, *Electroanalysis* **2003**, 15, 715.

30. Q. Wan, X. Wang, X. Wang, N. Yang, *Polymer* **2006**, 47, 7684.

31. X. Wang, N. Yang, Q. Wan, X. Wang, *Sens. Actuators B* **2007**, 128, 83.

32. B. Shen, M. Chen, *Electroanalysis* **2007**, 19, 1616.

33. J.Y. Heras, A.F.F. Giacobone, F. Battaglini, *Talanta* **2007**, 71, 1684.

34. S. Lupu, A. Mucci, L. Pigani, R. Seeber, C. Zanardi, *Electroanalysis* **2002**, 14, 519.

35. J. Mathiyarasu, S. Senthilkumar, K.L.N. Phani, V. Yegnaraman, *Mater. Lett.* **2008**, 62, 571.

36. K.C. Ho, W.M. Yeh, T.S. Tung, J.Y. Liao, *Anal. Chim. Acta* **2005**, 542, 90.

37. J. Li, X. Lin, *Sens. Actuators B* **2007**, 124, 486.

38. J.M. Zen, A.S. Kumar, *Acc. Chem. Res.* **2001**, 34, 772.

39. A. Walcarius, *Chem. Mat.* **2001**, 13, 3351.

40. M. Sadakane, E. Steckhan, *Chem. Rev.* **1998**, 98, 219.

41. A. Walcarius, *Electrochemistry with Micro- and Mesoporous Silicates*, in Ed.: V. Valtchev, S. Mintova, M. Tsapatsis, *Ordered Porous Solids*, Elsevier, Amsterdam **2009**, pp 523–555.

42. J.L. Bredas, G.B. Street, *Acc.Chem. Res.* **1985**, 18, 309.

43. U. Salzner, J.B. Lagowski, P.G. Pickup, P.A. Poirier, *Synth. Met.* **1998**, 96, 177.

44. M.G. Kanatzidis, *Chem. Eng. News* **1990**, 68(49), 36.

45. S. Brazovskii, N. Kirova, Z.G. Yu, A.R. Bishop, A. Saxena, *Optic. Mater.* **1998**, 9, 502.

46. J. Heinze, B.A. Frontana-Uribe, S. Ludwigs, *Chem. Rev.* **2010**, 110, 4724.

47. A.F. Diaz, J.I. Castillo, J.A. Logan, W.Y. Lee, *J. Electroanal. Chem.* **1981**, 129, 115

48. E.M. Genies, G. Biden, A.F. Diaz, *J. Electroanal. Chem.* **1983**, 149, 101.

49. T.A. Skotheim, J.R. Reynolds (Eds), *Handbook of Conducting Polymers*, 3rd Ed. CRC press, Boca Raton, **2007**.

50. J.E. Osterholm, P. Passiniemi, H. Isotalo, H. Stubb, *Synth. Met.* **1987**, 18, 213.

51. R.J. Waltman, J. Bargon, *Can. J. Chem.* **1986**, 64, 76.

52. M. Lemaire, W. Buchner, R. Garreau, H.A. Hoa, A. Guy, J. Roncali, *J. Electroanal. Chem.* **1990**, 281, 293.

53. E.W. Tsai, S. Basak, J.P. Ruiz, J.R. Reynolds, K. Rajeshwar, *J. Electchem. Soc.* **1989**, 136, 3683.

54. J.P. Ruiz, K Nayak, D.S. Marynick, J.R. Reynolds, *Macromolecules* **1989**, 22, 1231.

55. S.V. Lowen, D. Macinnes, B.L. Funt *J. Polymer Scein. Part A: Polymer Chem.* **1989**, 27, 4087.

56. G. Heywang, F. Jonas, *Adv. Mater.* **1992**, 4, 116.

57. M. Dietrich, J. Heinze, G. Heywang, F. Jonas, *J. Electroanal. Chem.* **1994**, 369, 87.

58. L. Greonendaal, G. Zotti, P. Aubert, S.M. Waybright, J.R. Reynolds, *Adv. Mat.* **2003**, 15, 855.

59. L. Groenendaal, F. Jonas, D. Freitag, H. Pielartzik, J.R. Reynolds, *Adv. Mat.* **2000**, 12, 481.

60. J.H. Chen, C. Dai, W. Chiu, *J. Polymer Scein. Part A: Polymer Chem.***2008**, 46, 1662.

61. J. Park, H.K. Kim, Y. Son, *Sens. Actuators B: Chem.* **2008**, 133, 244.

62. S. Kirchmeyer, K. Reuter, *J. Mater. Chem.* **2005**, 15, 2077.

63. L. Groenendaal, G. Zotti, F. Jones, *Synth. Met.* **2001**, 118, 105.

64. S.S. Zhu, T.M. Swager, *J. Am. Chem. Soc.* **1997**, 9, 795.

65. R. Kingsborough, T.M. Swager, *Adv. Mater.* **1998**, 10, 1110.

66. B. Piro, L.A. Dang, M.C. Pham, S. Fabiano, C. Tran-Minh, *J. Electroanal. Chem.* **2001**, 512, 101.

67. N. Sakmeche, S. Aeiyach, J.J. Aaron, M. Jouini, J.C. Lacroix, P.C. Lacaze, *Langmuir*, **1999**, 15, 2566.

68. N. Sakmeche, J.J. Aaron, S. Aeiyach, P.C. Lacaze, *Electrochim. Acta* **2000**, 45, 1921.

69. Lima, P. Schottland, S. Sadki, C. Chevrot, *Synth. Met.* **1998**, 93, 33.

70. B. Piro, L.A. Dang, M.C. Pham, S. Fabiano, C. Tran-Minh, *J. Electroanal. Chem.* **2001**, 512, 101.

71. D. Han, J. Kim, S. Park, *J. Phys. Chem. B* **2006**, *110*, 14874.

72. X.J. Wang, K.Y. Wong, *Thin Solid Films* **2006**, 515, 1573.

73. M.C. Morvant, J.R. Reynolds, *Synth. Met.* **1998**, 92, 57.

74. J. Ahonen, J. Lukkari, J. Kankare, *Marcomolecules* **2000**, 33, 6787.

75. M. Lapkowski, A. Pron, *Synth. Met.* **2000**, 110, 79.

76. E. Nasybulin, S. Wei, M. Cox, I. Kymissis, K. Lavon, *J. Phys. Chem. C* **2011**, 115, 4307.

77. A. Walcarius, *Electroanalysis* **1996**, 8, 971.

78. R.P. Townsend, *Stud. Surf. Sci. Catal.* **1991**, 58, 359.

79. A. Walcaius, *Electroanalysis* **2008**, 20, 711.

80. A. Walcarius, *Electroanalysis* **1996**, 8, 971.

81. A. Warcarius, *Anal. Chim. Acta* 1999, **384**, 1

82. M. Arvand, M. Vaziri and M. Vejdani, *Mater. Scien. Eng. C* **2010**, 30, 709.

83. A. Warcarius, T. Barbiase and J. Bessiere, *Anal. Chim. Acta* **1997**, 340, 61.

84. G. Marko-Varga, E. Burestedt, C. Svensson, J. Emnues, L. Gorton, T. Ruzgzs, M. Luiz, K.K. Unger, *Electroanalysis* **1996**, 8, 1121.

85. A. Walcarius, L. Lambers, E.G. Derouane, *Electrochim. Acta* **1993**, 38, 2257.

86. A. Walcarius, V. Vromman, J. Bessere, *Sens. Actuators B* **1999**, 56, 136.

87. J. Wang, A. Walcarius, *J. Electroanal. Chem.* **1996**, 404, 237.

88. J. Li, T. Peng, C. Fang, *Anal. Chim. Acta* **2002**, 455, 53.

89. V. Ganesan, R. Ramaraj, *Langmuir* **1998**, 14, 2497

90. A. Domenech, J. Perez-Ramirez, A. Ribera, G. Mul, F. Kapteijn, I.W.C.E. Arends, *J. Electroanal. Chem.* **2002**, 519, 72.

91. P. Zanello, *Inorganic Electrochemistry: Theory, Practice and Application*, RSC, **2003**.

92. H.E. Zittel, F.J. Muller, *Anal. Chem.* **1965**, 37, 200.

93. R.L. McCreery, *Chem. Rev.* **2008**, 108, 2646.

94. A.B. Moghaddam, A. Mohammadi, S. Mohammadi, D. Rayeji, R. Dinarvand, M. Baghi, R.B. Walker, *Microchim. Acta* **2010**, 171, 377.

95. R.M. De Carvalho, R.S. Freire, S. Rath, L.T. Kubota, *J. Pharm. Biomed. Anal.* **2004**, 34, 871.

96. M.E. Bosch, A.J.R. Sanches, F.S. Rojas, C.B. Ojeda, *J. Pharm. Biomed. Anal.* **2006**, 42, 291.

97. N.R. Goyal, V.K. Gurpta, M. Oyama, N. Bachheti, *Electrochem. Commun.* **2005**, 7, 803.

98. E. Wyszecka-Kaszubaa, M. Warowna-Grze, Z. Fija, *J. Pharm. Biomed. Anal.* **2003**, 32,1081.

99. S.J.R. Prabakar, S.S. Narayanan, *Talanta* **2007**, 72, 1818.

100. A.M. Larson, J. Polson, R.J. Fontana, *Hepatology* **2005**, 42, 1364.

101. J. Forshed, F.O. Andersson, S.P. Jacobsson, *J. Pharm. Biomed. Anal.* **2002**, 29, 495.

102. A. Yesilada, H. Erdogan, M. Ertan, *Anal. Lett.* **1991**, 24, 129.

103. F.A. Mohamed, M.A. Abdallah, S.M. Shammat, *Talanta* **1997**, 44, 61.

104. M.S. Bloomfield, *Talanta* **2002**, 58, 1301.

105. A. Marin, E. Garcia, A. Garcia, C. Barbas, *J. Pharm. Biomed. Anal.* **2002**, 29, 701.

106. L.A. Shervington, N.A. Sakhnini, *J. Pharm. Biomed. Anal.* **2000**, 24, 43.

107. F. Bohnenstengel, H.K. Kroemer, B. Sperker, *J. Chromotogr. B: Biomed. Sci. Appl.* **1999**, 721, 295.

108. S. Heitmer, G. Blaschke, *J. Chromotogr. B: Biomed. Sci. Appl.* **1999**, 721, 93.

109. L. Suntornsuk, O. Pipitharome, P. Wilairat, *J. Pharm. Biomed. Anal.* **2003**, 33, 441.

110. D. Easwaramoorthy, Y.C. Yu, H.J. Huang, *Anal. Chim. Acta* **2001**, 439, 95.

111. J. Chen, C.S. Cha, *J. Electroanal. Chem.* **1999**, 463, 93.

112. X. Kang, J. Wang, H. Wu, J. Liu, I.A. Akasay, Y. Lin, *Talanta* **2010**, 81, 754.

113. F.S. Felix, C.M.A. Brett, L. Angnes, *J. Pharm. Biomed. Anal.* **2007**, 43, 1622.

114. S.F. Wang, F. Xie, R.F. Hu, *Sens. Actuators B* **2007**, 123, 495.

115. R.N. Goyal, S.P. Singh, *Electrochim. Acta* **2006**, 51, 3008.

116. R.T. Kachoosangi, G.G. Wildgoose, R.G. Campton, *Anal. Chim. Acta* **2008**, 618, 54.

117. B.C. Lourencao, R.A. Medeiros, R.C. Rocha-Filho, L.H. Mazo, O. Fatibello-Filho, *Talanta* **2009**, 78, 748.

118. X. ShangGuan, H. Zhang, J. Zheng, *Anal. Bioanal. Chem.* **2008**, 391, 1049.

119. B. Habibi, M. Jahanbakhshi, M.H. Pournaghiazar, *Microchim. Acta* **2011**, 172, 147.

120. M. Li, L. Jing, *Electrochim. Acta* **2007**, 52, 3250.

121. P. Manisankar, S. Viswanathan, A. Pusphalatha, C. Rani, *Anal. Chim. Acta* **2005**, 528, 157.

122. V.S. Vasantha, S.-M. Chen, *J. Electroanal. Chem.* **2006**, 592, 77.

123. S. Mehretie, S. Admassie, M. Tessema, T. Solomon, *Anal. Bioanal. Electrochem.* **2011**, 3, 38.

124. S. Mehretie, S. Admassie, T. Hunde, M. Tessema, T. Solomon, *Talanta* **2011**, 85, 1376.

125. T.A. Skotheim, R.L. Elsenbaumer, J.R. Reynolds, *Handbook of Conducting Polymers*, Marcel Dekker, New York, **1998**.

126. A. Safavi, N. Maleki, O. Moradlou, *Electroanalysis* **2008**, 20, 2158.

127. D. Miner, J. Rice, R. Riggin, P. Kissinger, *Anal. Chem.* **1981**, 53, 2258.

128. O. Niwa, Y. Xu, H.B. Halsall, W.R. Heineman, *Anal. Chem.* **1993**, 65, 1559.

129. WHO (World Health Organization), *The Control of Schistosomiasis: Second Report of the WHO Expert Committee, WHO Technical Report Series*, Geneva, No. 830, **1993**.

130. S. Perrett, P.J. Whitfield, *Parasitol Today* **1996**, 12, 156.

131. G. Yang, W. Li, L. Sun, F. Wu, K. Yang, Y. Huang, X. Zhou, *Parasites Vectors* **2010**, 3, 84.

132. F.C. Churchill, D.N. Ku, *J. Chromatogr.* **1980**, 189, 375.

133. V. Lardans, C. Dissous, *Parasitol Today* **1998**, 14, 413.

134. W.E. Jones, *Am. J. Trop, Med. Hyg.* **1979**, 28, 300.

135. A. Korlkovas, *Essentials of Medical Chemistry*, Wiley, New York, **1988**.

136. G.E. Swan, J. *South Afr. Vet. Assoc.* **1999**, 70, 61.

137. E.C. Van Tonder, M.M. De Villiers, J.S. Handford, C.E.P. Malan, J.L. Du Preez, *J. Chromatogr. A* **1996**, 729, 267.

138. T.M. Schreier, V.K. Dawson, Y. Choi, N.J. Spanjers, M.A. Boogaard, *J. Agric. Food Chem.* **2000**, 48, 2212.

139. F. Onur, N. Tekin, *Anal. Lett.* **1994**, 27, 2291.

140. S.A. Abdelfattah, *Spectrosc. Lett.* **1997**, 30, 795.

141. H.G. Daabees, *Anal. Lett.* **2000**, 33, 639.

142. F.C. Abreu, M.O.F. Goulart, A.M. Oliveira Brett, *Biosens. Bioelectron.* **2002**, 17, 913.

143. H. Alemu, P. Wagana, P.F. Tseki, *Analyst* **2002**, 127, 129.

144. M. Ghalkhani, S. Shahrokhian, *Electrochem. Commun.* **2010**, 12, 66.

145. S. Mehretie, S. Admassie, M. Tessema and T. Solomon, Sens. Actuator **2012**, 168, 97.

146. J.H. Tocher, *Gen. Pharmacol.* **1997**, 28, 485.

147. P. Manisankar, S. Viswanathan, A. Mercy Pusphalatha, C. Rani, *Anal. Chim. Acta* **2005**, 528, 157.

148. S. Senthil Kumar, J. Mathiyarasu, K.L.N. Phani, V. Yegnaraman, *J. Solid State Electrochem.* **2006**, 10, 905.

149. Southampton Electrochemistry Group, *Instrumental Methods in Electrochemistry*, Ellis Horwood, Chichester, **2001**.

150. D.K. Gosser, Cyclic Voltammetry, Simulation and Analysis of Reaction Mechanisms, VCH Publishers, New York, **1993** p. 43.

151. P.W. Graebing, J.S. Chib, T.D. Hubert, W.H. Gingerich, *J. Agric. Food Chem.* **2004**, 52, 5924.

152. M. Jokanovic and M.P. Stojiljkovic, *Eur. J. Pharmacol.* **2006**, 553, 10.

153. M. Eddleston, *Q J Med.* **2000**, 93, 715.

154. M. Eddleston, *Med Trop* **2008,** 68, 385.

155. J. Bajgar, *Adv. Clin. Chem.* **2004**, 38, 151.

156. M. Gyenge, H. Kalasz, G.A. Petroianu, R. Laufer, K. Kuca and K. Tekes, *J. Chromatogr. A*, **2007**, 1161, 146.

157. M. Jokanovic and M. Prostran, *Curr. Med. Chem.* **2009**, 16, 2177.

158. S.M. Nurulain, D.E. Lorke, M.Y. Hasan, M. Shafiullah, K. Kuca, K. Musilek and G.A. Petroianu, *Neurotox Res*, **2009**, 16, 60.

159. M. Bodiroga, S.D. Agbaba, D. Ztvanov-stakics and R. Popovics, *J. Pharm. Biomed. Anal.* **1994**, 12, 127.

160. H. Kalasz, M.Y. Hasan, R. Sheen, K. Kuca, G. Petroianu, K. Ludanyi, A. Gergely and K. Tekes, *Anal. Bioanal. Chem.* **2006**, 385, 1062.

161. M. Gyenge, H. Kalasz, G.A. Petroianu, R. Laufer, K. Kuca and K. Tekes, *J. Chromatogr. A* **2007**, 1161, 146.

162. K. Karljikovic-Rajic, B. Stankovic, A. Granov and Z. Binenfeld, *J. Pharm. Biomed. Anal.* **1988**, 6, 773.

163. S. Issac and K.G. Kumar, *Anal. Methods* **2010**, 2, 1484.

164. L. Lonappan and K.G. Kumar, *Sensor Lett.* **2011**, 9, 541.

165. S. Mehretie, J. Losada, M. Tessema, S. Admassie, T. Solomon J. Perez-Pariente, I. Diaz, *Analyst* **2012**, 137, 5625.

166. E. Laviron, *J. Electoranal. Chem.* **1979**, 101, 19.

167. S. Chen, *J. Phys. Chem.* **2000**, 104, 663.

168. A Walcarius in: S.M. Aurbach, K.A. Carrado and P.K. Dutta (Eds.), *Handbook of Zeolite Catalysis and Microporous Materials*, Marcel Dekker, Chap. 14, **2003**.

169. E. Briot, F. Bedioui and K.J. Balkus Jr. *J. Electroanal. Chem.* **1998**, 454, 83.

170. J. Li, K. Pfanner and G. Calzaferri, *J. Phys. Chem.* **1995**, 99, 2119.

171. A. Walcarius, S. Rozanska, J. Bessière and J. Wang *Analyst*, **1999**, 124, 1185.

172. V.A. Petrosyan, M.E. Niyaxymbetov, E.V. Ulyanova, *Izv. Akad. Nauk SSSR, Ser. Khim.* **1990**, 3, 625.

173. A.B. Moghaddam, A. Mohammadi, S. Mohammadi, D. Rayeji, R. Dinarvand, M. Baghi and R.B. Walker, *Microchim. Acta* **2010**, 171, 377.

174. J.M. Potts (Ed.), *Essential urology: A Guide to Clinical Practice*, Humana press, **2004**.

175. B N Ames, R Cathcart, E Schwiers, and P Hochstein, *Proc Natl Acad Sci U S A* **1981**, 78, 6858.

176. D. Lakshmi, M.J. Whitcombe, F. Davis, P.S. Sharma, B.B. Prasad, *Electroanalysis* **2011**, 23, 305.

177. P. Pacher, J.S. Bechman, L. Liaudet, *Physiol. Rev.* **2007**, 87, 315.

178. M. Alderman, K.J. Aiyer, *Curr. Med. Res. Opin.* **2004**, 20, 369.

179. R. J. Johnson, D.-K. Kang, D. Feig, S. Kivlighn, J. Kanellis, S. Watanabe, K. R. Tuttle, B. Rodriguez-Iturbe, J. Herrera-Acosta, M. Mazzali, *Hypertension* **2003**, 41, 1183.

180. C. R. Raj, T. Ohsaka, *J. Electroanal. Chem.* **2003**, 540, 69.

181. H.K. Choi, D.B. Mount, A.M. Reginato, *Ann Intern Med.* **2005**, 143, 499.

182. T. Annanmaki, A. Muuronen, K. Murros, *Mov Disord.* **2007**, 22, 1133.

183. M.K. Kutzing, B.L. Firestein, *J. Pharmacol. Exper. Therap.* **2008**, 324, 1-7.

184. Y. Zhao, X. Yang, W. Lu, H. Liao, F. Liao, *Microchim. Acta* **2009**, 164, 1.

185. I.D.P. Wootton, H. Freeman, *Microanalysis in Medical Biochemistry*, 6th Ed. Churchill Livingstone, New York, **1982**.

186. C.K. Lim, D.E. Pryde, A.M. Lawson, *J. Chromatogr.* **1978**, 149, 711.

187. S.A. Wring, J.P. Hart, *Analyst* **1992**, 117, 1215.

188. S. Se, Y. Wen, W.D. Zhang, L.M. Gan, G.Q. Xu, *Electroanalysis* **2003**, 15, 1993.

189. S.A. John, *J. Electroanal. Chem.* **2005**, 579, 249-256

190. M. Mallesha, R. Manjunatha, C. Nethravathi, G.S. Suresh, M. Rajamathi, J.S. Melo, T.V. Venkatesha, *Bioelectrochemistry* **2011**, 81, 104.

191. J. Arguello, V.L. Leidens, H.A. Magosso, R.R. Ramos, Y. Gushikem, *Electrochim. Acta* **2008**, 54, 560.

192. S. Thiagarajan, S. Chen, *Talanta* **2007**, 74, 212-222.

193. L. Lin, J. Chen, H. Yao, Y. Chen, Y. Zheng, X. Lin, *Bioelectrochemistry* **2008**, 73, 11.

194. J. Huanga, Y. Liua, H. Houb, T. You, *Biosens. Bioelectron.* **2008**, 24, 632.

195. R.P. Silva, A.W.O Lima, S.H.P. Serrano, *Anal. Chim. Acta* **2008**, 612, 89.

196. S.A. Kumar, H. Cheng, S. Chen, *Electroanalysis* **2009**, 21, 2281.

197. Y. Li, X. Lin, *Sens. Actuators, B* **2006**, 115, 134.

198. P. Kalimuthu, S.A. John, *Talanta* **2010**, 80, 1686.

199. A. Babaei, M. Zendehdel, B. Khalilzadeh, A. Taheri, *Coll Surf B: Biointerfaces* **2008**, 66, 226.

200. A. Geto, M. Amare, T. Merid, S. Admassie, *Anal Bioanal Chem* **2012**, 404, 525.

201. M. Chao, X. Ma, X. Li, *Int. J. Electrochem. Sci.* **2012**, 7, 2201.

202. M.W. Tietz, Clinical Guide to Laboratory Tests, Thrid ed. Pa. WB Saunders Campany, Philadelphia, 1995 (from: www.mti-diagnostics.de Rev **2008**).